Evaluation of Existing Highway Bridge Systems

M. Ghosn
J.R. Casas

Monograph CIMNE Nº 30, February 1996

Evaluation of Existing Highway Bridge Systems

M. Ghosn
J.R. Casas

E.T.S. d'Enginyers de Camins, Canals i Ports
Universitat Politècnica de Catalunya

Monograph CIMNE Nº 30, February 1996

Internacional Center for Numerical Methods in Engineering
Gran Capitán s/n, 08034 Barcelona, España

The cover designed by: Jordi Pallí

First published, December 1995

Edited by:
International Center for Numerical Methods in Engineering
C/ Gran Capitán, s/n
08034 Barcelona, Spain

ISBN: 84-87867-62-6
Deposito Legal: B-10948-96

EVALUATION OF EXISTING HIGHWAY BRIDGE SYSTEMS

Michel Ghosn
and
Juan Ramón Casas

Centro Internacional de Métodos Numéricos en Ingeniería
Universidad Politécnica de Cataluña
Edificio C1, Gran Capitán, s/n
08034 Barcelona, España

1. INTRODUCTION

1.0 Problem Statement

Evaluation, repair and rehabilitation of bridges are increasingly important topics in current efforts to deal with the deteriorating infrastructure of developed countries. In fact, after several years of large scale construction projects to build new highway networks, the number of existing bridges is so large that current administrations need to invest increasingly large amounts of funds on the maintenance, diagnostic and repair of these bridges.

For example, in the United States about 40 percent of the nation's 570,000 bridges are classified as deficient and in need of rehabilitation or replacement according to the Federal Highway Administration's (FHWA) criteria [1]. In Europe, the most important infrastructure construction works were completed shortly after the end of World War II. Therefore, many of the existing bridges are now older than 40 years and the situation is quickly resembling the one encountered in the US. In fact, a report by the Organization for Economic Co–operation and Development (OECD) [2] states that more than 50 percent of existing European bridges are more than 25 years old.

In addition to aging, increased loading and environmental contamination are other main causes of bridge deterioration [3]. The percentage of bridges damaged due to accidental collisions is also very high. In fact, it has been reported [4] that about 0.9 percent of all US prestressed concrete bridges are damaged every year mostly due to collisions which account for 80 percent of the total observed damages [4,5].

Fortunately, despite the aging and deterioration of the bridge infrastructure, the rate of catastrophic bridge failures that is recorded is very low compared to other safety risks that the public is exposed to in its daily routine. This is because current bridge evaluation techniques are conservatively biased and implicitly or explicitly use high levels of safety factors. On the other hand, these current evaluation methods do not always provide an accurate measure of the true capacity of existing bridge systems. For

example, current design and evaluation techniques deal with individual members and use procedures which ignore the effect of the complete structural system [6,7,8,9,10]. As currently performed, the safety check verifies that the strength of each member is greater than the applied forces by a comfortable safety margin. The member forces are calculated using an elastic analysis while member capacity (when appropriate) may be calculated using inelastic member behavior. The safety margin is provided through the application of safety factors (load and/or resistance factors) that are calibrated based on experience and engineering judgment or using a combination of experience and structural reliability methods. In addition, a check of member serviceability criteria such as member cracking and maximum displacements under service loads is also performed [6,7,8,9,10].

While the member–oriented linear analysis approach has been successfully used for new designs, it does not provide an adequate representation of the safety of the complete bridge system. In many instances, the failure of an individual member does not lead to the failure of the complete system. On the other hand, because of possible large nonlinear deformations, the bridge may be inadequate for truck traffic at loads that are lower than those that will cause a system failure [11].

Loss of member capacity is also of concern. Bridge members are often subjected to fatigue stresses that may lead to fracture and the loss of the load carrying capacity of a main member. In addition, corrosion, fire or an accident such as collision by a truck, ship or debris, could cause the loss of a member or the severing of the prestressing strands. To ensure the safety of the public, bridges should be able to sustain these damages and still operate albeit at reduced capacity. Therefore, in addition to verifying the safety of the intact structure, the evaluation of a bridge's safety should consider the consequences of the failure of one critical bridge element [11,12].

Because of the system effects and the high costs of bridge repairs, the evaluation of damaged existing bridges requires a very careful analysis of the structural performance of the bridge system as well as an economic analysis of the options available. Facing a deteriorated or a damaged bridge, the evaluating engineer has to decide whether to replace the damaged member or to repair it in–place; whether to restore the member (or the bridge) to its original capacity or to permit a lower capacity. These decisions are currently often made under the pressure to restore the facility to service without performing an accurate structural safety analysis nor an economic analysis [13].

To avoid high costs of replacement or repair, the evaluation of an existing bridge must accurately reveal the present load carrying capacity of the structure and predict future loads and any future changes in bridge capacity due to deterioration. In addition, on a more global scale, the repairs and replacements of bridges belonging to a network, must be prioritized and optimized. This work requires an efficient decision making process. It is thus imperative to explore all available methods, theoretical and experimental, as well as previous practical experience and knowledge to devise a rational strategy to deal with the problem [13].

The need to develop accurate deterioration models and practical tools for field assessment of the degree of deterioration has been identified [13]. There is also a consensus that bridge evaluation criteria should be rationalized by basing them on state–

of–the–art methods, in particular on reliability theory [13]. Thus, a new generation of bridge evaluation and maintenance criteria should be based on probabilistic methods following a trend analogous to that used in the development of the current generation of bridge design criteria. Reliability has become an issue of increasing importance for highway bridges because of gradual increases in truck loads, difficulty of load enforcement and increase in traffic. A probabilistic treatment is thus appropriate to account for the influence of these trends [14].
Due to the gravity of the problem at hand, many studies on different aspects of bridge diagnostics, evaluation, rehabilitation techniques and management strategies have been initiated throughout the world. For example, new instrumentations and techniques for the detection, diagnosis and monitoring of bridge structures are being tested by several research organizations [15 through 22]. Models for deterioration rates of bridge members are also under investigation [23,24]. Innovative methods for bridge strengthening and rehabilitation are being implemented in current practice [25,26,27,28]. In addition, reliability–based techniques for bridge member as well as bridge system evaluation have been developed [29,30]. Finally, many US states and European countries are developing bridge management systems in an attempt to optimize the use of the limited resources available for bridge maintenance and rehabilitation [1,31,32,33]. The results of these investigations however, were never assembled into a comprehensive and coherent framework that can be directly used by a bridge engineer during the routine evaluation of existing bridges.

1.1 Research Objectives and Report Outline

The objective of this study is to develop a comprehensive framework for the evaluation of existing highway bridge systems based on reliability techniques and accounting for the nonlinear behavior of these structures. To achieve these objectives the following tasks are undertaken:

1) Develop analysis techniques to evaluate the true behavior and the actual capacity of existing bridge systems taking into account their capacity to redistribute the applied loads both longitudinally and transversely. The proposed methods should be simple enough yet sufficiently accurate for easy implementation in system reliability calculations.
2) Develop system reliability models to account for the uncertainties associated with determining bridge loads and system capacity.
3) Develop a framework to utilize results of nondestructive testing and bridge diagnostics in the safety evaluation of existing bridges using system reliability techniques. This framework should be usable by the evaluating engineer to devise optimum strategies for bridge evaluation and rehabilitation.

Chapter 2 of this report outlines a method to perform the nonlinear analysis of typical highway bridge systems. Chapter 3 develops system reliability models to evaluate the structural safety of highway bridge systems under the effect of truck loads. Chapter 4 develops a technique to evaluate the performance of damaged highway bridge systems and develop tools for optimum decision making based on bridge system reliability,

inspection reports and costs of rehabilitation. Chapter 5 summarizes the findings and outlines the direction of future research in the field of evaluation of existing bridge systems.

2. NONLINEAR ANALYSIS OF BRIDGE SYSTEMS

2.0 Introduction

Bridge system capacity is defined as the capability of a bridge to carry heavy loads due to the interlocking of members into a complete system. To study the nonlinear behavior of bridge systems until their ultimate capacity requires the investigation of member performance as well as transverse and longitudinal load redistribution. To calculate this system capacity the nonlinear analysis of a bridge system is required. Many computer programs are available to perform the linear elastic analysis of bridge systems. For example, reference [59] gives a list of some of these programs such as GENDEK [60], CURVBRG [61] and MUPDI [62]. These programs, however, are specialized for the analysis of specific bridge types and are capable of performing only linear elastic analyses. Therefore, they are not suitable for studying the complete nonlinear behavior of bridge systems.

Specialized nonlinear bridge analysis programs are also available. For example, Kostem and his co-workers developed programs BOVA [63] and BOVAS [64] to perform the nonlinear analysis of concrete and steel slab on girder bridge systems. Idriss and White [65] also developed a program to perform the nonlinear analysis of steel I-girder bridge systems. Similarly, Maheu [44] developed a program to perform the nonlinear elasto-plastic analysis of steel girder bridge systems. Scordelis and his co-workers developed programs for the nonlinear analysis of box type bridges [67]. For example, the program NOBOX [41] is used for the nonlinear analysis and ultimate strength of multi-cell reinforced concrete box girder bridges. The program NAPBOX [56] is used for the analysis of rectangular single-cell reinforced and prestressed concrete box girder bridges. Kostem and Hand, also developed a program for the inelastic analysis of spread box-beam bridges [68]. Each one of these programs was however designed to analyze one particular type of bridges. An engineer who is interested in studying the behavior of different types of bridges must therefore be familiar with the requirements and limitations of several such programs.

General purpose nonlinear finite element packages can also be used for the nonlinear analysis of any structure and in particular bridge structures. For example, FINITE [69] was used in reference [59] to analyze a variety of bridge structures but was only used to study the behavior in the linear elastic range although the program is capable of performing nonlinear analyses. The program ABAQUS [70] is an especially powerful program that can be adapted to perform the analysis of any type of structure. For example, ABAQUS [70] was used by Helba and Kennedy [71] to analyze the collapse loads of continuous skewed composite steel bridges. Other commercially available programs with similar capabilities include ANSYS [66], NONSAP [72], DYN3D [73] and many others. These programs are theoretically usable for any type of bridge structure. The problem with such general purpose commercial packages, especially for use in

the nonlinear range, is the complexity of the required input data and the specialized training required before an engineer becomes familiar with their use, capabilities and limitations. For example, the nonlinear behavior is studied using the basic principles of 3–dimensional plasticity and thus the program requires complete input information on the type of plastic flow model to be used and the definitions of failure in 3 dimensions. Because of the difficulty of adapting the general purpose programs for large scale analysis of many bridge types, this study uses a specially developed nonlinear bridge analysis program *NONBAN* which can be routinely used to analyze the nonlinear behavior of common type bridge structures. The advantages of the program *NONBAN* are:

1. The program requires simple input information such that it could be used on a routine basis without requiring lengthy preparation of input data.
2. The program is applicable for studying the nonlinear behavior of common type bridge structures including slab on I–beam bridges as well as box girder bridges.
3. The program gives a reasonably accurate representation of the global nonlinear behavior of bridge systems.

The program *NONBAN* as developed in a related project [11] and modified in this study uses a grillage (grid) analysis procedure. The program performs a nonlinear analysis of bridge systems using a modified stiffness matrix that accounts for material nonlinearity. In this program, the linear elastic stiffness matrices of the beam elements are modified to account for possible flexural and shear nonlinearities as explained in section 2.1. Section 2.2 provides a general description of the program logic. A discussion on the nonlinear material models used with *NONBAN* is provided in section 2.3. Sections 2.4 through 2.9 provide illustrations on the accuracy and the validity of the program by comparing the results of *NONBAN* to analytical and experimental results of tests on bridge members, as well as model and full scale field tests of bridge structures.

2.1 Stiffness Matrix Method for Bridge Analysis

The stiffness matrix method has been in use for several decades to perform the linear elastic analysis of structural frames. In Europe, where bridge design codes do not recommend simplified analysis approaches as currently provided by AASHTO's distribution factors [6], the stiffness matrix approach is the most widely used method for the linear elastic analysis and design of bridge systems. In most instances, the bridge superstructure is modeled as a grillage (grid) formed by linear elastic beam elements. This approach is used for slab bridges, slab on girder bridges, as well as spread box beam bridges and multicell box girder bridges. The latter types of bridges, however, require careful modeling to account for the torsional capacity of the boxes and the distortion of the cross section (in–plane deformations) [34].
In the derivation of the stiffness matrix for the linear elastic analysis of bridge systems, the bridge is divided into beam elements interconnected via nodes. The deflections and rotations of these nodes can be released or fixed depending on the boundary constraints. In the linear elastic range, the beam element stiffness matrices assume that the displacements at the ends of a beam element are equal to those of the nodes.

As the loads are incremented beyond the elastic limits and the beam elements go into the nonlinear range, it is often assumed that this plastification is concentrated at the ends of the beam elements [35]. This can be modeled as if the elastic part of the beam elements are joined to the nodes by means of flexible connections. When the plastification (or nonlinearity) is due to the effect of bending stresses, the flexible connections are modeled as rotational springs. The relationship between the moments and the rotations of these plasticized ends are represented by rotational stiffnesses. Although, these stiffnesses are not necessarily linear, they can be assumed to be piecewise linear [35]. Hence, this model can be used in an incremental nonlinear structural analysis of a bridge system as will be seen in section 2.2. The effect of shear nonlinearity is discussed further below when discussing the deformations due to shearing forces.

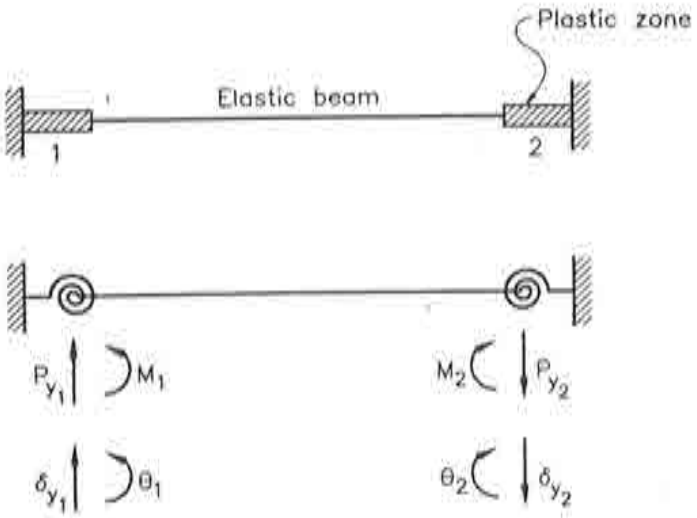

Figure 2.1. Definition of terms of a beam element with rotational springs

The derivation of the stiffness matrix of a beam element with rotational springs at its ends follows the approach recommended in reference [35]. The following derivation assumes a beam element in 2–D and uses the notation shown in Figure 2.1 where δ_{y1} and θ_1 are respectively the spring deflection and the spring rotation of end 1. p_{y1} and m_1 are the plastic force and the plastic moment at end 1. The relationship between the plastic forces and the plastic deformations of node 1 can be written in matrix form as:

$$\begin{bmatrix} \delta_{y1} \\ \theta_1 \end{bmatrix} = \begin{bmatrix} 0 & 0 \\ 0 & \frac{1}{\beta_1} \end{bmatrix} \begin{bmatrix} p_{y1} \\ m_1 \end{bmatrix}$$

or:

$$\boldsymbol{\delta}_1 = \mathbf{F}_{c1}\, \mathbf{p}_1 \tag{2.1}$$

where $\boldsymbol{\delta}_1$ is the vector of generalized spring displacements of end 1. $\boldsymbol{\delta}_1$ is formed by two terms δ_{y1} which is the vertical displacement and the rotation θ_1. $\mathbf{p}_1$ is the vector of generalized spring forces at end 1, it is formed by two terms p_{y1} which is the vertical

force and the moment m_1. $\mathbf{F}_{c1}$ is the spring flexibility matrix where β_1 is the stiffness of the rotational spring. β_1 is equal to infinity when the beam is rigidly connected to the node *i.e.* when the beam ends are still in the elastic range. On the other hand, β_1 is equal to zero when the plastic moment limit is reached. Figure 2.2.a shows an idealized moment versus plastic rotation curve modeling the plastification due to bending stresses of the ends of structural beam elements.

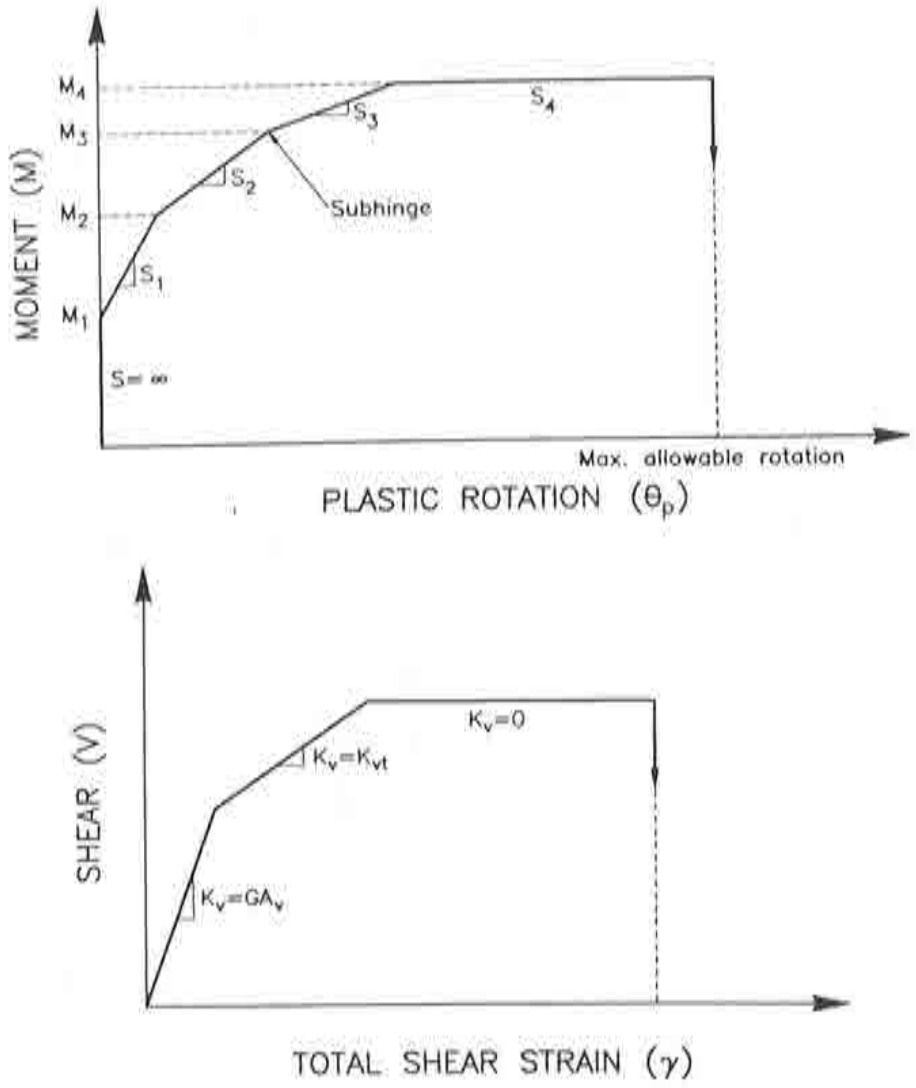

Figure 2.2. Material nonlinearity models used in *NONBAN*

An equation similar to equation 2.1 can also be written for end 2 with a flexibility matrix $\mathbf{F}_{c2}$ expressed in terms of β_2 the stiffness of the rotational spring at end 2.

$$\begin{bmatrix} \delta_{y2} \\ \theta_2 \end{bmatrix} = \begin{bmatrix} 0 & 0 \\ 0 & \frac{1}{\beta_2} \end{bmatrix} \begin{bmatrix} p_{y2} \\ m_2 \end{bmatrix}$$

or:

$$\boldsymbol{\delta}_2 = \mathbf{F}_{c2}\, \mathbf{p}_2 \tag{2.2}$$

The flexibility matrix of end 2 of the beam element when the bending stresses are still in the linear elastic range and accounting for shear deformations is given as:

$$\mathbf{F}_{m2} = \begin{bmatrix} \frac{L^3}{3\,EI} + \frac{L}{K_V} & \frac{L^2}{2\,EI} \\ \frac{L^2}{2\,EI} & \frac{L}{EI} \end{bmatrix} \tag{2.3}$$

where L is the length of the beam element, E is the elastic modulus, I is the moment of inertia and K_V is the shear rigidity. When the shear force applied on the beam element is still in the linear elastic range K_V is equal to GA_V where G is the shear modulus and A_V is the shear area of the section. As the shear force exceeds its elastic limit, K_V is modified to account for shear cracking and shear failure. Figure 2.2.b shows an idealized shear deformation curve modeling the effect of shear nonlinearity. Equation 2.3 assumes that as the bending stresses of the beam element go into the nonlinear range, the plasticized bending zone remains infinitely small and is concentrated at the ends of the beam element. Thus, the length of the part of the beam element where the bending stresses are still in the elastic range remains practically equal to the original length L. If the shear deformations are negligible then K_V is set equal to infinity. If shear nonlinearity is to be included in the analysis, the shear stiffness K_V can be updated as the applied loads are incremented beyond the shear elastic limits (see section 2.3.1).
To satisfy equilibrium, the plastic forces that develop in the spring at end 1 due to flexural nonlinearity will also create corresponding forces at end 2. These in turn will also create additional displacements at end 2. Therefore, the total displacements at end 2 are obtained by superposing the displacements due to the plastic forces directly applied at end 2, the displacements at end 2 due to the part of the beam where the elastic stresses are still linear and the displacements at end 2 due to the plastic forces that develop at end 1 to satisfy equilibrium. The final flexibility matrix for end 2 is obtained from the superposition of the flexibility matrix of end 2, the linear elastic flexibility matrix and the transformed flexibility matrix of end 1. This can be formulated as follows:

$$\mathbf{F} = \mathbf{F}_{c2} + \mathbf{F}_{m2} + \mathbf{H}^t\, \mathbf{F}_{c1}\, \mathbf{H} \tag{2.4}$$

where $\mathbf{H}$ is the equilibrium matrix which gives the relationship between the forces that develop at end 1 due to the plastic forces applied at end 2, $\mathbf{H}^t$ is the transpose of $\mathbf{H}$. The equilibrium matrix $\mathbf{H}$ is given by:

$$\begin{bmatrix} p_{y1} \\ m_1 \end{bmatrix} = \begin{bmatrix} 1 & 0 \\ L & 1 \end{bmatrix} \begin{bmatrix} p_{y2} \\ m_2 \end{bmatrix}$$

or

$$\mathbf{p}_2 = \mathbf{H}\, \mathbf{p}_1 \tag{2.5}$$

where

$$\mathbf{H} = \begin{bmatrix} 1 & 0 \\ L & 1 \end{bmatrix}$$

The beam element stiffness matrix gives the relationship between the forces applied on both ends of the beam and the displacements and rotations of the nodes. The part of the beam element stiffness matrix that gives the relationship between the forces at end 2 and the displacements at end 2 is obtained by inverting the flexibility matrix **F** [35].

$$\mathbf{K}_{22} = \mathbf{F}^{-1} \tag{2.6}$$

The part of the stiffness matrix that gives the relationship between the forces at end 1 and the displacements at end 1 is obtained by [35]:

$$\mathbf{K}_{11} = \mathbf{H}\,\mathbf{K}_{22}\,\mathbf{H}^t \tag{2.7}$$

The part of the stiffness matrix that gives the relationship between the forces at end 1 and the displacements at end 2 is obtained by:

$$\mathbf{K}_{12} = -\mathbf{H}\,\mathbf{K}_{22} \tag{2.8}$$

The final stiffness matrix for one beam element becomes:

$$\mathbf{K} = \begin{bmatrix} \mathbf{K}_{11} & \mathbf{K}_{12} \\ \mathbf{K}_{21} & \mathbf{K}_{22} \end{bmatrix} \tag{2.9}$$

where $\mathbf{K}_{21}$ is the transpose of $\mathbf{K}_{12}$. In addition to the terms due to bending and shear, the grid analysis requires the inclusion of the torsional effects in the stiffness matrix. These can be considered separately since the rotations due to torsion are uncoupled from the bending and shearing rotations and displacements. More details on the derivation of the stiffness matrix of beam elements with ends connected to rotational springs can be found in reference [35].

2.2 Nonlinear Bridge Analysis Program – *NONBAN*

The program *NONBAN* was written to perform the nonlinear analysis of multi–girder bridge systems using the incremental analysis technique [11]. To use *NONBAN*, the bridge should be discretized as a grid with longitudinal beam elements used to model the contributions of the longitudinal members such as main girders; and transverse beam elements used to model the contributions of transverse members such as slab, flanges and diaphragms. Figure 2.3 shows an example describing the discretization of a slab on I–girder bridge.

Material nonlinearities are only considered for bending about the main axis of each element and for shear deformations in the vertical direction. The nonlinear behavior of each element is represented by a moment versus plastic rotation ($M - \theta$) curve and a shear deformation curve as shown in Figure 2.2. The plastic rotation is defined as the

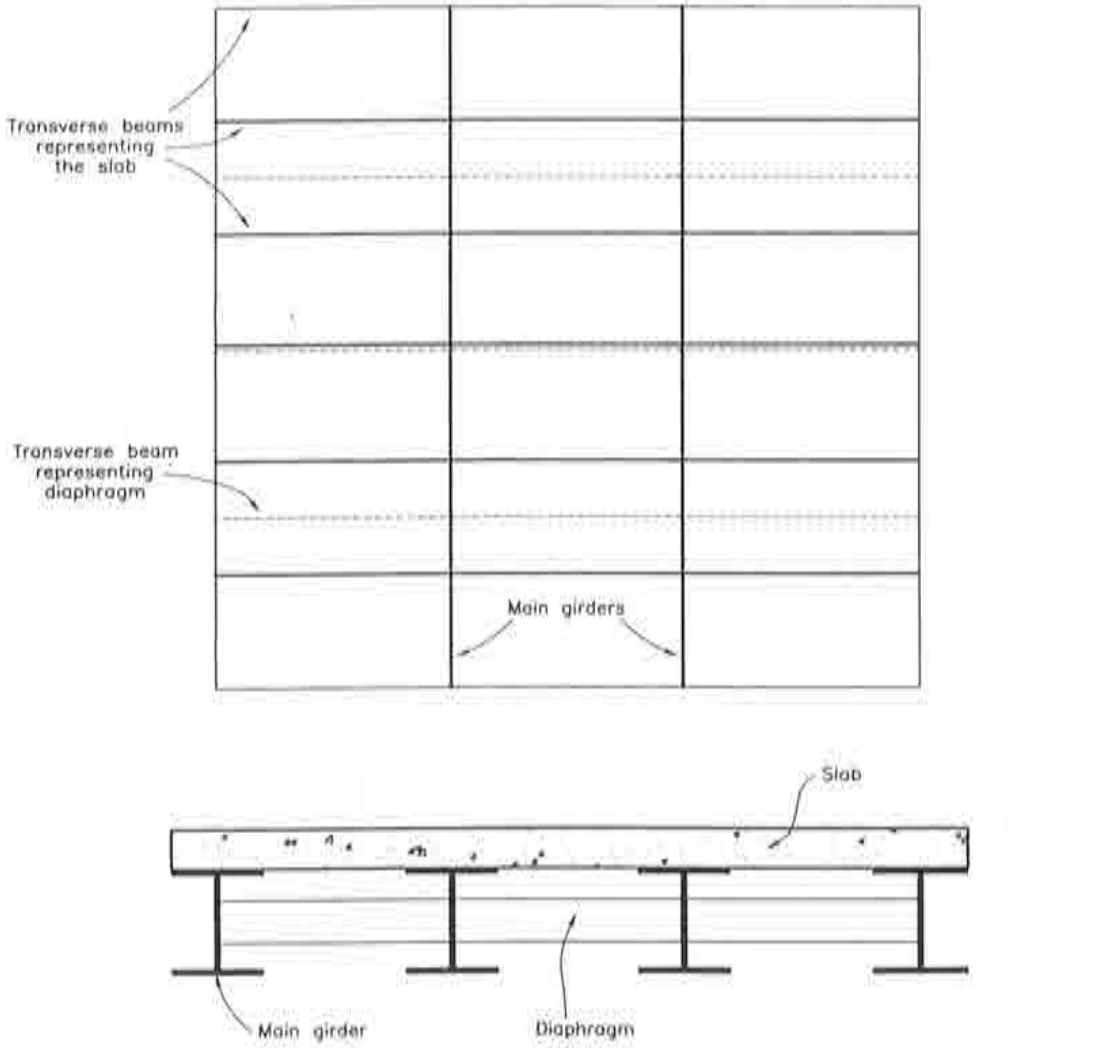

Figure 2.3. Typical grid model for bridge superstructure

total rotation minus the elastic rotation. The points of transition between segments of the $(M - \theta)$ curve will be referred to as "subhinges". When the moments and shear forces on a beam element are below the elastic limits, the calculation of the stiffness matrix assumes that β_1 and β_2 of equations 2.1 and 2.2 are equal to infinity and that K_V of equation 2.3 is equal to GA_V. When the moments or the shear forces on a beam element exceed the elastic limits, the appropriate values of β_1, β_2 and K_V are taken from the moment rotation and shear deformation curves and the stiffness matrix is calculated using the equations developed in section 2.1.

To consider the nonlinear behavior of the bridge system, the incremental loading technique is used. To perform the incremental analysis, it is first assumed that all beam elements are in their linear elastic range corresponding to the first segment of each element's $M - \theta$ and shear deformation curves. A load is then applied on the structure and the forces and deformations of each element are calculated. Each beam

element is then checked to calculate the factor by which the initial load should be multiplied in order to reach the level at which the next subhinge will form or the level at which a new slope is reached in the shear deformation curve. The load factor that is finally applied for the whole bridge system is the lowest factor obtained. The internal forces and deflections are calculated for the factored load. These are the final results of the first iteration.

The stiffness matrix of the element where a subhinge forms, or which reaches a level at which the shear deformation slope changes is updated using equation 2.9. This is achieved by using β values in equations 2.1 and 2.2 obtained from the appropriate segments of the moment rotation curves. Similarly, the value of K_V used in equation 2.3 is replaced by the appropriate shear deformation slope. A second elastic analysis is then performed with the updated stiffness matrix and with the original load. Every element is checked to find the lowest possible load factor by which the results of the second analysis should be multiplied to produce a new subhinge or to reach a new shear deformation slope. This load factor is the incremental load factor.

The results of the second analysis are multiplied by the incremental load factor and then added to the results of the first iteration. These are the results of the second iteration. The total load factor at this stage is the incremental load factor added to the load factor obtained in the previous iteration. The process is thus repeated until the structure becomes unstable or until a predetermined stopping criterion is met. Typical stopping criteria include a total deflection limit or a total rotation limit.

The results of the incremental analysis are typically presented in curves giving the load factor versus the response of interest. Common plots usually give the load factor versus maximum deflection.

A flow chart describing the logic used by *NONBAN* is provided in Figure 2.4.

2.3 Material Nonlinearity

In addition to the beam geometric and elastic material properties, the program *NONBAN* requires a representation of the nonlinear material behavior. To use the formulation developed in section 2.1, the material nonlinearity should be summarized in moment versus plastic rotation curves and in shear versus shear deformation relationships. Main bridge elements could be either concrete (reinforced or prestressed) or steel (composite or noncomposite). The behavior of these two types of materials is different and thus are treated separately in this study.

2.3.1 Nonlinearity of Concrete Members

The nonlinear behavior and the ductility of concrete beams is normally modeled using moment versus curvature relationships [36]. These relationships are developed using the principle of equilibrium in function of member geometry and the stress–strain relationships of the concrete and the reinforcing and/or prestressing steel. Moment versus plastic rotation curves can also be used to model the nonlinear behavior of concrete members. These curves can be obtained using a combination of analytical and empirical methods as explained below.

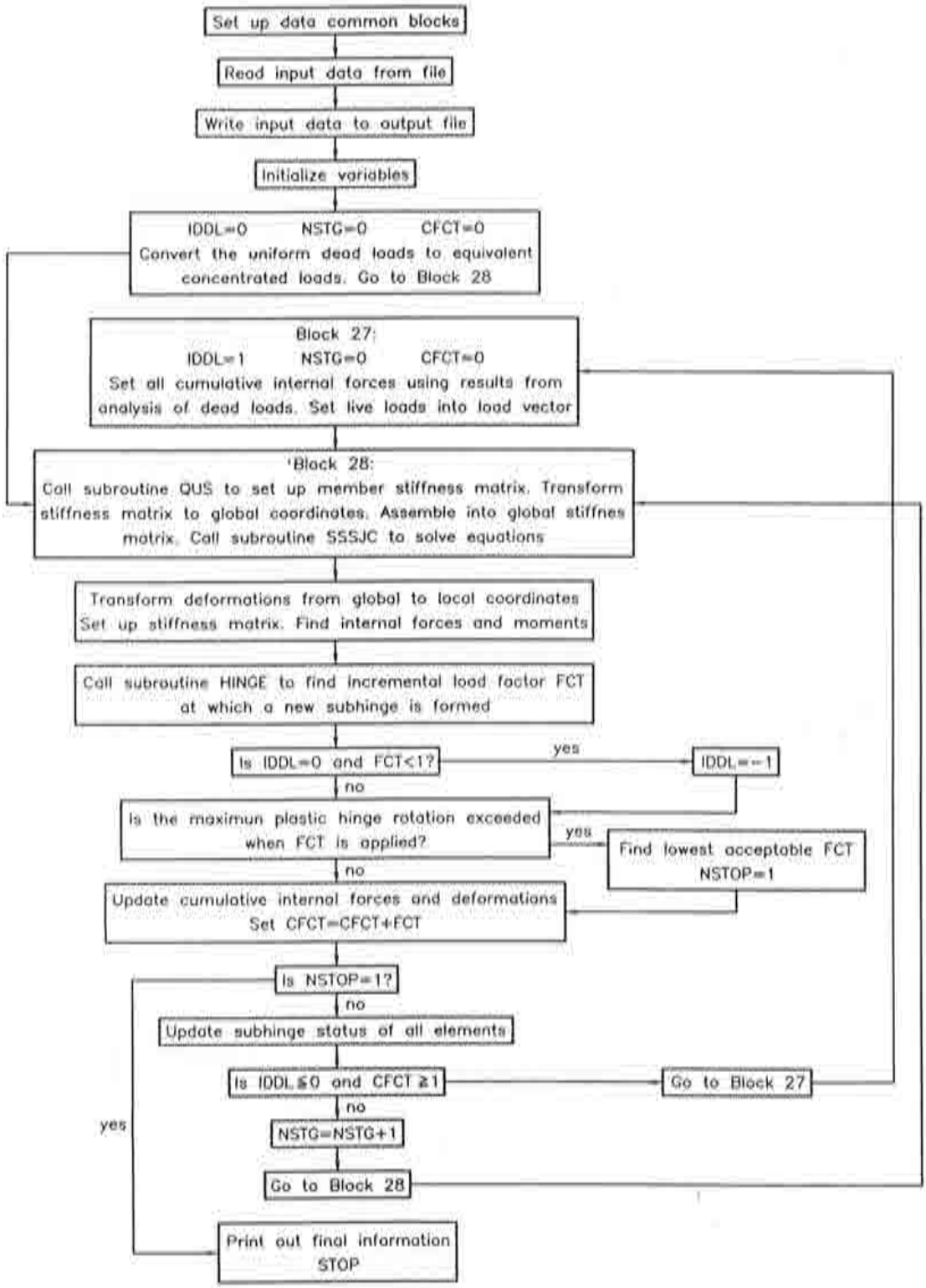

Figure 2.4. *NONBAN* **Flow chart**

Definitions

As the load applied on a concrete member increases, and the strains at some section go beyond the elastic limits, the section undergoes inelastic deformations. One measure of the total internal deformations of a section is the curvature ϕ defined as:

$$\phi = \frac{\varepsilon}{c} \tag{2.10}$$

Where ε is the strain of the extreme compression fiber and c is the distance from the extreme compression fiber to the neutral axis. In general, the total curvature ϕ can be divided into an elastic part ϕ_e and a plastic part ϕ_p

$$\phi = \phi_e + \phi_p \tag{2.11}$$

Knowing the stress–strain relationships for all the materials forming a section, the relationship between the internal bending moment applied on the section and the curvature can be calculated from equilibrium. Typical stress versus strain curves for concrete, reinforcing steel and prestressing steel are shown in Figure 2.5. Examples of moment versus curvature plots for typical reinforced concrete and prestressed concrete sections are given in Figures 2.6 and 2.7.
The total rotation θ of a section is related to the curvature ϕ by the differential equation:

$$d\theta = \phi \, dx \tag{2.12}$$

where dx is the differential length of the beam section under consideration.
If the total rotation is divided into an elastic rotation θ_e and a plastic rotation θ_p, then:

$$d\theta_p = \phi_p \, dx \tag{2.13}$$

As the plastic deformation spreads over a portion of the beam of length L_p, the total plastic rotation becomes:

$$\theta_p = \int_0^{L_p} \phi_p \, dx \tag{2.14}$$

where ϕ_p is the plastic curvature and L_p is the length of the plastic hinge. Since ϕ_p varies over L_p and since L_p is difficult to estimate, it is usual to assume that the curvature is constant over the length of the plastic hinge L_p which is usually estimated using empirical equations. In this case the plastic rotation can be calculated from the plastic curvature using the equation:

$$\theta_p = \phi_p \, L_p \tag{2.15}$$

Maximum Plastic Rotations

Concrete members will keep loading until they reach their ultimate moment capacity. As the section goes into the inelastic range, plastic hinge rotations will occur. These plastic hinge rotations are related to the strain in the member. Once the ultimate strain capacity is reached, it will result into a maximum possible plastic hinge rotation

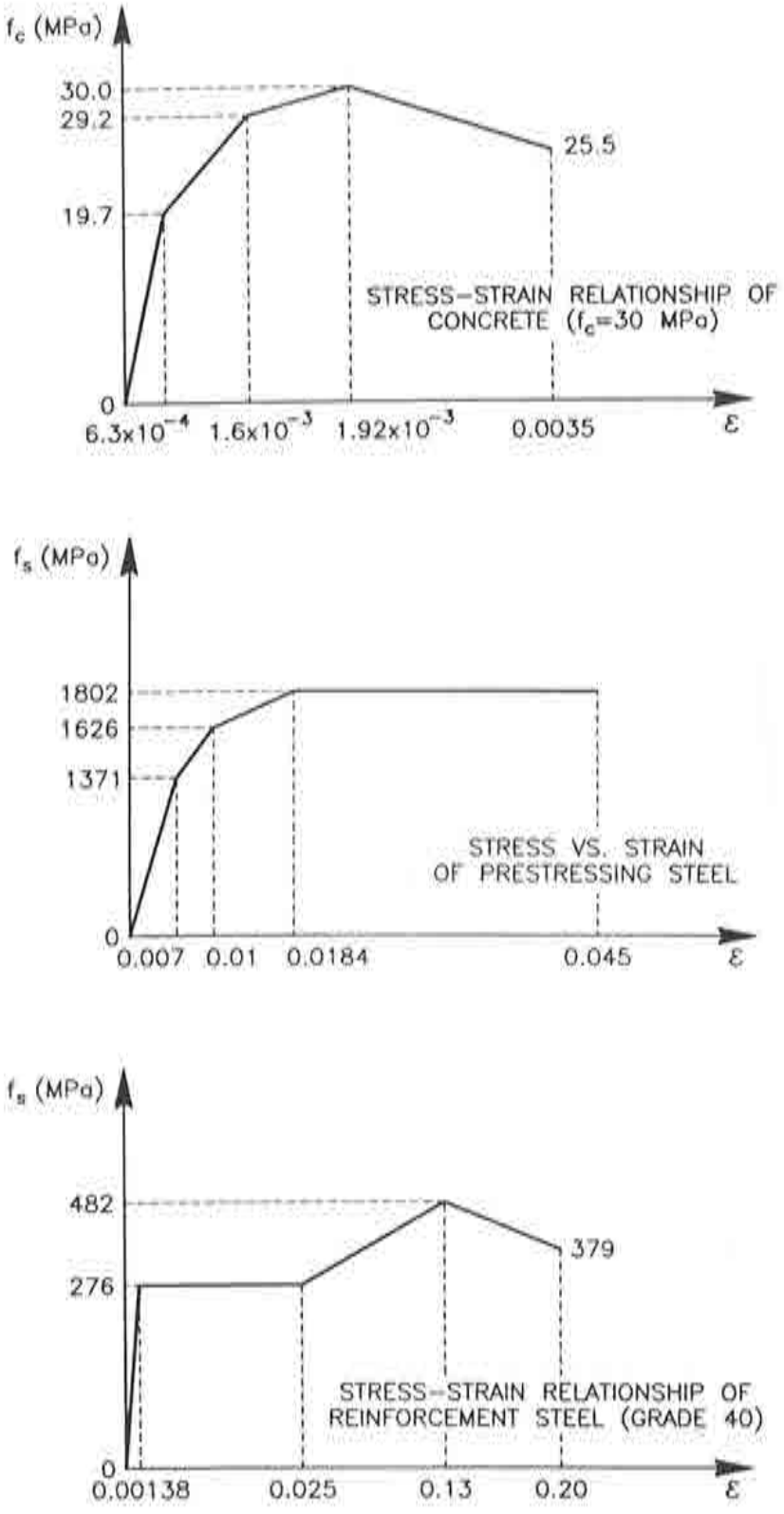

Figure 2.5. Typical stress–strain curves for concrete, reinforcing steel and prestressing steel

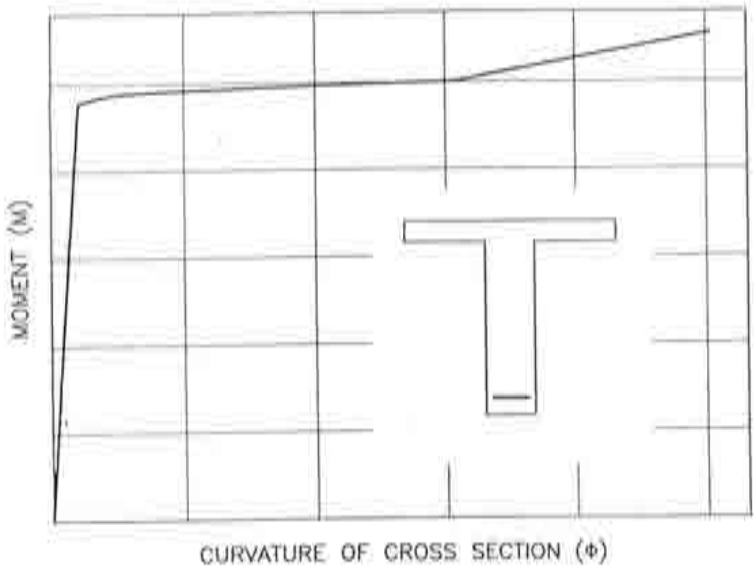

Figure 2.6. Example of moment versus curvature plot for a typical reinforced concrete section

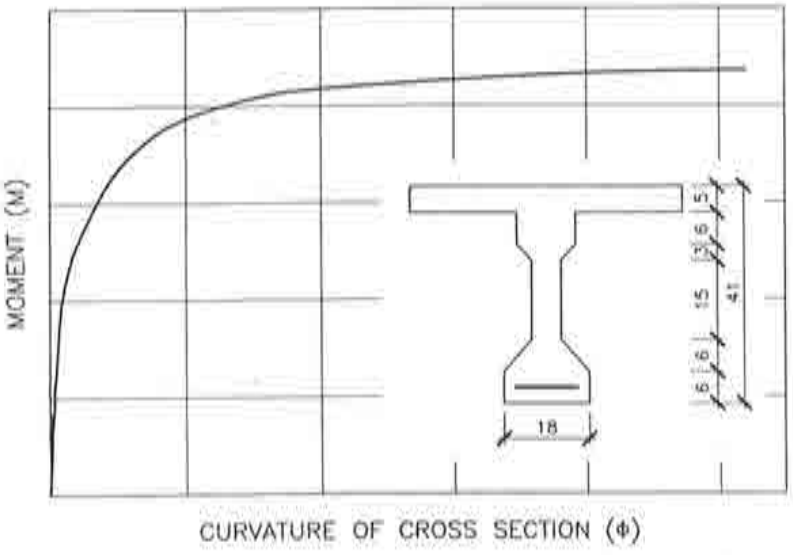

Figure 2.7. Example of moment versus curvature plot for a prestressed concrete section

at which point member failure will occur. Unloading will occur suddenly once this maximum plastic hinge rotation value is reached. It was observed that the maximum plastic hinge rotation that a section can sustain is a function of the section geometry, the reinforcement ratio and the level of lateral confinement [36].
Several methods have been proposed to estimate this maximum plastic hinge rotation. For example, Naaman proposed an empirical formula that gives the maximum plastic

hinge rotation in function of the distance to the centroid of the reinforcing steel, the plastic hinge length and the reinforcing index [37]. His equation was obtained by fitting a curve through analytically derived data points. His proposed equation is valid for reinforced, prestressed or partially prestressed concrete members and is given by:

$$\theta_{p\ max} = \frac{1.05 - 1.65\ W}{1300W - 40} \frac{L_p}{\frac{d}{2}} \tag{2.16}$$

where L_p is the length of the plastic hinge, d is the effective depth of the section and W is the reinforcing index which gives the ratio of the forces in the reinforcing steel to those in the concrete:

$$W = \frac{A_{ps}\ f_{ps} + A_s\ f_s + A'_s\ f'_s}{bdf'_c} \tag{2.17}$$

f_{ps} is the tensile stress in prestressing steel at the nominal ultimate moment capacity, f_s is the tensile stress in non–prestressed tensile steel, f'_s is the compressive stress in steel, f'_c is the compressive strength of concrete. A_{ps} is the cross sectional area of prestressed steel, A_s is the cross sectional area of non–prestressed steel and A'_s is the area of compression steel. b is the width of flange or web width of rectangular sections. d is the distance from extreme compression fiber to centroid of tensile force in steel.
The length of the plastic hinge can be estimated based on empirical formulas. For example, reference [36] proposes the following equation:

$$\begin{aligned} &\text{For unconfined concrete} \quad L_p = k_1\ k_2\ k_3\ (z/d)^{1/4}\ d \\ &\text{For confined concrete} \quad\ L_p = 0.8\ k_1\ k_3\ (z/d)\ c \end{aligned} \tag{2.18}$$

where k_1, k_2 and k_3 are constants reflecting the type of steel used, the level of axial load and the strength of concrete respectively. z is the distance of critical section to the point of contra–flexure. d is the effective depth of the member and c is the neutral axis depth at the ultimate moment of the member [36]. Naaman [37] showed that equation (2.16) gives a lower bound when compared to the experimental results of Mattock given in reference [38].

Moment Rotation Curves for Concrete Members

For the purposes of this study, the nonlinear behaviour of concrete members under bending is modeled following these steps:

1. Moment versus curvature relationships are plotted for every concrete section using the principle of equilibrium depending on each section's geometry and the stress–strain relationships of the concrete, reinforcing steel and/or prestressing steel.
2. Given the moment–curvature plots, moment versus plastic rotation curves are obtained using equations 2.15 and 2.18.
3. Equation 2.16 is used to determine the maximum plastic hinge rotation that each section can sustain. When the plastic hinge rotation of a section reaches this

maximum value, the section is assumed to fracture and will not be able to carry load and unloading occurs.

Shear Nonlinearity

In addition to nonlinearity under bending, concrete members exhibit nonlinear behavior due to shear. Shear behavior, however, is very difficult to model. Experimental results on the behavior of concrete members under shear show extremely wide scatter and the models available for predicting the ultimate shear capacity are extremely unreliable [36,39,40]. Although bridge field tests and model tests have shown that shear failures in bridges under high loads are not usual, modeling the shear transfer mechanism seems to be an important factor for the analysis of concrete box–gider bridges [41]. In this study, modeling the shear behavior of concrete members uses a multilinear shear deformation curve as proposed in reference [41] (see Figure 2.2). When the beam is still in the linear elastic range, the initial shear stiffness is given as:

$$K_{V0} = G\, A_V \tag{2.19}$$

where G is the shear modulus and A_V is the shear area. This is the slope of the first segment of the shear deformation curve. In this range, the shear forces are assumed to be mostly carried by the concrete and the longitudinal reinforcing steel. The slope remains constant until the concrete cracks at a load V_{cr}. If no shear reinforcement is provided, the member will fail at that load level. V_{cr} can be calculated using the empirical equation proposed by Zsutty [42] (see also reference [36]) by:

$$V_{cr} = 59 \left(\frac{f'_c\, \rho_w\, d}{a} \right)^{1/3} b_w\, d \tag{2.20}$$

where f'_c is the concrete compressive strength in psi, ρ_w is the flexural shear reinforcement to shear area ratio and a/d is the shear span ratio. b_w is the web width and d is the effective depth.
If shear reinforcement is provided, it would produce additional strength and the ultimate shear capacity would be due to a combination of the concrete strength and the strength due to the vertical shear reinforcing bars. The slope of the shear–shear deformation curve above the cracking level can be obtained using the equation derived by Park and Pauley [36] which is given as:

$$K_{vt} = \frac{\rho_v}{1 + 4\, n\, \rho_v} E_s\, b_w\, d \tag{2.21}$$

where E_s is the elastic modulus of the reinforcing steel, b_w is the web thickness, d is the effective depth, and ρ_v is the shear steel reinforcement ratio. n is the modulus ratio.
Ultimate shear capacity is normally calculated by summing the capacity at cracking V_{cr} to the capacity of the reinforcing steel V_s such that:

$$V_u = V_{cr} + V_s \tag{2.22}$$

where V_s is equal to:

$$V_s = \frac{A_t \, f_y \, d}{s} \tag{2.23}$$

A_t is the area of shear reinforcement within a distance s, f_y is the yield stress of steel, d is the effective depth of the section.
This model and similar models are widely used throughout the world although they are known to vastly underpredict the true shear capacity. This is because they ignore many of the physical phenomena that help provide additional shear capacity such as arch action, aggregate interlock etc. [39,40]. Many researchers are trying to develop better models based on the theory of fracture mechanics. These models however require further refinement before they can be used in actual practice [43].

2.3.2 Ductility of Steel Members

Considerable research on the inelastic behavior and the ductility of steel and composite bridge members took place since the mid–1960's. Observations made by researchers in this field are summarized by Maheu [44].
As reported in reference [44], experimental results showed that composite sections provide large shape factors (M_p/M_y) on the order of 1.5, while it is about 1.15 for naked steel sections. Failure of composite sections with relatively deep slabs was marked by crushing of the slab only after considerable strain hardening had occurred in the bottom flange of the beams. However, for sections where the plastic neutral axis is located in the steel section, the ultimate moment may not be reached since the concrete may crush before the steel section could yield throughout. Therefore the location of the plastic neutral axis is an important factor in determining both the capacity and the ductility of a composite section. Based on his literature survey, Maheu [44] also observed that a minimum number of connectors is needed to reach the maximum moment but beyond that, additional connectors did not contribute to the moment capacity.
Maheu [44] also reports that for negative bending, failure was usually caused by local buckling at the point of maximum negative moment; this was dependent on the slenderness of the flange and the web. Therefore, slenderness limits for compact sections and bracing requirements are important to prevent local buckling during plastic rotations. It was also observed that beams made of high strength steels, low strength concrete and thin slabs tended to lack ductility.
Schilling [45] summarizes the results of experimental studies on steel ductilities. These studies resulted in a number of moment–rotation curves that give the relationship between the applied moment and the plastic rotation of simple and continuous steel beams. Schilling's curves give the total plastic rotation over the finite length in which yielding occurs. Thus, the total plastic rotation is assumed to be concentrated in a small region representing an angular discontinuity, and the rest of the girder is otherwise assumed to be elastic. The curves that Schilling proposed were derived from experimental data which account for: Steel yielding including the effect of residual stresses; the spread of the yielding along the length as the loading progresses; cracking or local crushing of the slab; permanent distortion of the cross sectional shape; and

any other factors that cause permanent rotations. Different curves are proposed to cover composite and non–composite, compact and non–compact sections in positive and negative bending. The curves proposed by Schilling and discussed in this section are used in conjunction with the program *NONBAN* to perform the inelastic analysis of typical steel bridges.

Positive Bending of Composite Sections

The moment rotation curve for positive bending sections is given in Figure 2.8.a. The ordinate gives the ratio of the applied moment to the plastic moment M_p. Yielding begins at a moment level equal to 0.2 M_p due to the presence of residual stresses. The moment rotation curve reaches Mp at a plastic rotation of 15 milli–radians and is assumed to remain constant at M_p thereafter. Unloading occurs at such a very high rotation level that it can be ignored. Schilling [45] observed that the slab normally provides sufficient support to the compression flange to prevent premature unloading due to local or lateral buckling. Therefore, this curve applies for both compact and non–compact sections. The inelastic behavior is mainly due to concrete crushing at shear studs and yielding of the steel.

Positive Bending of Non–Composite Sections

For non–composite sections in positive bending, Schilling recommends to use the curve shown in Figure 2.8.b. The same curve is appropriate for both compact and non–compact, non–composite sections in positive bending. This is based on the assumption that the slab provides sufficient support to the compression flange to prevent premature unloading due to local or lateral buckling even if the section is not composite. This assumption is consistent with the new proposed AASHTO LRFD specifications [9] as well as the AASHTO ASD method [46]. The inelastic rotations result from the residual stresses in the steel. The maximum plastic hinge rotation that the section can take is 63 mrad (0.063 rad). Beyond this point, the section unloads and instability occurs.

Negative Bending of Compact Sections

Schilling assumes that all sections in negative bending act as non–composite sections. The effect of the steel reinforcement in the deck is ignored even if shear studs connect the steel beams to the deck in the negative bending region. The same curve used for positive bending of non–composite sections shown in Figure 2.8.b is therefore used for compact sections in negative bending.

Negative Bending of Non–Compact Sections

If the section in the negative bending region is non–compact it will not be able to reach its full plastic capacity because of local and lateral buckling. Nonlinear behavior starts at a load level equal to 0.7 M_y due to residual stresses. As soon as the moment reaches the yield capacity of the section, it becomes unstable and starts to unload. Schilling observed that this will occur at a plastic rotation roughly equal to 5 mrad. Unloading

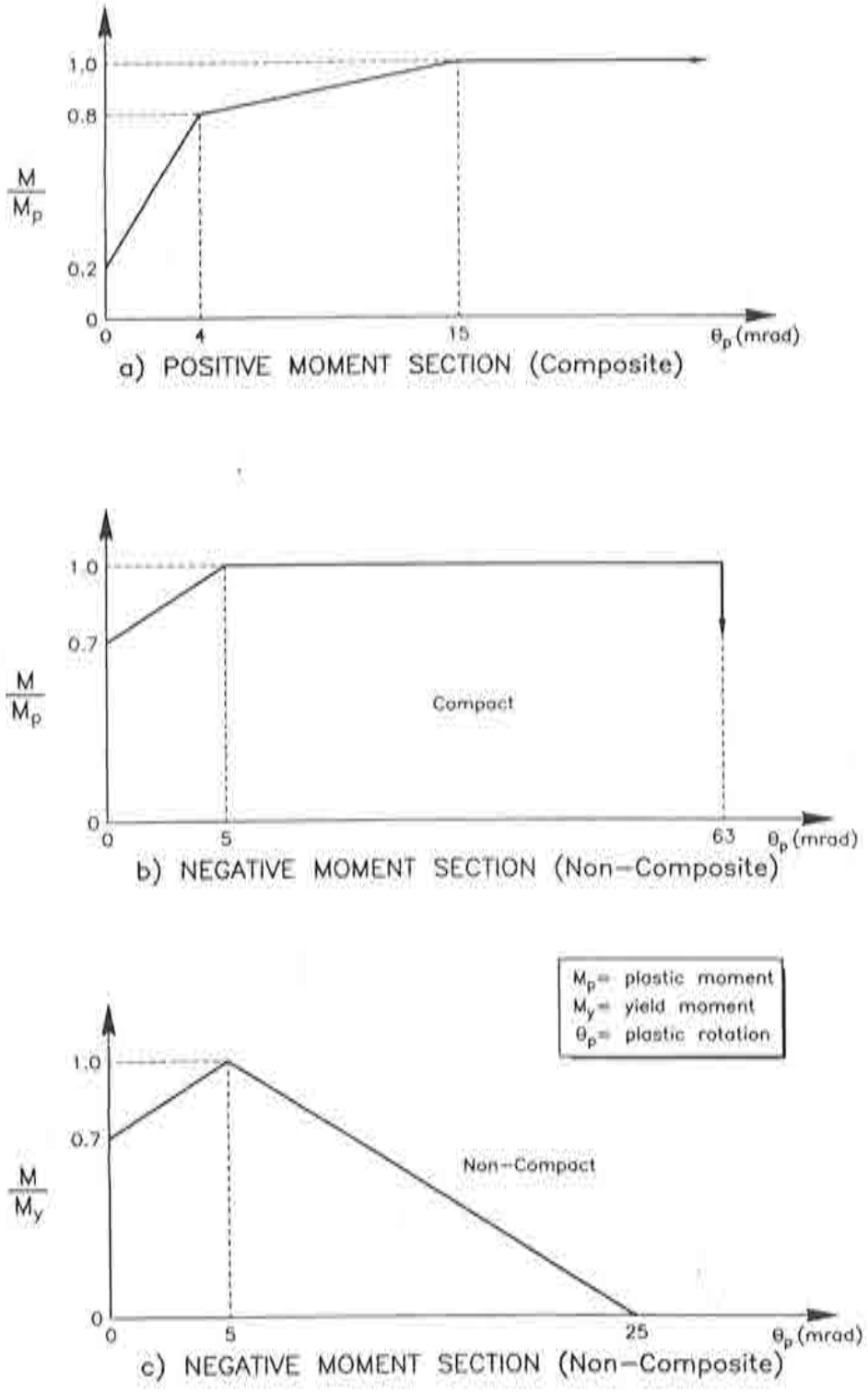

Figure 2.8. Moment rotation curves for steel members

will continue until the plastic rotation reaches a value of 25 mrad where all load–carrying capacity of the section is lost. This behavior is modeled as shown in Figure 2.8.c.

2.4 Nonlinear Analysis of Beam Models in Bending

To verify the validity of the approach proposed in this study for the analysis of bridge structures, several comparisons between published experimental results and the results of *NONBAN* were undertaken. For example, Rabbat *et al.* [47] performed an extensive experimental investigation to determine the behavior and strength of prestressed concrete girders with draped and blanketed strands after subjecting them to repetitive loading. The girders were then tested to destruction under static load. Rabbat *et al.* observed that the ultimate strength capacity was not affected by the cyclic loading if the repetitive loading did not cause cracking in the concrete. This was true for both the blanketed and the draped specimens. Plots showing the applied load versus maximum deflection for the static tests were given in reference [47]. The dimensions and material properties of the specimens were also given. Specimen G14 with blanketed strands was chosen for this comparison. Figure 2.9 compares the test results obtained by Rabbat *et al.* to the results obtained using *NONBAN*. The comparison shows good agreement for the whole range of behavior including the determination of the failure point.

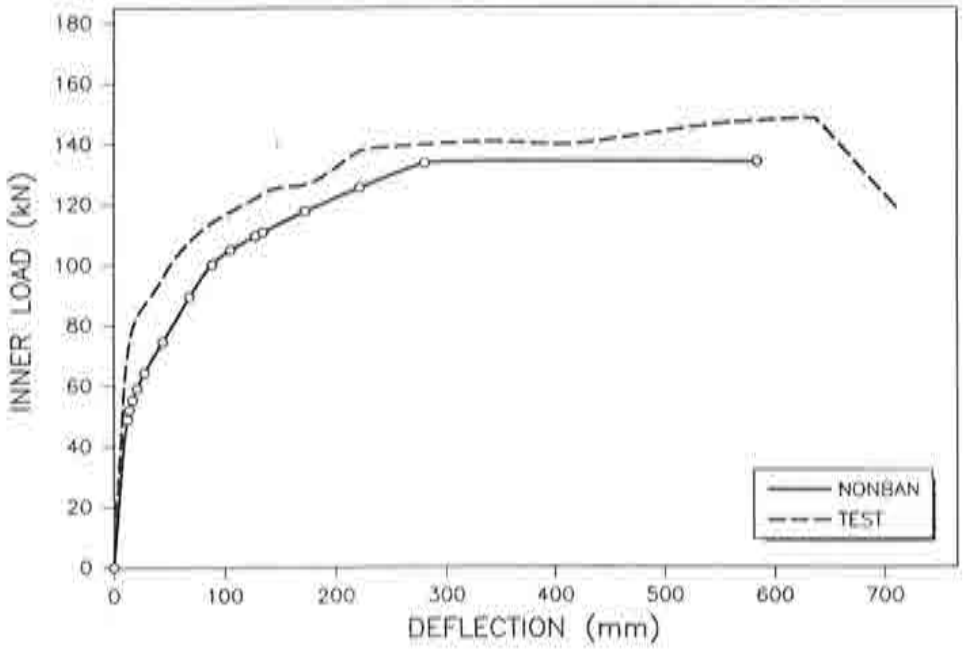

Figure 2.9. Comparison between prestressed beam test (Rabbat *et al.)* and *NONBAN*

Hawkins, Sozen and Siess [48] give the results of 22 tests of two span continuous pretensioned prestressed concrete beams. They plotted load deflection curves for two tested specimens. The two specimens were quite similar except for the amount of longitudinal steel reinforcement. The behavior of the specimens under static load tests was monitored until failure. Figure 2.10 shows a comparison between the results given

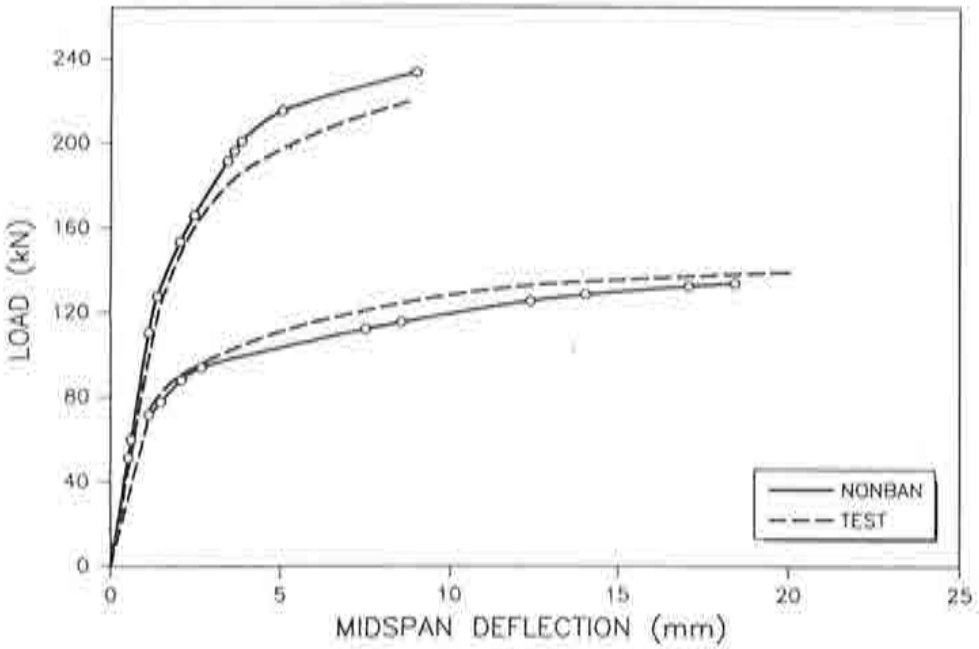

Figure 2.10. Comparison between prestressed beam test (Hawkins *et al.*) and *NONBAN*

in reference [48] and the results obtained using *NONBAN*. Here again, good agreement is observed between the results including the determination of the failure point.

2.5 Nonlinear Analysis of Concrete Beam Models in Combined Bending and Shear

To test the validity of the approach proposed in section 2.3.1 to include shear effects in the analysis of concrete beams, the example published by López [49] is reanalyzed herein using the program *NONBAN*. López performed a nonlinear finite element analysis to predict the behavior of prestressed concrete bridge members under combined bending, torsion and shear. In one example, he compared the results he obtained for a prestressed concrete beam under combined bending and shear to experimental results obtained by Serrano [50]. *NONBAN* was run using the models proposed in section 2.3.1 to account for the nonlinear behavior of the beam. Figure 2.11 shows the cross section and the profile of the tested prestressed concrete beam. The material properties are also shown in Figure 2.11. Figure 2.12 shows a comparison between the results obtained by *NONBAN* and the experimental results obtained by Serrano [50] and the finite element results obtained by López [49]. The results indicate that the calculation of the cracking shear capacity as calculated in equation (2.20) is fairly accurate as are the slopes calculated from equation (2.21). On the other hand, the ultimate shear capacity as calculated from equations (2.22) and (2.23) is extremely conservative underpredicting the actual capacity by more than 40 percent.

A similar analysis is performed to compare the models proposed in this study to the experimental results performed by Serra and Marí at UPC [51]. The experimental results

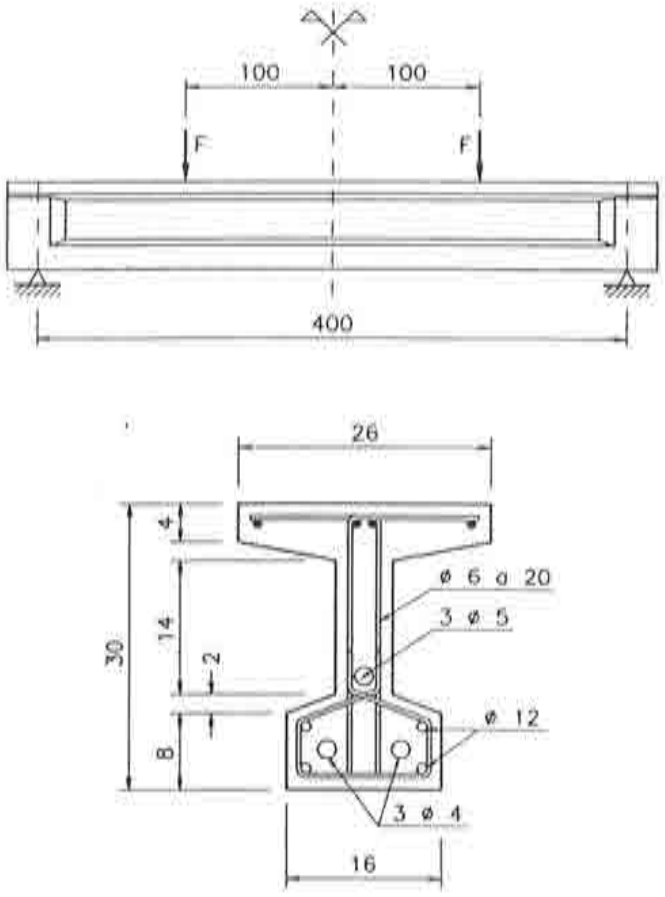

f_c = 45 MPa	A_l = 4.52 cm^2	f_t/s = 2.83 cm^2/m
f_{yl} = 457 MPa	A_p ø4 = 0.76 cm^2	ø4 f_{py} = 1690 MPa
f_{yt} = 474 MPa	A_p ø5 = 0.59 cm^2	ø5 f_{py} = 1510 MPa

Figure 2.11. Description of beam model analyzed by López

for a reinforced concrete beam under combined bending and shear are compared to the results of the program *NONBAN*. Once again, the loads causing flexural cracking as well as the loads causing shear cracking and the slope of the load–deflection curves obtained by *NONBAN* are very similar to the values obtained experimentally as seen in Figure 2.13. The ultimate failure load however predicted using equations (2.22) and (2.23) was

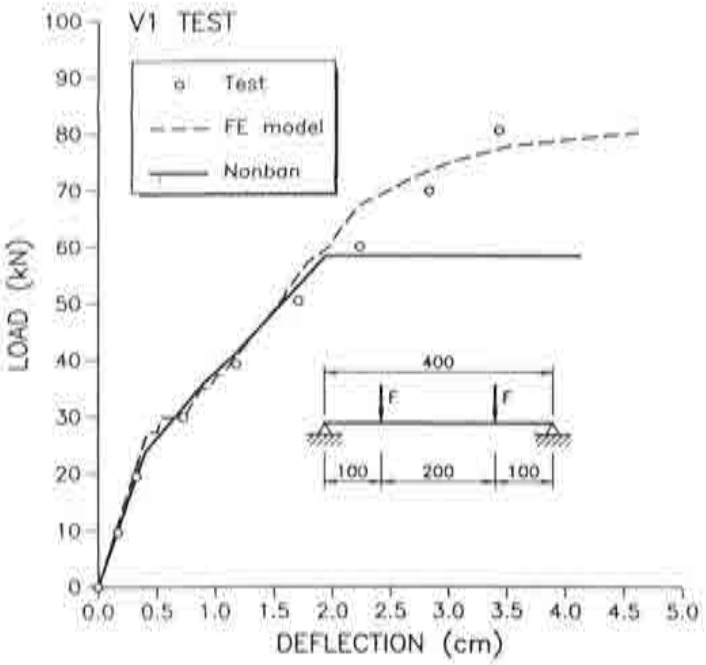

Figure 2.12. Comparison of results from FEM, *NONBAN* and test results

found to be much lower than the value measured experimentally the difference being on the order of 20 percent.
The observed "conservativeness" in the prediction of the ultimate shear capacity of concrete beams was highly expected. In fact, Park an Pauley [36] have shown that there is very wide scatter in the results of shear capacity tests and that the currently used shear strength models only provide lower bounds to these test results.

2.6 Analysis of Box Beams under Torsion

The program *NONBAN* is designed to model a bridge as a system of one dimensional beam elements. The program accounts for the torsional deformations of the beam elements in the linear elastic range using the torsional rigidity of each member represented by GI_x where G is the elastic shear modulus and I_x is the torsional inertia. This approach can be used for the analysis of slab on I–beam type bridges where the torsional inertia of the longitudinal beams is relatively small and does not significantly contribute to the lateral distribution of the load. For box bridges, where the torsional properties of the members are extremely important, Hambly [34] proposes a model that accurately accounts for the torsional capacity as well as the in–plane deformations of the boxes. The model, however, does not account for out–of–plane deformations such as those due to warping. The model proposed by Hambly can be summarized as follows:

1. To account for the flexural capacity of box girder bridges, each web of a box girder is assumed to act as a one dimensional beam element in the longitudinal direction

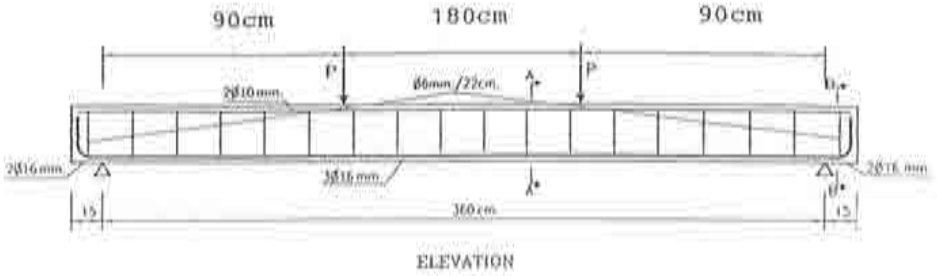

ELEVATION

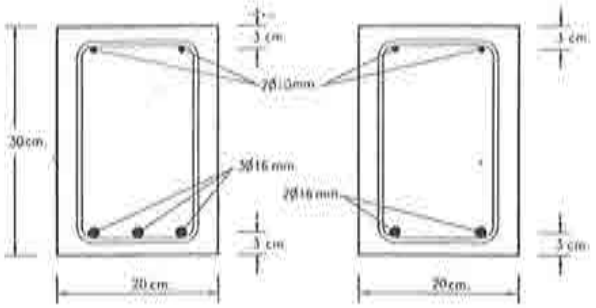

CROSS SECTION A CROSS SECTION B

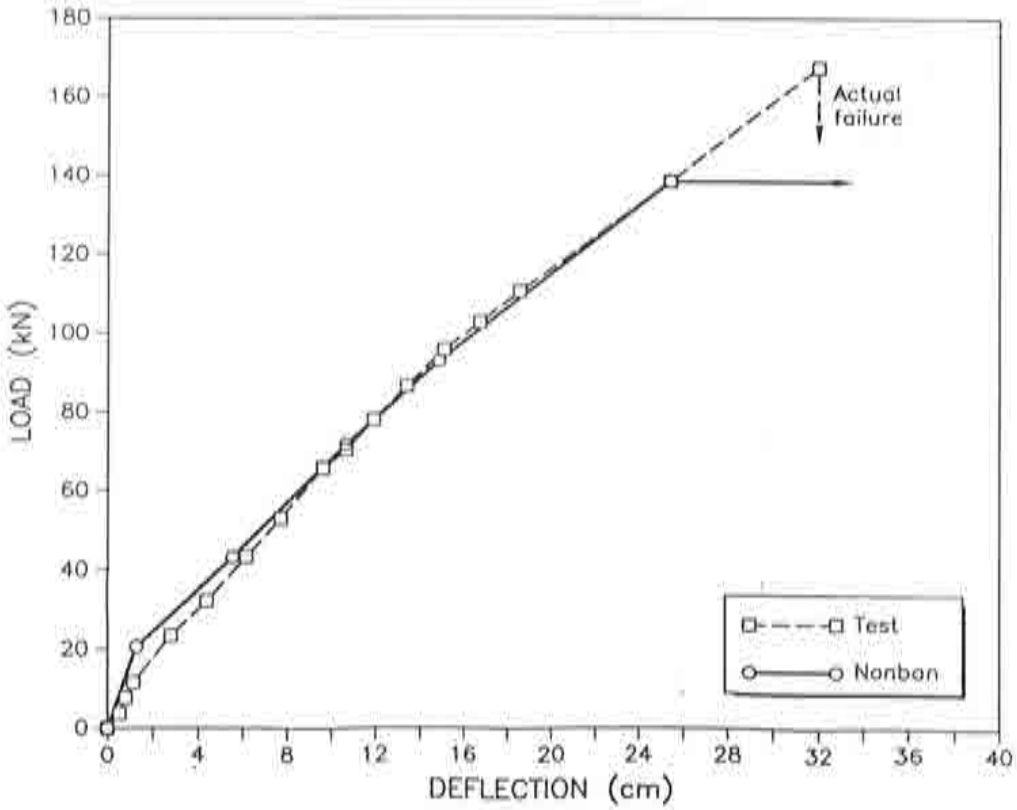

Figure 2.13. Comparison of *NONBAN* to Serras test

with a moment of inertia equal to $1/n$ of the total moment of inertia of the box. (where n is the number of webs). Another option involves the use of weighting factors where the weighting factors are functions of the location of the center of gravity of the whole girder and the tributary area of each web. Although more theoretically sound, Hambly suggests that the second option does not significantly improve the accuracy of the results.

2. To account for the torsional capacity of the box girder, the total torsional inertia of the box is divided to each longitudinal beam (representing the contribution of a web) and to the transverse beams (representing the contribution of the upper and lower flanges including the effect of the slab). Each web will carry $1/2n$ of the total torsional inertia and each transverse beam carries $s/2B$ of the total torsional inertia (where s is the spacing between the transverse beams and B is the total width of the box girder).
3. To account for the in–plane deformations of the cross section (or cross–sectional distortions), Hambly assumes that the flange of the box acts in the transverse direction as a shear beam. The moment of inertia of this transverse beam is calculated from the moment of inertia of the top flange (including the deck slab for composite box girders) and the bottom flange. The shear area of this transverse beam is calculated as a function of the capacity of the box to resist in–plane forces applied on the whole box.

The scheme proposed by Hambly ignores the effect of out–of–plane deformations such as warping effects etc. In fact, Soliman *et al.* [58] have shown that out–of–plane deformations are negligible for box girders with support diaphragms. Since normal bridge designs includes diaphragms at the supports, it is concluded that the out–of–plane deformations can be ignored without significantly affecting the results.

This modeling scheme is summarized in Figure 2.14. Hambly [34] proposed his method to model the linear elastic behavior of bridges using a grillage analysis. The nonlinear torsional behavior of structural members is extremely difficult to model because of the interaction between the torsional capacity with the shear and moment capacities of structural members [52]. It is herein assumed that for a bridge system, torsional loads will remain in the linear elastic range and that the nonlinear behavior of the bridge is only due to bending and shear. The validity of this assumption for the nonlinear analysis of box bridges is verified in sections 2.8 and 2.9 by comparing the results obtained by *NONBAN* using the Hambly modeling scheme to experimental and analytical results obtained by other researchers.

To test the applicability of Hambly's approach for the linear elastic analysis of boxes, an example taken from Calgaro J.A. and Virlogeux, M., [53] is analyzed. The properties of the box example and the applied loading are shown in Figure 2.15. The box is fixed at both ends and a uniformly distributed torsion is simulated by an antisymmetric distributed load applied on top of the webs. To solve this type of torsional problems, Calgaro and Virlogeux developed an analytical method based on the principles of equilibrium. The method they developed resulted in a differential equation similar to that obtained for beams on elastic foundations. Closed–form solutions were possible

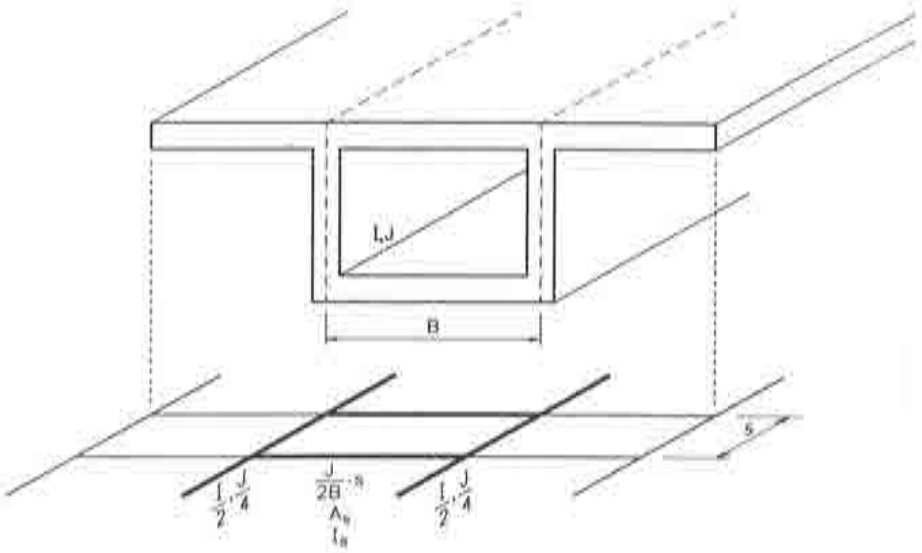

Figure 2.14. Summary of Hamblys modelling scheme for box girder

for simple boundary conditions such as simple supports or fixed supports similar to those used in the example shown in Figure 2.15. The model ignores the effect of web shear deformations as well as the effect of out–of–plane (e.g. warping) deformations. The beam properties used in the *NONBAN* analysis are shown in Figure 2.15. The results obtained from *NONBAN* are compared to the theoretical results obtained by Calgaro and Virlogeux in table 2.1. For example, using *NONBAN*, the maximum bending moment in a longitudinal member was found to be equal to 18.9 kN.m resulting in a maximum stress of 6.10 MPa. The maximum stress calculated theoretically was found to be equal to 6.27 MPa. On the other hand, the maximum deflection calculated theoretically was found to be equal to 1.49 10^{-5} m while the grillage analysis yielded a deflection of 1.77 10^{-5} m. Using concentrated point loads at the mid–span rather than the uniform loads over the full length, yielded a maximum displacement of 6.93 10^{-7} m using the theoretical approach of Calgaro while *NONBAN* yielded a maximum displacement equal to 7.0 10^{-7} m. Since the analytical approach proposed by Calgaro and Virlogeux does not account for out–plane deformations nor does it account for shear deformations in the webs of the boxes, so to be consistent with the latter assumption, *NONBAN* was used assuming infinitely large web shear areas. *NONBAN* does not account for out–of–plane deformations.

The modeling scheme proposed by Hambly was also tested by comparing the results of *NONBAN* to the results obtained by Seible for the linear elastic analysis of boxes under torsion. Two concrete boxes one with a base of 3 ft and the other with a base of 9 ft under loads producing high levels of torsions were analyzed by Seible and compared to previously published analytical results. The results obtained are summarized in Figure 2.16. For the 3 ft wide box, the model proposed by Hambly and used in *NONBAN* seems

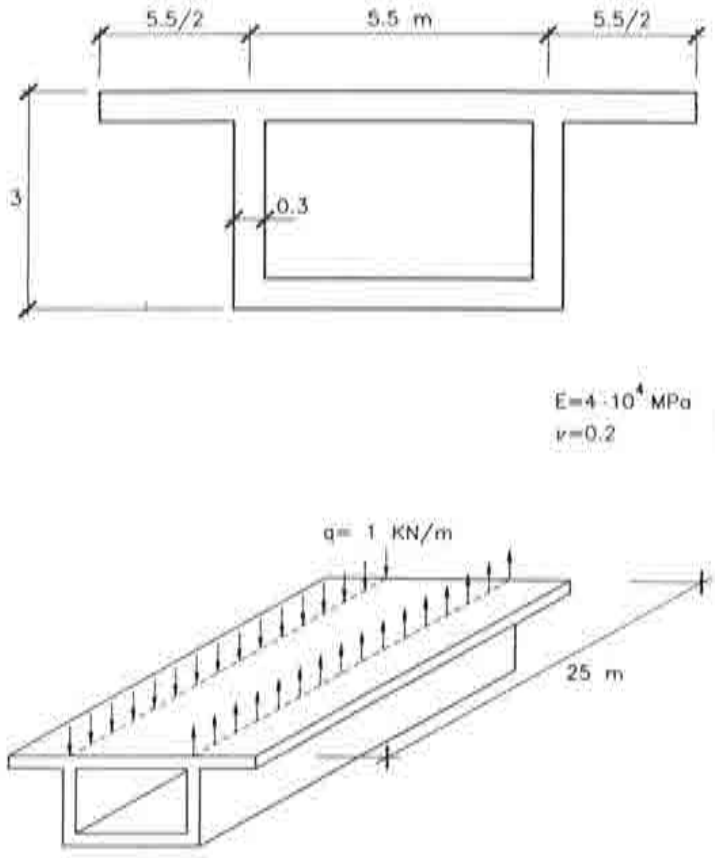

Figure 2.15. Properties of box beam analyzed by Calgaro *et al.*

Case	Calgaro *et al.*	*NONBAN*
Distributed load		
Max. Stress	6.27 MPa	6.10 MPa
Max. Displacement	1.49 E–5 m	1.77 E–5 m
Concentrated load		
Max. Displacement	6.93 E–7 m	7.00 E–7 m

Table 2.1. Comparison of Results of Calgaro *et al.* to *NONBAN*

to overpredict the maximum deflection when *NONBAN* includes the shear deformations in the webs. The maximum deflection obtained with *NONBAN* is 4.2 10^{-5} ft compared to 2.93 10^{-5} ft obtained by Seible. When the shear deformations are not included, then the maximum deflection calculated by *NONBAN* becomes 2.80 10^{-5} ft which is reasonably close to the results of Seible. On the other hand, as shown in Figure 2.16 for the box with the 9 ft base, Seible obtained a maximum deflection of 10.26 10^{-5} ft

compared to 8.70 10^{-5} ft with *NONBAN* including web shear deformations. For the case when the web shear deformations are not included, *NONBAN* produces a deflection of 5.93 10^{-5} ft The theoretical model of Calgaro and Virlogeux for the box with the 9 ft base produced a maximum deflection of 5.58 10^{-5} ft.

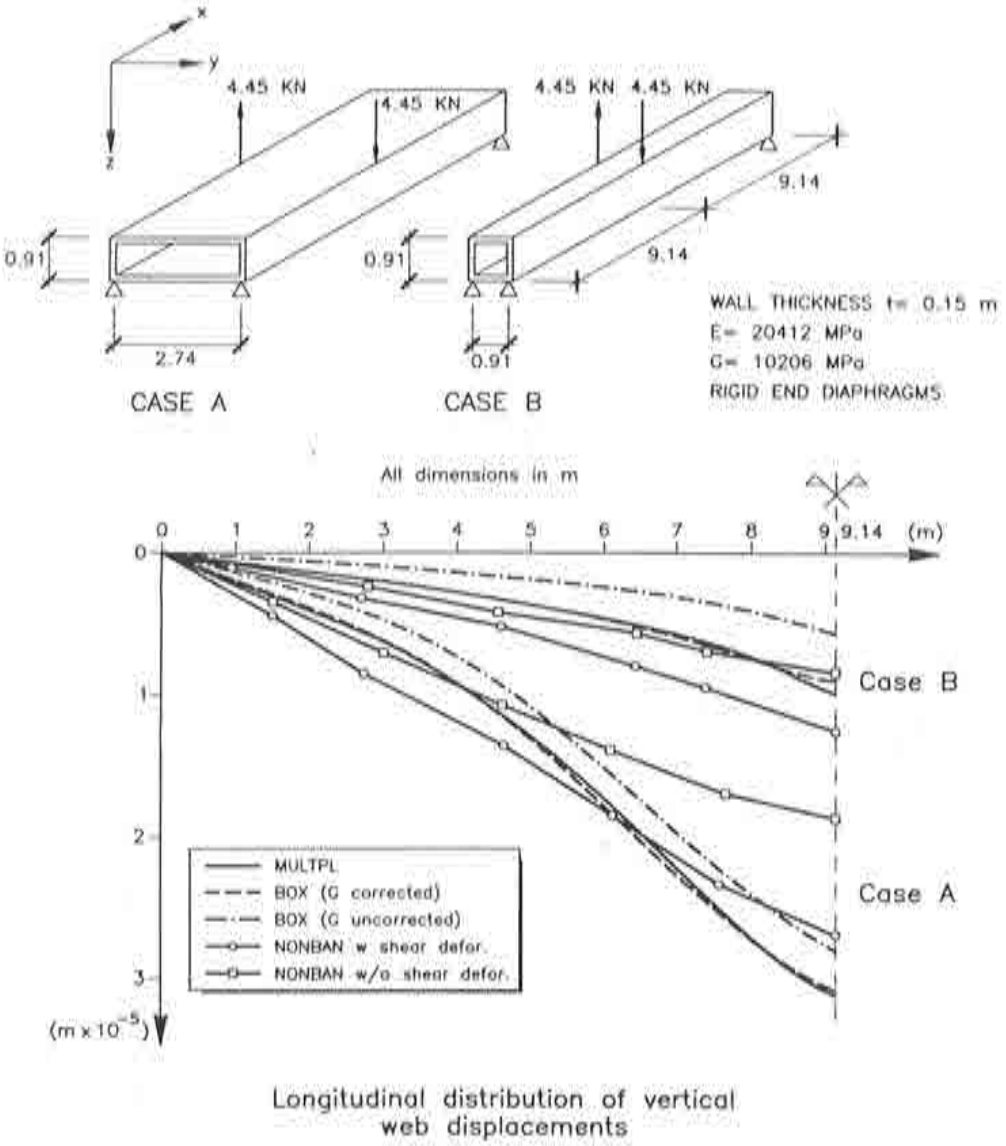

Figure 2.16. Comparison of *NONBAN* to torsion examples of Seible

The conclusion drawn from these examples indicate that:

1. The modeling scheme proposed by Hambly [34] produces deformations under high torsional loads similar to those obtained analytically by Calgaro *et al.* [53]. This ignores the effect of web shear and out-of-plane deformations such as the effect of warping.

2. The effect of warping and web shear deformations are negligible for torsionally rigid boxes under relatively small torsional loads such as the 3 ft box beam tested by Seible. Hence, Hambly's modeling scheme and Calgaro's analytical methods are valid.
3. Hambly's modeling scheme and Calgaro's method underpredict the deformations in box girders where warping is important under high torsional loads. This is because in such cases, the out-of-plane deformations and the web-shear deformations become more significant.

Since the torsional loads applied on bridge structures are not normally the dominant loading conditions and since the presence of diaphragms will reduce the effect of deformations due to warping, it is herein concluded that Hambly's modeling scheme is accurate enough to account for the correct load distribution of concrete box girder bridges. This assumption will be further verified in the examples analyzed in sections 2.8 and 2.9.

2.7 Nonlinear Analysis of Slab on I-Beam and T-Beam Bridges

To check the validity of the program *NONBAN* to analyze slab on I-beam bridges, the results of a composite steel I-beam bridge previously analyzed in the nonlinear range by other researchers are compared to those obtained by *NONBAN*. In addition, the published results of three full scale bridge field tests are compared to those obtained by *NONBAN*. The three full scale tests are for a reinforced concrete T-beam bridge, a prestressed concrete I-beam bridge and a non-composite steel I-beam bridge.

Comparison of *NONBAN* to Other Nonlinear Analysis Programs

The program *NONBAN* was tested by analyzing one of the bridges used by Maheu in a study for the Ontario Ministry of Transportation [44]. The bridge is a slab-on-girder steel structure composite in both the positive and negative bending regions. The five-girder two-lane bridge has two continuous spans of 13.8 m each. The bridge was modeled as a grid by Maheu [44] and the analysis was performed assuming elasto-plastic behavior of the longitudinal members *i.e.* no transverse hinges are included in the analysis. This assumption was based on the observation made by Maheu [44] that experimental tests have shown that deck slabs possess much greater strengths than their flexural resistances would suggest and thus failure of slabs in the transverse direction is unlikely. The steel sections were assumed to be compact and fully braced. The bridge was symmetrically loaded using four OHBDC vehicles as shown in Figure 2.17. The results of the analysis are presented in Figure 2.18. The figure shows the total applied live load versus maximum deflection. The dashed line gives the results as published in reference [44]; the solid line gives the results obtained using the program *NONBAN*. The comparison indicates that the post-elastic behavior obtained using *NONBAN* is very close to the curve obtained by Maheu.

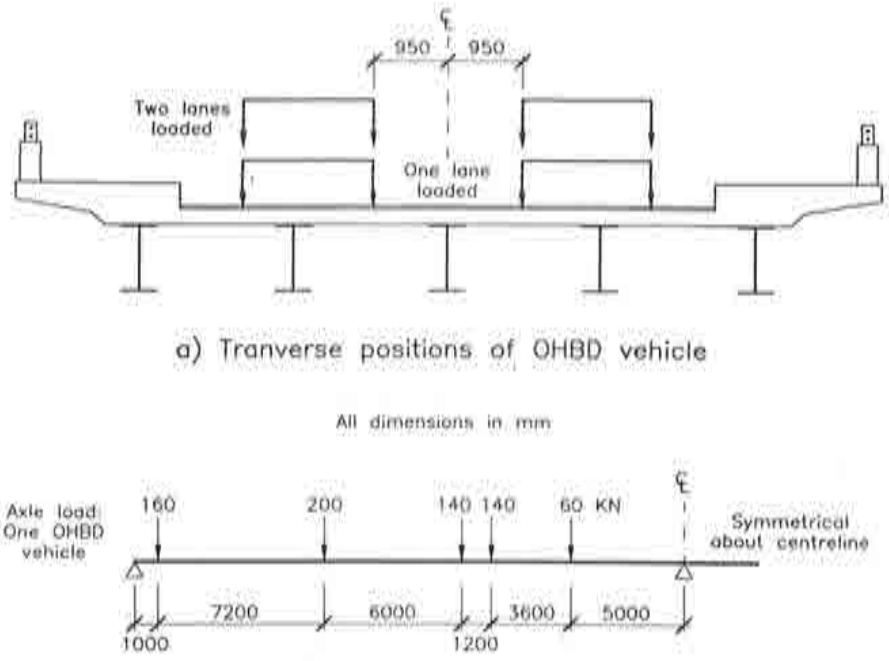

Figure 2.17. Loading and layout of bridge analyzed by Maheu

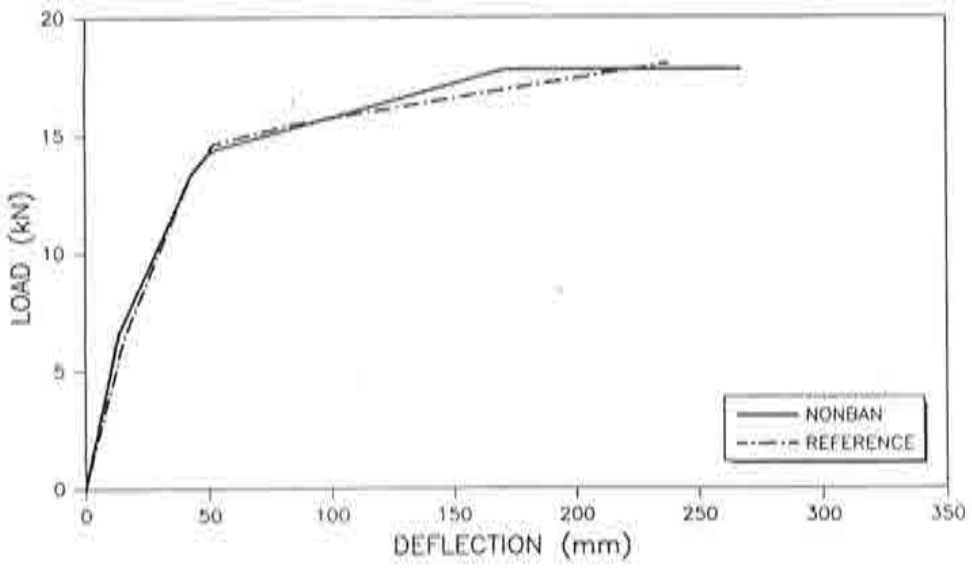

Figure 2.18. Comparison between results of Maheu and *NONBAN*

Comparison to full–scale Bridge Tests

Figure 2.19 gives the layout and the properties of the simply–supported reinforced concrete bridge tested by Buckle *et al.* [54]. During the test, the researchers observed

that the handrail on the bridge added to the capacity of the bridge as long as composite action between the handrail and the deck slab was maintained. At near-ultimate conditions, the curb separated from the slab and the contributions of the handrail to the bridge load capacity diminished rapidly. Although shear failures were observed in the deck, transverse load distribution continued. Only minor damage was observed in the diaphragm. The researchers also observed that compressive membrane action in the slab contributed significantly to the reserve strength of the bridge. Figure 2.20 gives a comparison between the results obtained in the field to those obtained from *NONBAN*. Reference [54] indicated that the ultimate bridge capacity was found to be 1480 kN although the maximum displacement for that load was not available, *NONBAN* produced a maximum load capacity of 1600 kN for a maximum deflection of about 130 mm. This constitutes a difference of about 8 percent in the estimation of the ultimate capacity. According to Buckle *et al.* (who also overestimated the ultimate capacity) the discrepancies between the test results and the analysis may be due to errors in estimating the material properties and also due to ignoring the possibility of damage to the bridge due to shear and torsional effects. The bridge when tested was quite old and the core samples used to estimate material properties showed high variability due to deterioration. This variability was ignored in the analysis. Nevertheless, the agreement with the test results were reasonably good given the simple models used in the analysis.

Bridge	Barkers bridge
Location	SH1, Warkworth
Date built	1940
Date tested	March 1981
Span(s) (m)	3.66, 12.80, 3.66 (12', 42', 12')
Beams	
Spacing (m)	4 at 2.03 (6' 8")
Section (mm)	762 × 330 (30" × 13")
Mid-span steel	5732 mm² (8.884 in.²)
Slab thickness (mm)	178 (7")
Width (m) (curb to curb)	7.32 (24' 0")
Diaphragm (mm)	Yes; 660 × 203 (26" × 8")

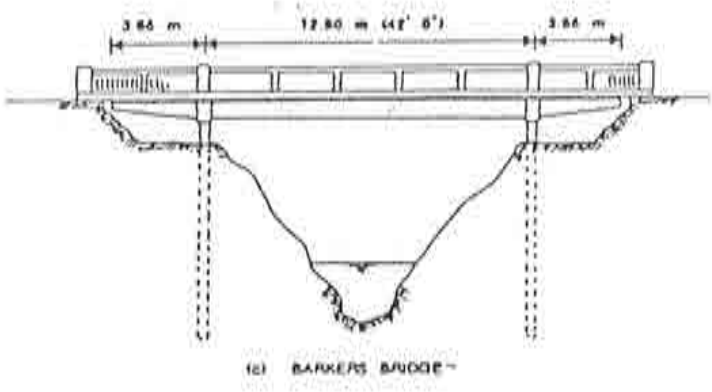

(a) BARKERS BRIDGE

Figure 2.19. Layout of bridge tested by Buckle

Figure 2.21 describes a simple span prestressed concrete bridge tested by Burdette and Goodpasture [55]. The bridge consists of four, type III AASHTO girders acting compositely with a 7 in. thick deck slab. The behavior of the bridge was monitored until failure. Overall behavior of the bridge was not affected by cracking of the diaphragm or

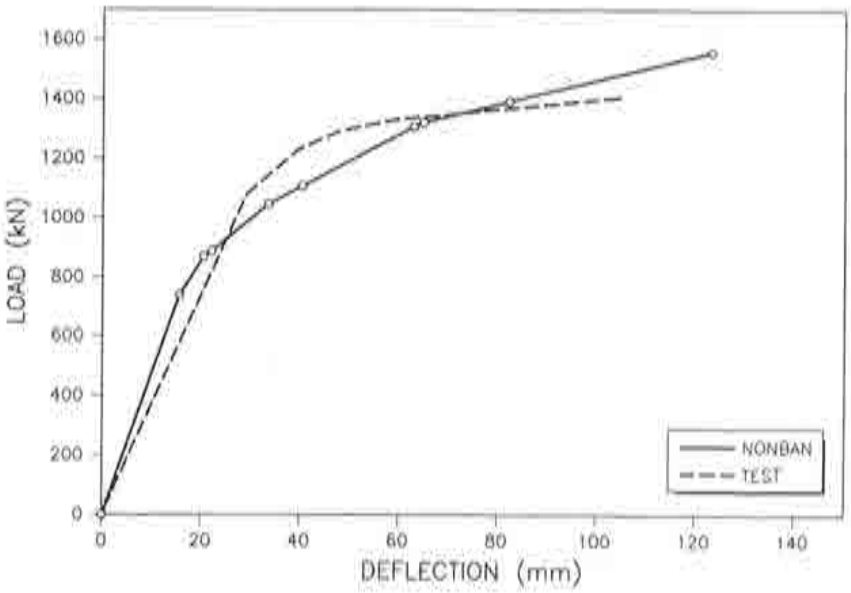

Figure 2.20. Comparison between results of Buckle and *NONBAN*

the interior girders. However, when the composite action between the deck and girder broke loose, crushing of the interior sections followed resulting in the redistribution of the load to the exterior girders. Failure occurred at a load of 1140 kips when the interior girders completely failed. Figure 2.22 gives a comparison between the results obtained using *NONBAN* and the field tests. The maximum load capacity was estimated to be 1190 kips and good agreement is observed for the whole range of behavior.

A two–lane non–composite steel girder bridge was also tested by Burdette and Goodpasture [55]. The three–span continuous bridge had four 27 in., rolled beams at 7 ft 4 in., center to center. The load versus deflection curve given in reference [55] is compared to the results of *NONBAN* in Figure 2.23. The agreement is quite good except for the slope of the linear elastic loading portion of the curve. In this region, Burdette and Goodpasture [55] observed considerable composite action which dissipated as the ultimate capacity is reached. The model used with *NONBAN* assumed non–composite behavior throughout the test range. The sequence of hinge formation observed using *NONBAN* followed the same pattern observed during the field test. *NONBAN* predicted that the peak load was reached when the maximum deflection was 27.3 in. The field test showed that the peak load was reached when the maximum deflection was 26.4 in. The difference between the maximum load capacity estimated by *NONBAN* and that measured in the field was less than 4 percent. The field test however, was continued beyond the peak load until the deflection reached 38.4 in.

2.8 Nonlinear Analysis of Box Girder Bridges

Another verification of the validity of the analysis approach proposed in this study has been performed by comparing the results obtained by *NONBAN* to the results of Choudhury and Scordelis [56]. These authors developed a finite element model to

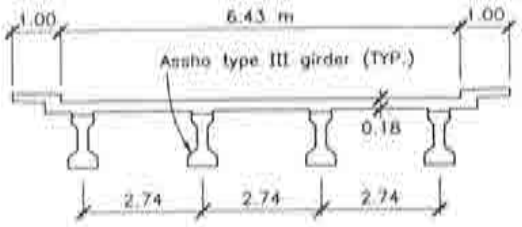

BRIDGE CROSS SECTION

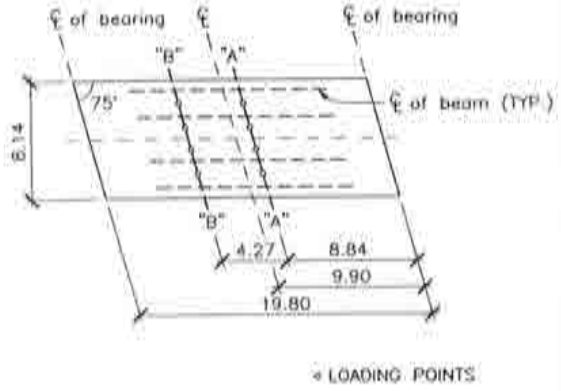

PLAN OF BRIDGE SHOWING POSITION OF LOADS

Figure 2.21. Layout of prestressed concrete bridge tested by Burdette & Goodpasture

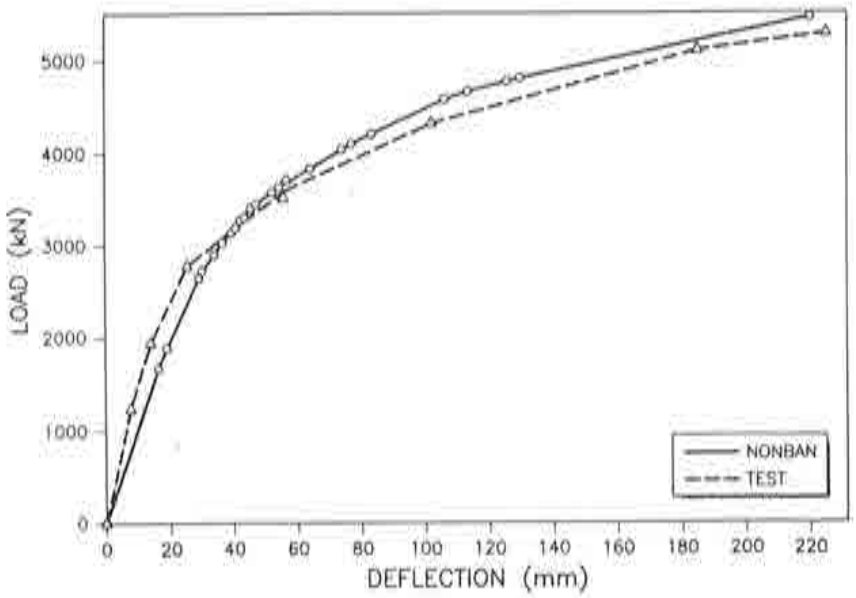

Figure 2.22. Comparison between results of Burdette and Goodpasture and *NONBAN*

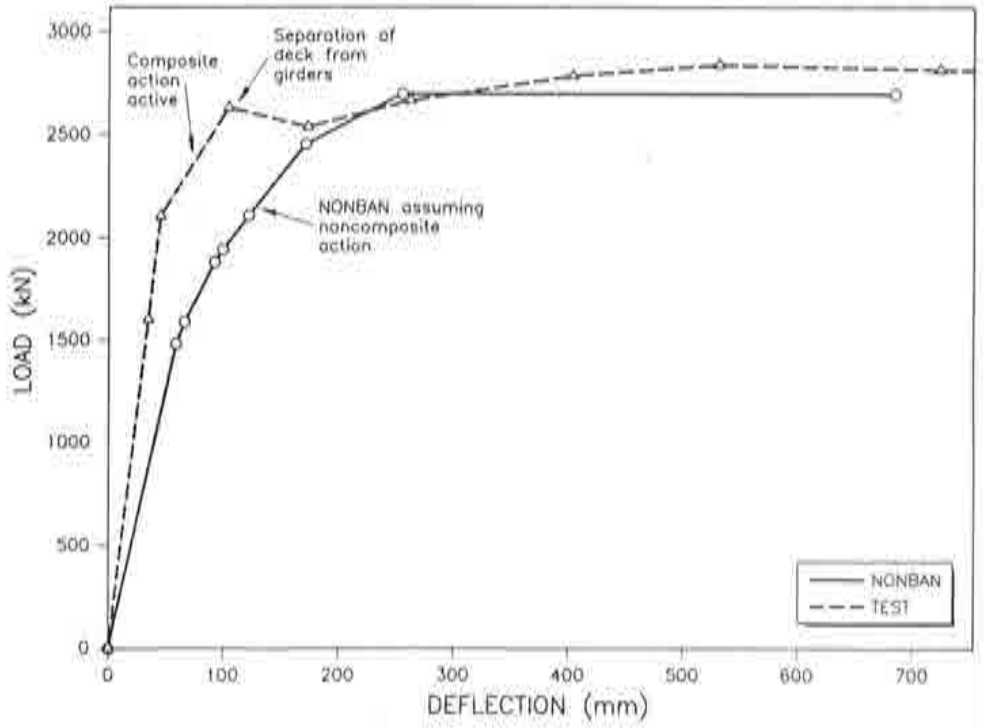

Figure 2.23. Comparison between steel bridge test and *NONBAN*

perform the nonlinear analysis of box girder configurations. Although their program was tested in the linear elastic range against experimental results, it was not tested in the nonlinear range because of the "inavailability of experimental data". They used their program to study the behavior of one example bridge under Cal Trans special permit vehicles [56]. The bridge is a unicell, three–span (160', 200', 160') continuous prestressed concrete curved box girder bridge designed to satisfy AASHTO's HS–20 and Cal–Trans requirements. The bridge geometry and material properties are as shown in Figure 2.24. For this example, the bridge model and member properties used with *NONBAN* follow the scheme outlined by Hambly [34]. The *NONBAN* input data is as shown in Table 2.2. In this example, it was assumed that material nonlinearities are only due to flexure. Also, to simplify the input data preparation, the moment versus rotation curves for each section was assumed to be bilinear *i.e.* elasto–plastic behavior of the members was assumed. Shear deformations are included in the *NONBAN* analysis but the shear is assumed to remain in the linear elastic range. The results obtained from *NONBAN* are compared to the analytical results of Choudhury as shown in Figure 2.25. The results show good agreement between *NONBAN* and the published results. As expected, the curve produced with *NONBAN* is somewhat stiffer than the published curve because of the simplifications used in developing the moment–rotation curves used in *NONBAN*. *i.e.* the fact of using bilinear moment–rotation curves. *NONBAN* somewhat underpredicts the ultimate load due to possible overestimation in the dead

load and also due to minor changes in the loading conditions. (Figure 2.24 shows the loading condition used in referene [56] and that used with *NONBAN*). The results of this example emphasize that even with a rough approximation of the moment rotation curves, *NONBAN* produces reasonably good agreement with the results of specialized finite element programs for the nonlinear analysis of box girder bridges. It should be noted herein, that if shear failure was included in the analysis, the ultimate capacity of the bridge would have been highly underpredicted. This is because the currently used shear strength models of equation 2.22 underpredict the shear capacity of the webs. This would have predicted a load factor at ultimate of only 1.2 rather than the value of 5.6 predicted in reference [56].

Concrete	Reinforcing Steel		Prestressing steel
	Longitudinal	Transverse	
$f_c'' = 4{,}000$ psi $E_{ci} = 3.605 \times 10^6$ psi $f_1 = 500$ psi $\epsilon_{cu} = 0.004$ $\beta = 0.85$ $\nu = 0.20$ $\tau_{cr} = 190$ psi $\beta_1 = 0.85$	$f_y = 60$ ksi $E_{s1} = 29{,}000$ ksi $E_{s2} = 0$ $\epsilon_{su} = 0.03$	$f_{yt} = 60$ ksi $E_{st} = 29{,}000$ ksi	$\epsilon_1 = 0.00715$; $\sigma_1 = 196.6$ ksi $\epsilon_2 = 0.00900$; $\sigma_2 = 220.0$ ksi $\epsilon_3 = 0.01150$; $\sigma_3 = 240.0$ ksi $\epsilon_4 = 0.01350$; $\sigma_4 = 245.0$ ksi $\epsilon_5 = 0.05800$; $\sigma_5 = 270.0$ ksi $E_p = 27{,}500$ ksi
Anchorage slip each jacking end :	$\Delta_a = 0.25$ in.		
Wobble friction coefficient :	$K = 0.0002$/ft		
Curvature friction coefficient :	$\mu = 0.25$/radian		
Unit weight of composite structure :	$w = 155$ pcf		
Tension stiffening coefficient :	$k' = 0$		

Table 2.2. Material Properties of Box Girder Bridge

2.9 Nonlinear Analysis of Multi–Cell Box Bridges

To test the validity of *NONBAN* and the approach proposed by Hambly [34] for modeling the behavior of multi–cell box bridges, the results of a model bridge tested by Scordelis *et al.* [57] and analyzed by Seible [41] are compared to the results obtained using *NONBAN*. The bridge model is a reinforced concrete continuous (two spans) four–cell bridge. The bridge was symmetrically loaded with two point loads in each span.
The bridge geometry is as shown in Figure 2.26. Figure 2.27 shows the discretization used by Seible and gives the section properties and the reinforcement of each element. In the *NONBAN* analysis the bridge model was discretized as done by Seible except for the element at the mid–support (No. 11) which was divided into two elements to better model the high flexural and shear rigidities of the support conditions. The moment versus rotation relationships for each element were obtained separately for positive and negative bending depending on the amount of reinforcement. The results obtained for this case are compared to those obtained by Seible (Nobox) and to the experimental results in Figure 2.28. It is observed that a very good match between the results is obtained for this bridge with the model used. It should be noted, however, that the

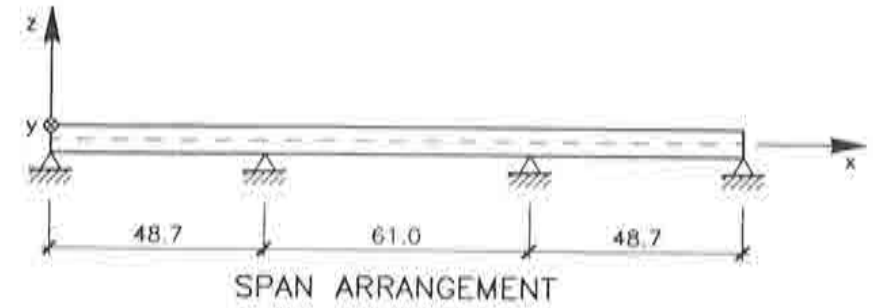

SPAN ARRANGEMENT

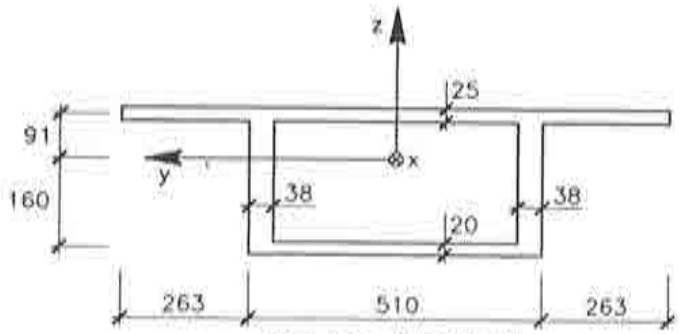

CROSS SECTION

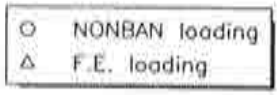

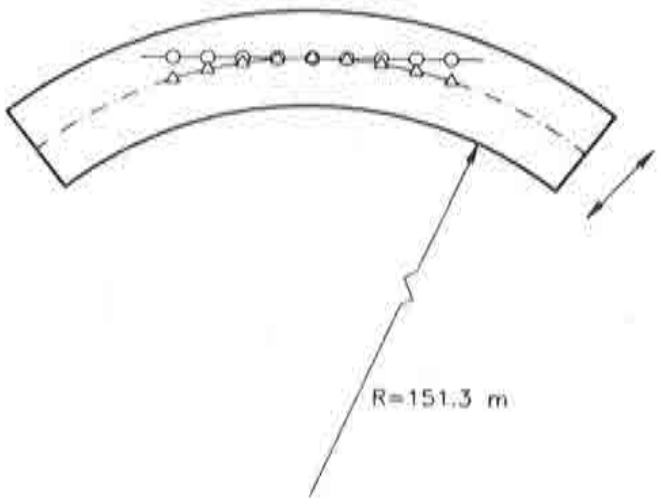

Figure 2.24. Properties of box girder bridge

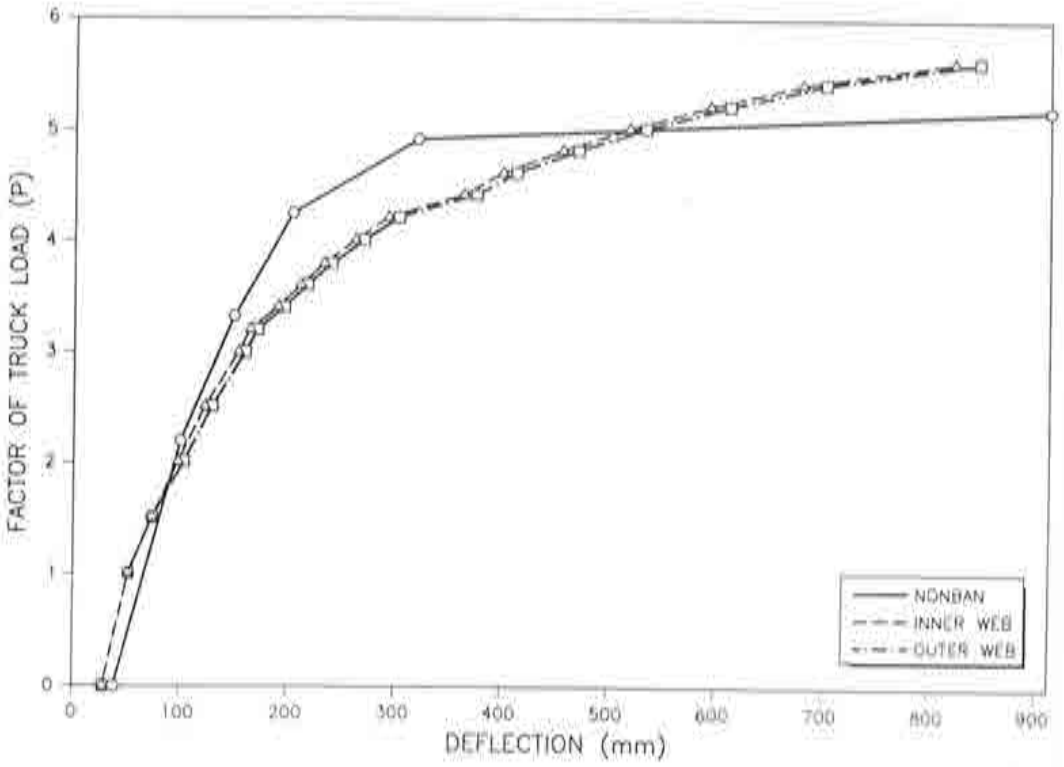

Figure 2.25. Comparison between *NONBAN* and FE analysis of box girder bridge

results of *NONBAN* seem to be quite sensitive to the assumed length of the plastic hinge L_p used while deriving the moment versus rotation curves. This sensitivity is believed to be caused by the scale effect due to the relatively deep thickness of the box compared to the total length of the bridge model and the length of the elements. Based on a sensitivity analysis performed as part of the analysis of this bridge, it appears that using moment versus rotation curves with an L_p value obtained from equation 2.18 provides the best results with the additional condition that L_p be always less than 1/2 the length of the element. It should also be noted that here again using equation 2.22 to check the shear ultimate capacity of the bridge model would have underpredicted the observed failure load by about 50 percent.

2.10 Conclusions

This chapter developed a simple technique to study the nonlinear behavior of bridges using a grillage discretization based on the approach proposed by Hambly. The method developed is valid for steel and concrete (prestressed and reinforced) slab on I–beam bridges as well as box girder bridges. A nonlinear analysis program *NONBAN* was developed to perform such an analysis. Nonlinearity due to bending is accounted for by using moment versus plastic rotation curves. Multi–linear shear deformation curves are used to account for the effect of shear nonlinearities. Several comparisons between the

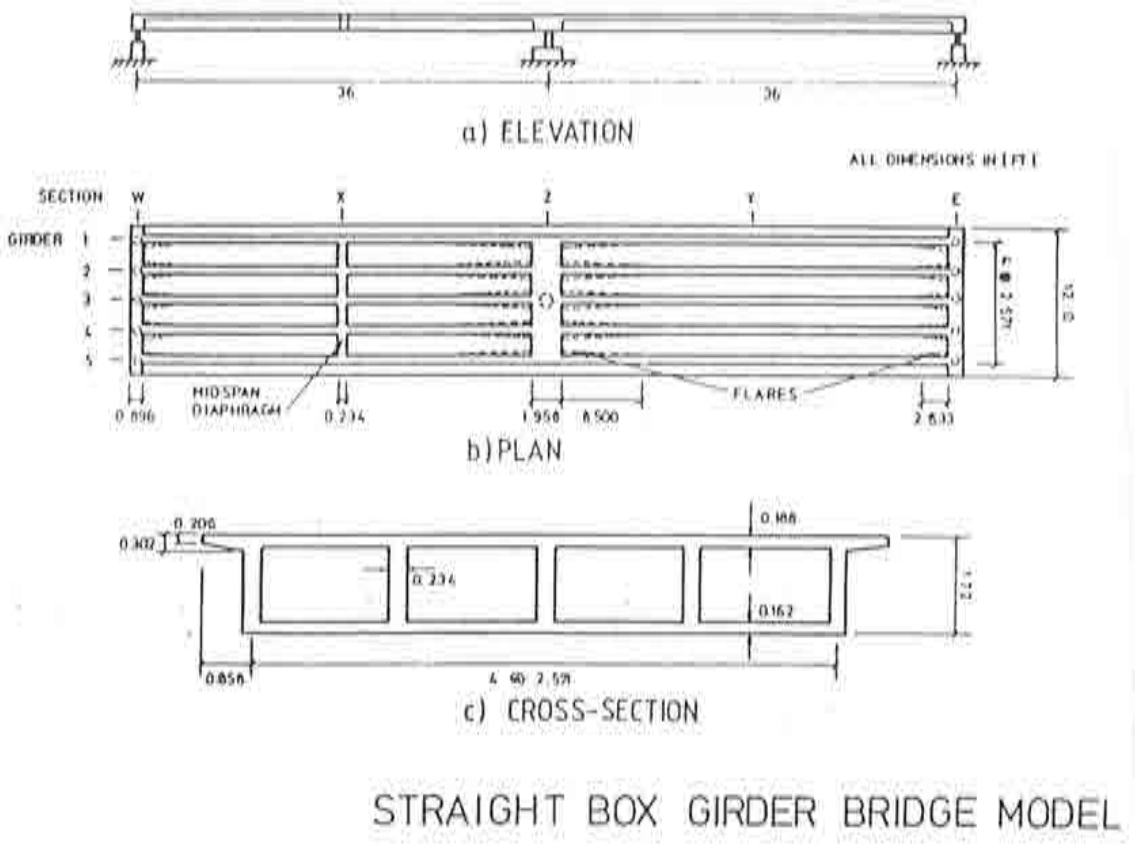

Figure 2.26. Geometric properties of multi–cell concrete box girder bridge model (from Ref. 41)

results obtained by *NONBAN* and other published numerical results as well as published experimental results of full scale and model bridges were performed. The results obtained verified the validity of the program and Hambly's modeling scheme for the nonlinear analysis of bridges subjected to truck traffic loads and proved that *NONBAN* can model the global behavior of common type bridge structures with sufficient accuracy. The proposed model is applicable to situations where the dominant loading condition is due to bending with relatively low levels of shearing and torsional loads. Because available shear strength models seem to highly underpredict the shear capacity of typical bridge structures, best correlation with other numerical and experimental results are obtained when shear failures are ignored.

3. RELIABILITY MODEL FOR BRIDGE SYSTEMS

3.0 Introduction

To account for the uncertainties associated with determining member resistances and applied loads, recent studies have used reliability-based models to perform the safety evaluation of existing and new bridges [5,9,14,20,22]. Most of these efforts, however, were

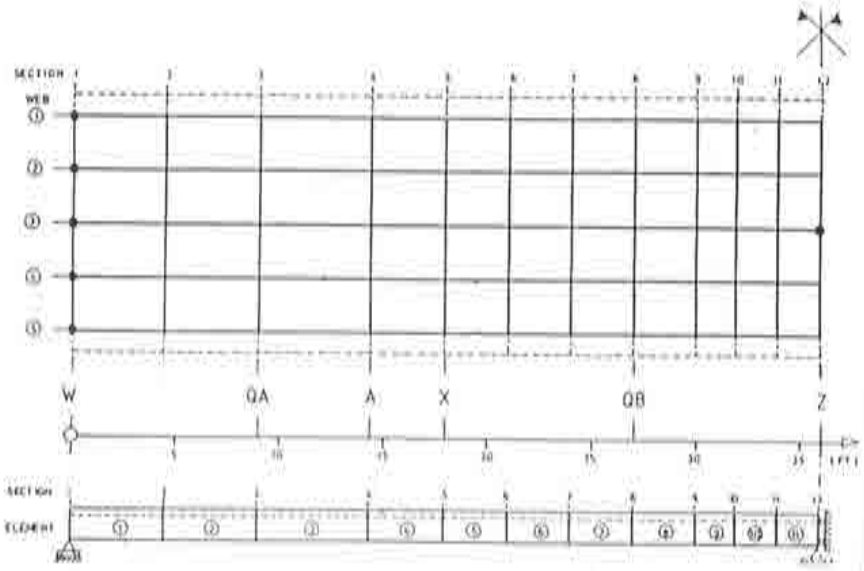

-DISCRETIZATION FOR GRILLAGE MODEL

SLAB REINFORCEMENT AND WEB THICKNESS
FOR LONGITUDINAL BEAM ELEMENTS

BEAM ELEMENT NO.	LONGITUDINAL REINFORCEMENT AREA				WEB THICK-NESS	SHEAR STIRRUP REIN-FORCE-MENT AREA
	TOP SLAB		BOTTOM SLAB			
	INTERIOR GIRDER	EXTERIOR GIRDER	INTERIOR GIRDER	EXTERIOR GIRDER		
	[in²]	[in²]	[in²]	[in²]	[ft]	[in²/in]
1	0.59	0.59	1.96	0.88	0.252	0.012
2	0.59	0.59	2.35	1.27	0.234	0.0077
3	0.59	0.59	2.74	1.47	0.234	0.0077
4	0.59	0.59	2.74	1.47	0.234	0.0077
5	0.59	0.59	2.74	1.47	0.234	0.0077
6	0.59	0.59	2.35	1.27	0.234	0.0077
7	0.59	0.59	1.42	0.79	0.234	0.012
8	2.55	1.87	1.37	0.64	0.279	0.014
9	3.19	2.60	0.80	0.59	0.324	0.018
10	3.53	2.75	0.80	0.59	0.354	0.015
* 11	5.00	4.00	0.80	0.59	1.286	0.018

*CENTER BENT ELEMENT

f'_c = 4500 psi $E_s = 2.9 \cdot 10^6$ 1 in = 25.4 mm

E_c = 550 600 kip/ft² f_{sy} = 60 ksi 1 ft = 0.305 m

G = 220 200 kip/ft² 1 kip = 4.448 kN

Figure 2.27. Mesh and material properties of multi-cell concrete girder bridge (from Ref. 41)

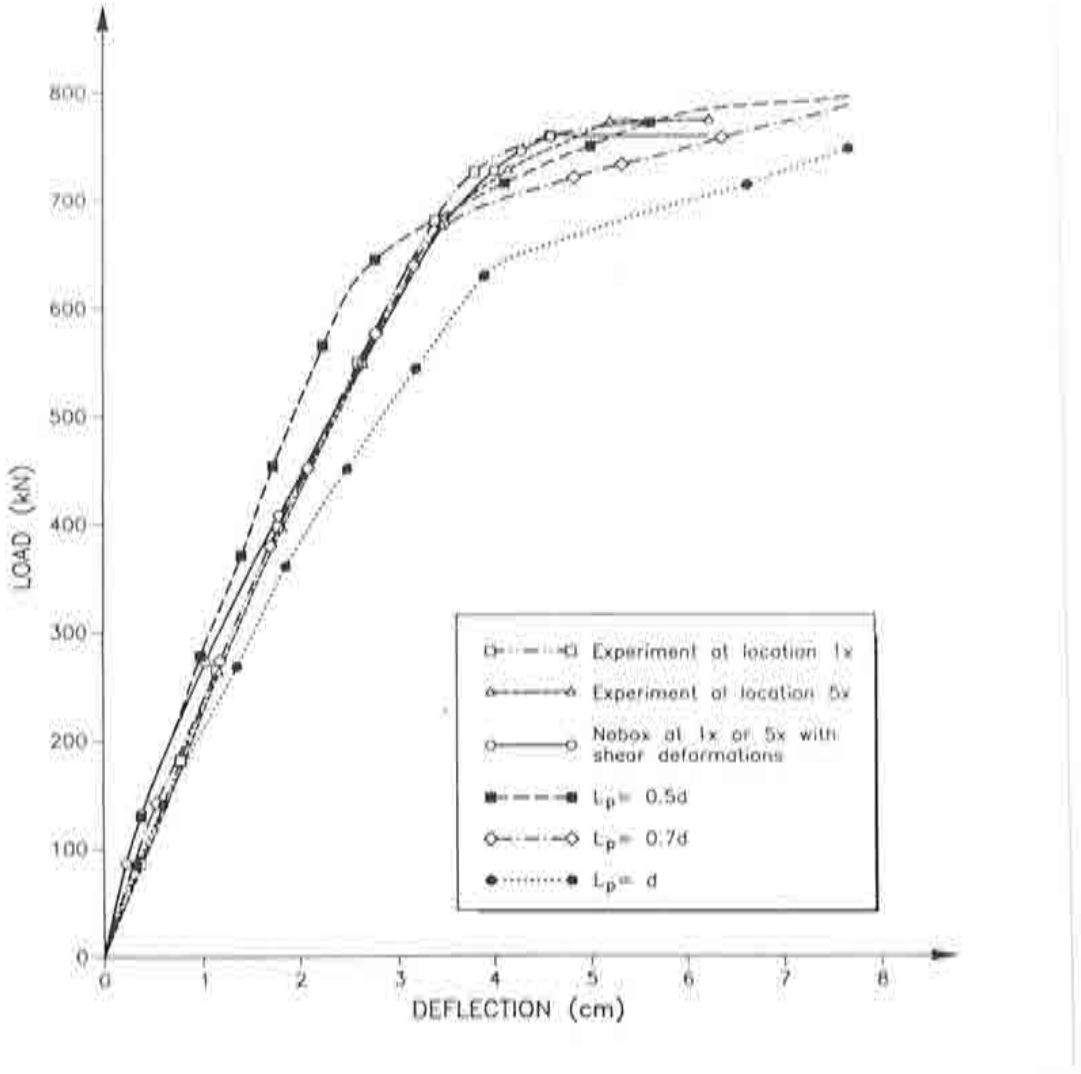

Figure 2.28. Comparison between *NONBAN* and results of Seible

concerned with the reliability of individual structural members. The theory of reliability has also been extended by researchers such as Ang, Moses and Cornell [74,75,76,77] to account for the interaction of members into one structural system with several possible failure modes and to account for the true nonlinear behavior of the system. The system reliability methods that were first developed for the analysis of offshore platforms were later applied to bridge structures. Studying the reliability of complete bridge systems in the nonlinear range is very complicated due to the need of enumerating all the pertinent failure modes and studying the statistical correlation between the members' resistances. To reduce the complexity of the problem, many approximate methods have been developed. These include efficient simulation techniques as well as approximate numerical methods [78,79]. Cornell [80], however, made the observation that for systems under static loading, "the probabilistic effects of randomness in element capacity upon system capacity are small compared to load variability". Therefore, it would be sufficient

to perform a deterministic analysis of a system using the median element properties in order to estimate the reliability of the whole system... although the coefficient of variation (COV) of the system is usually somewhat smaller than those of the elements' capacities.

This chapter proposes simple reliability models for the reliability analysis of bridge systems under traffic loads. Section 3.1 of this chapter gives a brief review of the basic concepts of structural reliability and its application to bridge members and its extension to bridge systems. Section 3.2 reviews the applicability of available truck live load models for the analysis of bridge systems. Section 3.3 illustrates how these models can be used for the analysis of two typical bridge systems.

3.1 Reliability Theory

Load intensity, bridge response and structural strength are not known with certainty. The aim of structural reliability theory is to account for the uncertainties in evaluating the load carrying capacity of structural systems or in the calibration of safety factors for structural design codes. Such uncertainties may be represented by random variables and their probability distributions. [81]

The value that a random variable can take is described by its probability law which is characterized by a probability distribution function. That is, a random variable may take a specific value with a certain probability and the ensemble of these values and their probabilities are described by a distribution function. The most important characteristics of a random variable are its mean value or average, and the standard deviation which gives a measure of dispersion or a measure of the uncertainty in determining the variable. The standard deviation of a random variable R with a mean $\overline{R}$ is defined as σ_R. A nondimensional measure of the uncertainty is the coefficient of variation (COV) which is the ratio of standard deviation divided by the mean value. For example the COV of the random variable R is defined as V_R such that:

$$V_R = \frac{\sigma_R}{\overline{R}} \tag{3.1}$$

Typical COV's for structural applications range from 8 to 15 percent for material strength, 5 to 10 percent for dead load, and 15 to 30 percent for live load and even higher for wind and seismic effects.

Codes often specify safe or nominal values for the variables used in the design equations. A nominal value is related to the mean value through a bias. The bias is defined as the ratio of the mean to the nominal value used in design. For example, if R is the member resistance, the mean of R ($\overline{R}$) can be obtained from the nominal or design value R_n using a bias factor such that:

$$\overline{R} = b_r \, R_n \tag{3.2}$$

where b_r is the resistance bias and R_n is the nominal value as specified by the design code. For example, A36 steel has a nominal design yield stress of 36 ksi but coupon tests show an actual average value close to 40 ksi. Hence the bias of the yield stress is 40/36 or 1.1.

In structural reliability, safety may be described as the situation where capacity (strength, resistance, fatigue life, etc.) exceeds demand (load, moment, stress ranges, etc.). Probability of failure, *i.e.*, probability that capacity is less than applied load, may be formally calculated; however, its accuracy depends upon the availability of detailed data on the probability distributions of loads and resistances. Since such data is often not available, approximate models are often used to execute the calculations.
Let the safety margin of a bridge component be defined as, Z, where:

$$Z = R - S \tag{3.3}$$

R is the resistance or member capacity, S is the total load effect.
The safety index (β) which is often used as a measure of risk is defined as:

$$\beta = \frac{\overline{Z}}{\sigma_z} \tag{3.4}$$

where $\overline{Z}$ is the mean safety margin and σ_z is the standard deviation of the safety margin. Probability of failure P_f is the probability that the resistance R is less than the total applied load effect S. This is symbolized by the equation:

$$P_f = Pr\ [Z < 0] \tag{3.5}$$

If R and S follow independent normal distributions then:

$$P_f = \Phi\ [-\beta] \tag{3.6}$$

Where Φ is the normal cumulative probability function that gives the probability that the normalized random variable is below a given value. β gives the number of standard deviations that the mean margin of safety falls on the safe side.
β as defined in equation (3.4) provides an exact measure of risk (probability of failure) if all the given variables follow normal distributions. Although β was originally developed for normal distributions, similar calculations can be made if the variables are lognormally distributed. A random variable whose logarithm is normally distributed is said to have a lognormal distribution. For lognormal distributions, the equation for β can be approximated as:

$$\beta = \frac{ln\left(\frac{\overline{R}}{\overline{S}}\right)}{\sqrt{V_R^2 + V_S^2}} \tag{3.7}$$

where $\overline{R}$ and $\overline{S}$ are the mean values of the resistance R and the load S and V_R and V_S are the coefficients of variation of R and S.
In general, β' s from either normal or lognormal models are used as estimates of the reliability of a structural member even if its capacity and applied load are neither normal nor lognormal. To improve on these estimates "Level II" methods have been developed. Level II methods involve an iterative calculation to obtain an estimate to the probability of failure. This is accomplished by approximating the failure surface ($Z = 0$) by a tangent multi-dimensional plane at the point on the failure surface closest

to the origin. A more detailed explanation of these principles and derivations of the equations given in this chapter can be found in reference [81].

Code Calibration

The safety index has been used by many code writing groups throughout the world to express structural safety for individual structural elements. β in the range of 2 to 4 is usually specified as an acceptable target value for different structural applications. As β increases, the probability of failure P_f decreases. Structural safety calculations for bridge members differ somewhat from other applications because truck loads (which constitute the dominant live load) increase with time due to new truck regulations and increases in truck volume. Meanwhile member capacity may be decreasing due to environmental or corrosion effects. Thus, for new bridge constructions, β is relatively high, say on the order of 3.5. But, over a bridge's life span, as member capacity decreases due to strength degradation and environmental effects, a typical β may fall to about 2.5. A β of 3.5 implies about a 0.000233 lifetime risk or a probability of failure of about 0.0233 % while a β of 2.5 corresponds to a probability of failure on the order of 0.621. These β values usually correspond to the failure of a single component. If there is adequate redundancy, the failure of one component may not result in the failure of the complete system. Thus, it is often observed that overall system safety indices for the ultimate capacity of the bridge $\beta_{ult.}$ will be higher than the safety indices for single components. For example, for some bridge structures with five parallel members, Tabsh and Nowak [30] found that the safety index of the bridge system $\beta_{ult.}$ may be roughly equal to $1 + \beta_{member}$.

The safety index is not calculated solely for making statistical risk statements but rather for recommending the proper load and strength safety factors for design or evaluation specifications. One commonly used approach is that each type of structure should have uniform or consistent reliability levels over the full range of applications; *e.g.* similar β values should be obtained for bridges of different span lengths, number of lanes, simple or continuous spans, roadway categories, etc. Thus, normally, a single target β must be achieved for all applications. Some engineers and researchers on the other hand are suggesting that higher values of β should be used for more important structures such as longer spans or for bridges that carry more traffic. This latter approach has not been accepted and no practical mechanism has been developed to determine the distribution of β with span length or traffic intensity.

Appropriate target β values are often calibrated based on existing designs. That is, if the safety performance of bridges designed according to current criteria has generally been found satisfactory, then the average safety index obtained from current designs is used as the target that any new design should satisfy. This calibration with past performance also helps to minimize any inadequacies in the data base as has been previously reported [14]. After calibration, a new bridge code should produce more uniform safety index values than those observed from current codes.

Alternate Format for Safety Index

The safety index for bridge members is normally calculated using equation (3.7) after statistical data on member resistances, dead load and live load effects are assembled. Another approach would consist of expanding the safety margin Z (3.3) as a function of the live load margin $R - D$ and the applied live load L. For example, if the total load effect S is due to the combined effects of the dead load D and the effect of the live load L, then equation (3.3) can be rewritten as:

$$\begin{aligned} Z &= R - S \\ Z &= R - D - L \\ Z &= (R - D) - L \end{aligned} \tag{3.9}$$

where the live load margin $R-D$ determines the capacity of a bridge member to support the applied live load. Current bridges are designed for a 75 year lifespan, thus, L is the maximum expected truck load effect that will be applied on the bridge in its 75 year life. Both the live load margin $R-D$ and the live load effect L can be normalized with respect to the effect of two side-by-side AASHTO HS-20 trucks. The safety margin can then be written as:

$$\begin{aligned} Z &= (R - D) - L \\ Z &= [LF_1 - LL_{75}] \times E_{HS20} \end{aligned} \tag{3.10}$$

where E_{HS20} is the effect of two HS-20 trucks. LF_1 gives the factor by which the effect of two HS-20 trucks is multiplied to cause the bridge member to reach its maximum capacity represented by $(R-D)$. LL_{75} gives the factor by which the effect of two HS-20 trucks is multiplied to produce the same effect as the maximum expected truck load in the 75-year lifetime of the bridge. Thus, LF_1 becomes a normalized measure of the strength capacity of the member and LL_{75} is a normalized measure of the applied live load effects.

Failure will occur when Z in eq. (3.10) is less than zero or when LF_1 is less than LL_{75}. Both LF_1 and LL_{75} are random variables. LF_1 is random due to the uncertainties associated in estimating the resistance R and the dead load effect D. LL_{75} is random due to the uncertainties associated with predicting the maximum expected lifetime load. LL_{75} in this model accounts for the truck load effects including the effect of multiple truck occurrences in one or several lanes as well as the dynamic impact. Using a lognormal format, the safety index for a bridge member becomes:

$$\beta_{member} = \frac{ln\left(\frac{\overline{LF_1}}{\overline{LL_{75}}}\right)}{\sqrt{V_{LF}^2 + V_{LL}^2}} \tag{3.11}$$

$\overline{LF_1}$ is the mean value of the random variable LF_1. It can be calculated from analytical and experimental studies on bridge behavior. $\overline{LL_{75}}$ is the mean value of the random variable LL_{75}, it can be obtained from statistical studies on truck traffic and their effect

on bridges. V_{LF} is the coefficient of variation of the load factor which is typically on the order of 15 %. V_{LF} accounts for the uncertainties in determining R and D. V_{LL} is the coefficient of variation of the maximum expected live load which is typically on the order of 20 %. V_{LL} includes the uncertainties in determining the truck traffic intensity, the truck weights, their axle configurations, the multiple occurrence of trucks on the bridge as well as their dynamic impact.

Safety of Bridges

While the calculation of the safety index for one member is normally used for the calibration of new codes, it does not provide an adequate representation of the safety of the complete bridge system. In fact, due to the presence of reserve strength and nonlinear effects, the failure of an individual member may not necessarily lead to the failure of the complete bridge system. On the other hand, because of possible large nonlinear deformations, the bridge may be unsafe for truck traffic at loads that are lower than those that will cause system failure or in certain cases at loads lower than those that will cause the failure of one member. Also, in addition to verifying the safety of the intact structure, the evaluation of a bridge redundancy should consider the consequences of a damage or the failure of one critical bridge member. Thus, to be safe, a bridge system should: a) provide a reasonable safety level against first member failure, b) should not produce large deformations under regular traffic conditions, c) should provide an adequate level of safety before it reaches its ultimate system capacity under extreme loading conditions, and d) should be able to carry regular traffic loads after damage or the loss of a main load-carrying member.
In summary, four different limit states are identified:

1) Member failure. This is a check of individual member safety using elastic analysis. The capacity of a bridge member to resist member failure is represented by the factor LF_1.
2) System Serviceability limit state. The capacity of a bridge system to resist reaching a serviceability limit is represented by the factor LF_s.
3) Ultimate limit state. This is defined as the ultimate capacity of the bridge system or the formation of a collapse mechanism. The capacity of the structure to resist collapse is represented by the factor LF_u.
4) Damaged condition limit state. This is defined as the ultimate capacity of a damaged bridge system. The capacity of a damaged bridge to resist collapse is represented by the factor LF_d.

In addition, two different loading conditions are also identified, these are:

1) Extreme loading conditions. This is defined as the maximum expected lifetime load. It is a function of the number of trucks that cross the bridge simultaneously, the positions of the trucks on the bridge deck, the weight of the trucks, the distribution of the weight to the individual axles, and the axle configuration. In addition, the load will be a function of the dynamic impact. The design life of

a bridge is normally equal to 75 years [82]. This extreme loading condition is normally used in the evaluation of member safety and safety for the ultimate limit state.

2) Regular Traffic Conditions. Regular traffic conditions are defined as recurrent loads expected to be regularly applied on the bridge. A two-year exposure period is used to define the maximum load expected under regular traffic conditions. This condition is used in association with the analysis of the serviceability limit state and for the analysis of the damaged bridges.

Using a format similar to that used in equation (3.10) for bridge members, the safety index for the ultimate limit state, system serviceability limit state and the damaged condition can be obtained by either assuming lognormal distributions (equation 3.10) or performing a level II iteration.

Reliability-Based Measures of Bridge Redundancy

Redundancy is defined as the capability of a bridge structure to continue to carry load after the failure of one of its members. A comparison between the safety index of one member and the safety indices for the ultimate capacity, $\beta_{ult.}$, the serviceability limit state, $\beta_{serv.}$, and the damaged condition, $\beta_{damaged}$, will then provide a measure of bridge redundancy. Relative safety indices are defined as:

$$\begin{aligned} \Delta\beta_u &= \beta_{ult.} - \beta_{member} \\ \Delta\beta_s &= \beta_{serv.} - \beta_{member} \\ \Delta\beta_d &= \beta_{damaged} - \beta_{member} \end{aligned} \tag{3.12}$$

These relative safety indices give measures of the additional safety provided by the complete bridge system compared to the safety obtained when a traditional check of individual members is performed. Thus, these relative safety indices provide a reliability-based measure of redundancy.

3.2 Probabilistic Live Load Models for Highway Bridges

To perform the reliability calculations, statistical data on bridge (member or system) strength as well as the loads expected to be applied on the bridge structure in its lifespan are required. For bridges, the variables associated with the highest level of uncertainties are the applied loads. The major loads applied on highway bridges include the dead load, live load and environmental loads. The dominant component of the live load is the truck traffic load. The traffic loading problem is characterized by the occurrence of millions of different loading events during the life of the structure. Each traffic loading event is characterized by the arrival of one or more vehicles whose load effects may superimpose. These vehicle arrivals are random in regard to their occurrence and their location in different lanes. In addition, each vehicle can be independently classified according to its number of axles, weight of each axle, spacing between axles, gross weight and speed. These random factors affect the truck's static loading. In addition,

the dynamic properties of the truck axles and the truck's suspension system influence the dynamic bridge response.
Many studies have been recently performed in various countries and jurisdictions to study the bridge loading problem. The goal of these studies is to develop bridge live load models that can capture the essential characteristics of the truck traffic patterns in each jurisdiction and model their effect on bridge structures. Due to the high levels of uncertainty associated with determining the characteristics of these live load effects, it has long been recognized that only probabilistic models can be effectively used to represent the effect of truck loads on the safety of existing or new bridges. Despite some differences in the methods adopted in each research study, the basic concepts used are essentially similar. The object of this section is to compare the different load models recently developed and determine the main truck traffic factors that influence their effect on highway bridges.

Load Modeling Techniques

Bridges are designed to safely withstand the maximum load expected over their service lifetime. In short to medium span bridges, the maximum live load is usually due to the occurrence of several heavy trucks simultaneously on the bridge. Methods to model this maximum response can be essentially divided into three categories: 1) Monte Carlo simulation, 2) convolution or integration method, and 3) closed form probability model or the theory of stochastic processes.
The Monte Carlo approach consists of randomly simulating independent sample values for each factor involved in the maximum response. These values are combined to produce a loading event. Each loading event produces one maximum bridge response calculated from the known structural behavior of the structure represented by an influence surface. By repeating the sampling many times, it is possible to simulate the probability distribution of the maximum response for one event. The probability distribution of the maximum lifetime response is calculated from the one event distribution if the number of independent events in the lifetime of the structure is known. Because many of the events do not produce extreme responses, Monte Carlo simulations in general are slow to accurately converge especially if the response depends on a large number of random variables such as the case with the bridge loading problem.
The convolution or integration technique uses a sum over all possible combinations of the factors involved in a loading event to produce the probability distribution of the maximum response of a single event. As a simple example, if the maximum response for one event, m, is a function of only two random variables x and y:

$$m = g(x, y) \tag{3.13}$$

the frequency distribution of m is calculated from the equation:

$$f_m(m_i) = \sum_k \sum_j \quad f_x(x_k)\, f_y(y_j) \tag{3.14}$$

such that $g(x_k, y_j) = m_i$, the function f_m denotes the discrete probability distribution

histogram:

$$f_m(m_i) = Pr\,(m_{i-} < m < m_{i+}) \tag{3.15}$$

m_{i-} and m_{i+} are closely spaced discrete values defining the histogram's increment size around point m_i. The convolution approach has the advantage that it allows the concentration of the calculation effort in the regions that are most significant. This is effected by reducing the increment sizes in the regions that produce high load effects and increasing the increments in other parts of the histograms.
A more direct approach for calculating the maximum lifetime response is by observing that the load on the bridge is varying with time. The value of the bridge response at a given time t is the outcome of a random variable. The calculation of the maximum response over a period of time T can be obtained by looking at the probability that the stochastic process exceeds a known bound. This problem is usually known as the barrier crossing problem. The advantage of the stochastic process approach is that it usually provides a closed form solution to the load modeling problem which can account for a large number of random variables. The disadvantage is the difficulty associated with the numerical solution of the equations obtained.
Several research studies developed different load models for use during the reliability calibrations of bridge design codes in different countries. This section reviews some of these studies and verifies their applicability for the Spanish truck traffic conditions.

Ghosn-Moses Model

Ghosn and Moses [14] used a convolution method to calibrate an empirical formula that is valid for typical US truck traffic patterns on two-lane highway bridges. In their convolution, they divided the bridge surface into four different slots. A loading event was defined as the case when at least one of the slots is occupied by a truck. Knowing the probability that the other slots are also occupied, a headway probability is obtained for each loading event. These headway probabilities were obtained from measured truck traffic data on two-lane US interstate highway sites.
In addition, each truck involved in the event is classified based on its type as either a single unit or a semi-trailer. Depending on its type, each truck is associated with a fixed axle configuration and a random gross weight drawn from a measured histogram. Given the truck positions, truck configurations and the gross weights for all the trucks in the event, the maximum response for one event is calculated from the bridge's influence line. The response of the bridge due to this one loading event is associated with a probability equal to the product of the headway probability and probabilities of the gross weights. This assumes independence between the headway (or truck positions), the truck types and the gross weights.
Given the maximum response and the probability for one event, a cumulative probability distribution function for one loading event is obtained. Knowing the expected number of events in a bridge lifetime, the cumulative distribution function of the maximum lifetime response is calculated assuming independence between the loading events.
The gross weight histograms and the truck traffic data used in the analysis were collected at various bridge sites in the state of Ohio. Results from the convolution with only

four possible slots were compared to a more refined convolution that allowed various numbers of trucks in various positions on the bridge. The comparison showed that for spans less than 60 m (200 ft) in length, results from the convolution using four slots were very similar to the results of the refined convolution. A sensitivity analysis using data from different bridge sites verified that the most important parameters controlling the maximum lifetime response was the tail end of the gross weight histogram. For typical US sites with about 20 % single unit trucks and 80 % semi-trailers, it was found that the maximum response was influenced by the gross weight histogram of the single unit trucks for short span bridges. For longer spans, the histograms of the semi-trailer trucks influenced the maximum response. The convolution assumed that an average interstate site is subjected to about 2000 loading events per day. However, it was also found that only significant changes in the number of loading events produced any noticeable difference in the maximum expected response. For example, assuming that the number of closely spaced trucks is proportional to the truck traffic intensity, it was found that a change in the number of lifetime events by a factor of 10 produced a change in the maximum response on the order of 17 % for bridges on the order of 60 m (200 ft) in length. The difference was found to be smaller for shorter span lengths.

Based on the results of the convolution program, Ghosn and Moses developed an empirical formula to give the maximum expected lifetime moment response for typical bridges. The proposed formula reflects the most important aspects of truck traffic characteristics. These include truck configuration, truck weight intensity, and multiple presence. The proposed formula is:

$$M = a\, m\, W_{95}\, H \tag{3.16}$$

where:

"M" is the maximum expected lifetime moment.

"a" is the moment effect of a representative vehicle with a typical configuration and a one unit total gross weight. a is a deterministic value and can be calculated from the influence line of the bridge. It was found that for typical US truck traffic composition, it is best to use a representative semi-trailer truck configuration for spans greater than 50 ft. While a single unit truck gives more consistent results for the shorter span lengths.

"m" is a random variable representing the variation of the effect of a random truck from the effect of the representative truck. If the representative vehicle has the configuration of an average truck, m is then close to 1.0 with a coefficient of variation that varies from 15 to 4 % depending on the span length. The longer the span length, the smaller is the influence of the truck configuration on the moment thus the smaller is the COV.

W_{95} is the characteristic value representing the intensity of the gross weight histogram. The 95 percentile value was chosen as the representative gross weight. For the spans where the single unit trucks dominate the response *i.e.* spans less than 15 m (50 ft) in length for typical US sites with 20 % single unit trucks, W_{95} is obtained from the gross weight histograms of the single trucks. For longer

spans, the gross weight histograms of the semi-trailer trucks is used.

"H" is the headway multiplicative factor. It reflects the number of typical trucks with the W_{95} weight needed to produce the maximum lifetime load effect. H was found to be a function of the span length and traffic composition reflecting the fact that the longer the span length the more likely it is to have many heavy vehicles simultaneously on the bridge. Similarly, the heavier the truck traffic is the more likely it is to have many heavy vehicles on the bridge. Values of H are tabulated for different span lengths, truck traffic intensities and projection periods (or service lifespan).

A model such as the one proposed in equation (3.16) is extremely powerful because of its flexibility and adaptability to any individual bridge site, local, state or national jurisdiction. In the next sections, the results obtained from the model proposed in equation (3.16) are compared to the published results and the models proposed by other research studies.

University of Michigan Model

A series of studies conducted at the University of Michigan culminated in the development of the live load model for the AASHTO LRFD specifications [82]. The calculations were based on the truck survey data performed in 1975 by the Ontario Ministry of Transportation. The original data was biased because it covered a selected number of heavily loaded trucks. The authors however, believed that the data is representative of current US truck traffic.

The maximum moment and maximum shear effects for each surveyed truck was calculated for a number of span lengths. The results were assembled into plots of histograms of the cumulative distribution functions. By assuming that the plotted data represents two weeks of traffic, the authors extrapolated the histograms to obtain the expected maximum effect of a single truck in a 75 year life of a bridge. A simulation is performed to account for the possible presence of other trucks in a lane of traffic. The simulation assumed various degrees of correlation between the weights of consecutive trucks. The weights of the trucks used in the simulation were drawn from the original survey data using various assumptions about the frequency of the occurrence of consecutive trucks on a bridge. Similar assumptions were made to account for the possible presence of trucks in two adjacent lanes. The results of these simulations were presented in tables as a function of span length and assumed bridge lifespan or return period.

Reference [82] shows that the two lane moment is about 2 times 0.85 times the one lane moment. Also, the authors found that the results obtained are similar to the results that would be obtained using the AASHTO HS-20 vehicle in addition to a 14.6 N/m (640 lb/ft) distributed load. Thus, the AASHTO LRFD code writers chose to use the HS-20 truck with the 14.6 N/m (640 lb/ft) distributed load as the design truck live load. When comparing the models used in references [82] and [14], it is observed that the frequency of multiple presence used in the Michigan studies were much higher than the ones observed in the field data of reference [14]. However, the fact that the

assumed number of total truck events was lower than that used in reference [14] may offset some of the effects of the difference in the frequency of multiple presence. In addition, the Michigan study assumed some level of correlation between truck weights of consecutive and adjacent trucks while reference [14] assumed independence between the truck weights. Finally, it is also observed that the truck gross weight data used in the Michigan study is biased toward the heavy trucks and is much different than the data collected in reference [14]. Despite these differences in the two analysis procedures, the empirical equation (3.16) derived in reference [14] is found to be valid and can be used to corroborate the results obtained by the University of Michigan.

For example, looking at a 12 m (40 ft) simple span bridge, the results presented in reference [82] indicate that the maximum moment effect for a two lane bridge for a 50 year lifespan is equal to two times 0.85 times the maximum effect of the one lane load. The tables provided in reference [14] show that the one lane moment is equal to 1.74 times the moment effect of the HS-20 truck which is equal to 610 kN.m (450 kip-ft). This will produce a maximum 50 year moment effect for a 50 year life equal to 1800 kN.m (1330 kip-ft). If we use equation (3.16) for the same span length, the multiple presence factor, H, is obtained as H=2.69. Reference [82] does not give the weight histogram used but it plots the cumulative probability distribution of the moment effect for single trucks. The plots can then be interpreted as plots of the cumulative distribution of a m W. Taking the value corresponding to 95 percentile (z = 1.65) and interpolating for the 12 m (40 ft) span, we obtain that the effect of a truck with the weight corresponding to the 95th percentile is equal to 1.078 times the effect of the HS-20 truck (610 kN.m). Multiplying H = 2.69 times 1.078 times 610 produces a maximum 50 year moment effect equal to 1770 kN.m (1304 kip-ft). This is only 2 % different than the 1800 kN.m (1330 kip-ft) value obtained earlier.

Similar comparisons between the results of equation (3.16) and the results of the Michigan studies are shown in Table 3.1 for different span lengths. The average difference is about 4 % with a maximum of 8 %. The results confirm the validity of equation (3.16) for predicting the results of live load simulations. The advantages of using equation (3.16) over the University of Michigan results is in the fact that the formula can be used for site-specific data while the results of the Michigan study are only applicable for the gross weight data collected for the Ontario truck survey. This observation is further confirmed in the sections that follow.

The Swiss Load Modeling Study

Bez in reference [83] developed a program to study the truck traffic loads on Swiss highways. The program uses a Monte Carlo simulation that considers the randomness in vehicle type, the vehicle configuration, the vehicle gross weight, the lane occupied, and the distance of the vehicle relative to the preceding vehicle. Two traffic conditions are considered separately: 1) Free flow of traffic and 2) Congested traffic. The distances between vehicles for the free flowing condition are simulated from actual field data. For the congested traffic case, vehicle spacing is assumed to be 1 m. Also, a dynamic impact factor is added for free flowing traffic but no dynamic factor is included for traffic congestion. Different number of congestions in a bridge lifetime are assumed. However,

Span length (m)	Eq. (3.16) (kN.m)	Michigan (kN.m)	Difference
12 m	1750	1790	- 2 %
18 m	3440	3300	1 %
24 m	5300	5030	5 %
30 m	7440	6970	7 %
45 m	12250	11900	3 %
60 m	19800	18300	8 %

Table 3.1. Comparison between Results of Michigan Model and eq. (3.16)

it was found that the maximum response for long lifespans converges asymptotically. The author also found that the results from the free flowing traffic with a dynamic impact factor of about 1.2 are approximately equal to the results of the congested traffic.

The most common truck on Swiss highway network seems to be the four axle semi-trailer. Reference [83] does not provide any information about the configuration of this vehicle. For this example, it is assumed that the configuration is similar to that of 4-axle semi-trailer Spanish trucks as published by Sobrino in reference [84]. The gross weight histograms published in reference [83] show that W_{95} of the 4-axle semi-trailer is equal to about 295 kN. To compare the prediction of the maximum expected lifetime load obtained from equation (3.16) to the results published in reference [83], two different situations are considered. First, it is assumed that truck traffic density is about the same as that encountered in US highways i.e. a typical site will be exposed to about 2000 truck arrival events per day. Taking the results published in reference [83] for congested traffic and dividing by a factor of 1.2 should produce the results for flowing traffic. These are compared to the results of equation (3.16) as shown in Table 3.2. The results show that the error varies between +17 % to -8 % with an average error on the order of 2 %.

On the other hand, it is reasonable to assume that as the truck traffic on a site increases, the loading situation will approach that of congested traffic. Therefore, it is herein suggested to compare the results of the congested traffic as published in reference [83] to the results of equation (3.16) using H for the heavy traffic condition. The results are shown in Table 3.2. In this case, the error varies between +3 % to -7 % with an average error on the order of 3.5 %.

The Spanish Load Modeling Study

Sobrino in reference [84] presented a research study on load modeling and reliability analysis of Spanish highway bridges. Analysis of truck traffic patterns produced observations very similar to those reported in reference [14]. For example, semi-trailer trucks with 4 and 5 axles were the most frequent trucks observed on Spanish

Span length (m)	Eq. (3.16) (kN.m)	Swiss (kN.m)	Difference
Flowing traffic			
33	3244	2783	17 %
50	5811	5600	4 %
60	7468	7850	- 5 %
70	9293	10100	- 8 %
Congested			
33	3428	3340	3 %
50	6522	6720	- 3 %
60	8740	9420	- 7 %
70	11240	12120	- 7 %

Table 3.2. Comparison between Results of Swiss Model and eq. (3.16)

highways. Although, the average truck weights seem to be higher than those observed in other countries, the truck weight histograms have the shape of bi-normal distribution functions. The author used a variation on the simulation program developed by Bez in reference [83]. The simulation considers both fluid and congested traffic conditions on two lane bridges with different compositions of truck traffic. Traffic in one direction as well as traffic in opposite directions are considered. The truck configurations and weights are classified according to the trucks' number of axles. Bridges are assumed to have a lifetime or return period of 75 years. Characteristic values of the maximum lifetime response are defined as the 95 th percentile values. The author noted that the maximum lifetime response can best be modeled as a Gumbel distribution. The characteristic maximum response was plotted for different span lengths. This includes the effect of flowing traffic and possibilities of congestion. Different numbers of congestions per month and different truck traffic intensities were considered. To check whether the formula given in equation (3.16) is valid for the Spanish truck traffic conditions, the results obtained in reference [84] for 2000 trucks/day are chosen for comparison. The most common truck type on Spain's highways is the five axle semi-trailer truck with a 2-axle cab and a rear tridem. This truck is chosen as the representative truck. A representative truck with a one unit gross weight (1kN) on a 50 m bridge gives a maximum moment effect equal to 10.6 kN.m. The truck gross weight histogram shows that the 95th percentile (W_{95}) is equal to 559 kN. Reference [14] shows that for the 50 m (165 ft) simple span the multiple presence factor H is equal to 2.94. Assuming that the semi-trailer is a truly representative truck configuration, the m factor would be equal to 1.0. The multiplication of a, m, W_{95} and H for this span length produces a mean maximum lifetime moment effect equal to 17421 kN.m.

Plots of characteristic (95 percentile) maximum moment effects are given in reference [84] for different span lengths. For the 50 m span with 10000 vehicles per day of which 20 % are trucks, the characteristic moment value is estimated to be on the order of 20000 kN.m. Reference [84] shows that the maximum response follows a Gumbel distribution with a COV on the order of 7 %. This would indicate that the 95 percentile is about 3 % higher than the mean value. In this case, the mean maximum response is on the order of 17700 kN.m. Compared to the value of 17421 kN.m obtained using equation (3.16) this shows a difference on the order of 1.5 %. The COV obtained in reference [84] is only 7 % because it does not account for site-to-site variability.
A random selection of simple and continuous span lengths was also chosen for further comparison using the steps outlined in the previous example. Table 3.3 shows the results obtained from the simulation and the results obtained using equation (3.16). It is noted that the difference observed for all the cases considered is less than 5.3 %. This seems to confirm that equation (3.16) is also valid for the Spanish truck traffic patterns.

Span length (m)	Eq. (3.16) (kN.m)	Spanish (kN.m)	Difference
33	9930	9495	5 %
50	17420	17670	- 2 %
60	22160	22970	- 4 %
70	30090	30600	- 2 %

Table 3.3. Comparison between Results of Spanish Model and eq. (3.16)

The Dutch Load Modeling Study

As part of the development of a bridge design code, Vrouwenvelder and Waarts [85] performed a study on traffic loads on bridges. Statistical data on 16000 vehicles were assembled to study their truck types and gross weights. Statistical models for truck axle loads were also derived. The most common truck types were found to be the 3-axle, 4-axle and 5-axle semi-trailers which together constituted 26 % of all truck traffic.
A probabilistic traffic flow model was constructed accounting for three types of traffic: free, congested and stopped. The truck traffic intensity was assumed to be 6700 trucks/day with 90 % of the trucks in the slow lane. It is assumed that 94 % of the loading situations involve free traffic, 5 % involve congested traffic and 1 % involve stopped traffic. The assumed headway between trucks for free traffic is about 12.5 m, for congested traffic is between 4 to 10 m and for stopped traffic is 1 to 5 m.
The authors used a simplified approach to estimate the design load for a 100 year reference period. The design load was defined as the load that will have a probability of exceedance equal to 0.62 % in the 100 year period. Knowing the number of trucks expected in the 100 year period and knowing the probability distribution of the truck

weights, the design load is calculated for one lane bridges assuming a single truck occurrence in each loading event. For lane loading, an average headway distance is used to define slots on the bridge. The probability of having a truck in each slot is calculated from the traffic intensity data accounting for the possibility of convoy formation. The probability distribution of the one lane response is thus calculated. The design load is then calculated from the probability distribution curves. Similar calculations are performed for traffic in multiple lanes. The results of the simplified model were corroborated using a Monte Carlo simulation.
To compare the results of reference [85] and those obtained from equation (3.16), it is assumed that the 4-axle truck is the dominant vehicle. The 95 percentile gross weight for this type of trucks is obtained as 391 kN for the Dutch traffic data. The influence coefficient of this trucks for a 50 m simple span, a, is calculated as 10.47 kN.m/kN. Assuming heavy traffic condition reference [14] gives an H value equal to 3.30 for the 50 m span. This would produce an expected 50 year maximum response equal to 13509 kN.m. Equation (3.16) given above was calibrated to give the median response for a 50 year lifespan. According to reference [85], this would correspond to about a 100 year return period. The results of the 50 m simple span bridge with a 100 year return period for two lanes in one direction (one slow and the other fast) give a distributed load q equal to 46.67 kN/m. This would produce a maximum moment response of 14583 kN.m which is 8 % higher than the value obtained from equation 3.16.

3.3 Application: System Performance of I-Beam and Spread Box Beam Prestressed Concrete Bridges

3.3.1 Introduction

As an application of the reliability models developed in the previous sections, this section performs a reliability analysis of two alternate bridge designs with the same simple span length of 25 m. The first configuration has 11 parallel prestressed I-girder beams. The alternate design consists of three spread box beams. These two configurations are chosen herein because they are the most common configurations currently used in Spain. In fact, prestressed concrete I-girder bridges are very common because they have had a long history of excellent performance under regular truck traffic loads as well as overloads. In addition, I-girder bridges are economical and easy to construct and are known to have high levels of system reserve strength and system redundancy. On the other hand, the use of spread box girder bridges has become more common in recent years because, in addition to their good structural performance, they are more aesthetically pleasing than I-girder bridges. For this reason, the Spanish bridge authorities have abandoned the use of parallel prestressed concrete I-girder bridges in favor of spread box beam girder bridges for all overcrossings.
The object of this section is to compare the structural performance of these two bridge types. To perform such a comparison, two example bridges with the same span length of 25 m and satisfying the same Spanish code requirements are designed. The first configuration has 11 parallel prestressed I-girder beams at 1.15 m center to center. The alternate design consists of three prestressed concrete spread cell box beams at 5 m

center to center. Figures 3.1 and 3.2 describe the two alternate bridge configurations. Chapter 2 of this report described a program used to analyze the nonlinear behavior of precast I-girder and precast spread box beam bridges. The program is used to compare the capacities of the two alternate bridge systems. The capacity of these bridges to support truck loads is studied for four different limit states discussed in section 3.1: a) First member failure assuming linear elastic behavior. b) Ultimate capacity accounting for the nonlinear material behavior. c) A system serviceability limit state. And d) Ultimate capacity assuming damaged conditions. The results of the deterministic analysis for these four limit states are used to estimate the reliability of the two alternate designs. Reliability indices for first member failure as well as system failure are obtained and used to compare the redundancy of the two structural systems.

3.3.2 Limit States

One important issue in the analysis of structures is the definition of failure or the definition of the limit states. Current design methods require that the forces be distributed to individual structural members using a linear elastic analysis. Failure is assumed to occur when the elastic member forces exceed member capacity. This definition of failure is widely used although normally member capacity is only reached after extensive plastification. In addition to verifying member capacity, member serviceability conditions are also checked. These include member deflections, member cracking and fatigue stresses. Member serviceability criteria are not normally related to the strength performance of the system.

To study the performance of a structural system, the complete nonlinear behavior of the structure should be monitored until system failure. Failure of a bridge system occurs when the structure is no longer capable of carrying any additional load or when its ultimate capacity is reached. This is defined as the load at which a mechanism forms *i.e.* the load that causes an infinitely large deflection, or the point at which the structure is so damaged that unloading occurs. On the other hand, it is often observed that a bridge structure ceases to function effectively at load levels lower than the loads that will cause failure. These conditions are known as system serviceability limit states [86]. Loss of member capacity is also of concern. Bridge members are often subjected to fatigue stresses that may lead to fracture and the loss of the load carrying capacity of a main member. In addition, corrosion, fire or an accident such as collision by a truck, ship or debris, could cause the loss of a bridge member or the severing of prestressing strands. To ensure the safety of the public, bridges should be able to sustain these damages and still operate albeit at reduced capacity. Therefore, in addition to verifying the safety and serviceability of the intact structure, the evaluation of a bridge's safety and redundancy should consider the consequences of the failure of critical members.

In summary, it is herein concluded that the linear analysis of a bridge structure is not sufficient to verify the safety and the functionality of a bridge structure. It is also important to verify the adequacy of its ultimate capacity for intact as well as damaged conditions and to verify its system serviceability. For concrete bridges, ultimate capacity is reached when a mechanism forms or when unloading begins due to extensive concrete damage. It has been observed that unloading begins at a load level close to the point

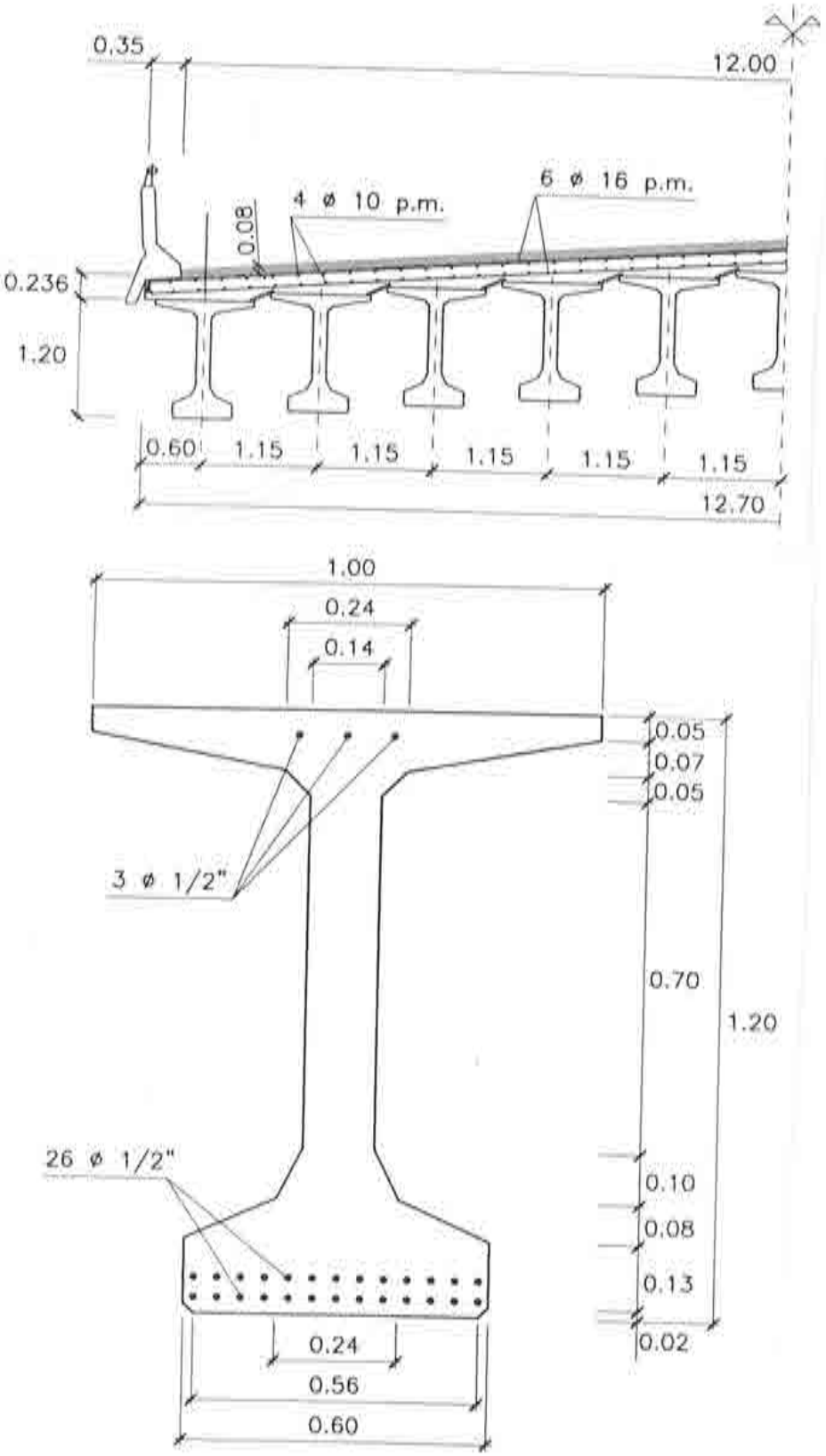

Figure 3.1. Description of the 11 I girder bridge

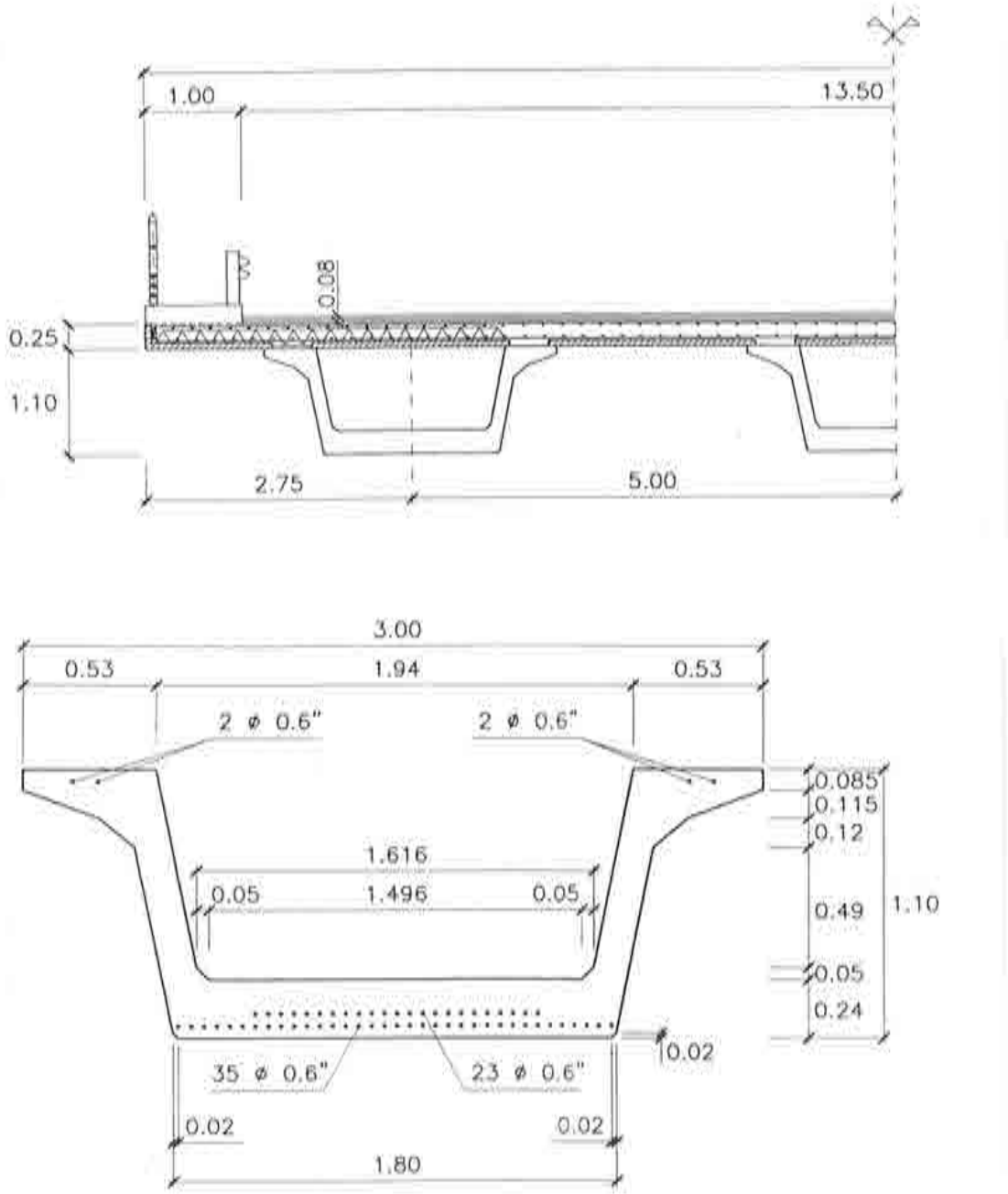

Figure 3.2. Definition of the 3 box girder bridge

when concrete crushing in a main longitudinal member occurs [36,87]. Therefore, this point is used herein to define system failure. Based on the recommendations of reference [86], it appears that the most suitable serviceability limit state for bridges is a deflection to span length ratio limit. A displacement limit equal to the span length/200 was proposed in reference [11] and is used herein as a system serviceability limit state. This serviceability limit is a system serviceability criterion and is different from the member serviceability criteria that are routinely checked in current design procedures. Finally,

the capacity of the structure to carry load after the complete damage or ductile failure of a main load carrying member should also be performed. As previously done in reference [11] it is herein recommended to verify the safety of a bridge under damaged conditions by assuming a damage scenario where one main longitudinal member is completely removed from the structural model.

3.3.3 Analysis of Bridge Models

To perform the nonlinear analysis using *NONBAN*, the two bridge systems described above are discretized as grillages with longitudinal and transverse beam elements following the modeling scheme proposed by Hambly [34]. Although Hambly proposed his scheme for the analysis of bridges in the linear elastic range, chapter 2 demonstrated that this scheme was also sufficiently accurate to study the global nonlinear behavior of typical I-beam as well as box beam bridge configurations. The properties of the longitudinal and transverse beams are shown in Figure 3.3 for the eleven-girder bridge and in Figure 3.4 for the three-box beam bridge. The nonlinear incremental analyses are performed under the effect of two side-by-side trucks with a minimum lateral distance of 1.2 m between the axles of the adjacent trucks. Each of the applied trucks is assumed to have the configuration of the average semi-trailer truck observed over the Spanish road network as shown in Figure 3.5. Both bridges are assumed to have simple pin supports at the ends of every longitudinal beam such that vertical displacements are restrained but all end rotations are free. For the box beams this assumes a single pin at each end located at the center of the end section.

In a first step, a linear elastic analysis of the two structures is performed. First member failure is assumed to occur when the most heavily loaded longitudinal member reaches its maximum capacity. The maximum capacity is reached when concrete crushing occurs. The concrete stress-strain relationships used for the derivation of the nonlinear material properties assume that concrete crushes when the compression strain is equal to 0.0035. Using the results of the linear analysis, it is found that first longitudinal member failure would occur in the 11-girder bridge when the weights of the two side-by-side trucks are incremented by a load factor of 8.98. For the three-box girder bridge, the load factor that would produce first member failure assuming linear elastic response is 8.53. For both bridges, the most critical loading position was obtained when the two trucks are transversely placed on the extreme edge of the bridge and the rear axle placed at the middle of the span. In both cases, failure occurred at the midpoint of the external longitudinal girder.

In a second stage, a complete nonlinear analysis using the material properties shown in Figures 3.3 and 3.4 is performed for the same trucks and loading positions described above. The truck loads are incremented and the weights of the trucks that produce system failure are obtained. System failure is defined as the load at which concrete crushing occurs. For the 11-girder bridge, system failure occurred at a load factor of 10.40. In this case, failure occurred when the exterior girder under the load reached its maximum plastic rotation at the middle of the span. For the three-box girder bridge, system failure occurred at a load factor of 9.18. At this load factor, failure occurred transversely in the slab section joining the web of the exterior box girder and the middle

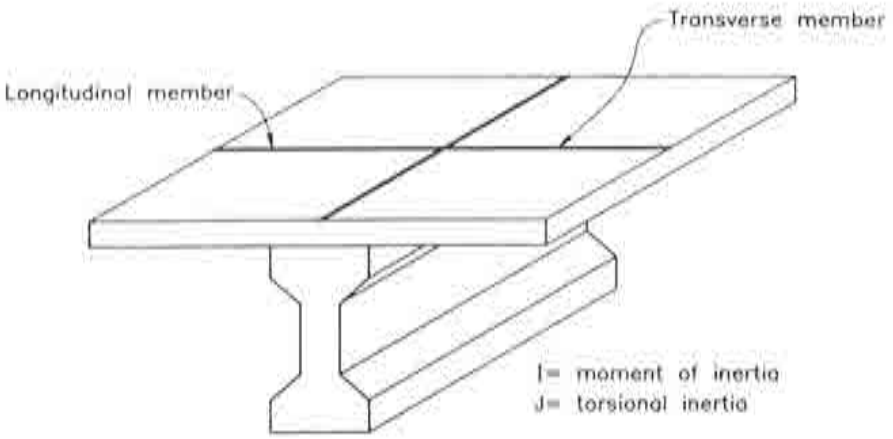

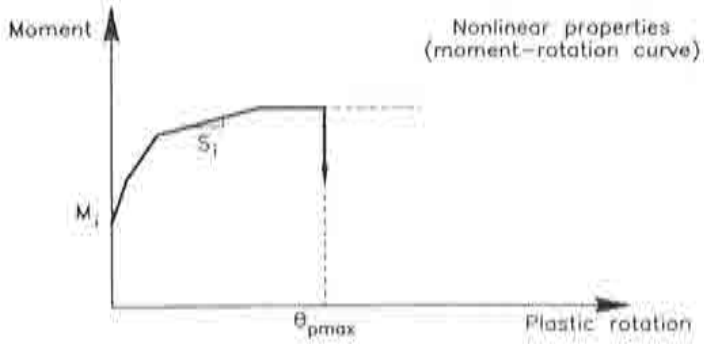

Longitudinal member properties:
(positive bending only)

I= 0.2167 m4
J= 0.0015 m4

M1= 490 T.m	S1= 105000 T.m/rad
M2= 590 T.m	S2= 27300 T.m/rad
M3= 690 T.m	S3= 11300 T.m/rad
M4= 710 T.m	S4= 0 T.m/rad

θ_{pmax}= 0.021 rad

Transverse member properties:
(positive bending only)

I= 0.0017 m4
J= 0.0033 m4

M1= 6 T.m	S1= 9900 T.m/rad
M2= 18 T.m	S2= 3500 T.m/rad
M3= 24 T.m	S3= 150 T.m/rad
M4= 25 T.m	S4= 20 T.m/rad

θ_{pmax}= 0.020 rad

Figure 3.3. Mechanical properties of model elements of the 11 I girder bridge

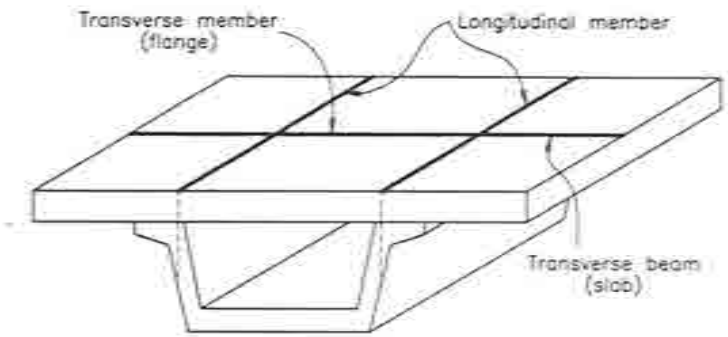

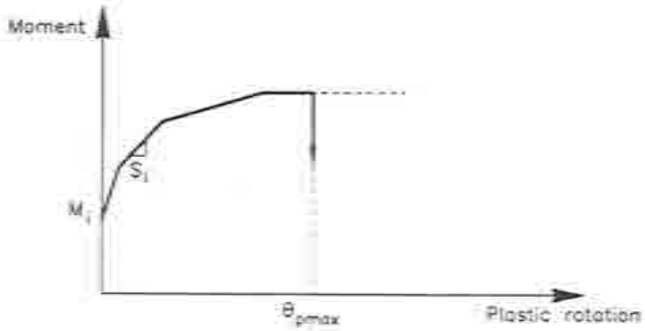

Longitudinal member properties:
(positive bending only)

I= 0.3220 m4
J= 0.1725 m4

M1= 790 T.m	S1= 211500 T.m/rad
M2= 900 T.m	S2= 51000 T.m/rad
M3= 1070 T.m	S3= 2400 T.m/rad
M4= 1120 T.m	S4= 0 T.m/rad

θ_{pmax}= 0.026 rad

Transverse member properties
(FLANGE OF BOX):

I= 0.449 m4
J= 0.40 m4
A_s= 0.00615 m2 (shear area)

Flange of boix is assumed to remain
in elastic range

Transverse member properties (SLAB):
(positive bending)

I= 0.0035 m4
J= 0.0065 m4

M1= 8 T.m	S1= 16200 T.m/rad
M2= 25 T.m	S2= 14000 T.m/rad
M3= 40 T.m	S3= 2300 T.m/rad
M4= 42 T.m	S4= 200 T.m/rad

θ_{pmax}= 0.0112 rad

Transverse member properties (SLAB):
(negative bending)

I= 0.0035 m4
J= 0.0065 m4

M1= 10 T.m	S1= 23000 T.m/rad
M2= 35 T.m	S2= 5500 T.m/rad
M3= 55 T.m	S3= 950 T.m/rad
M4= 56 T.m	S4= 170 T.m/rad

θ_{pmax}= 0.0143 rad

Figure 3.4. Mechanical properties of model elements of the 3 box girder bridge

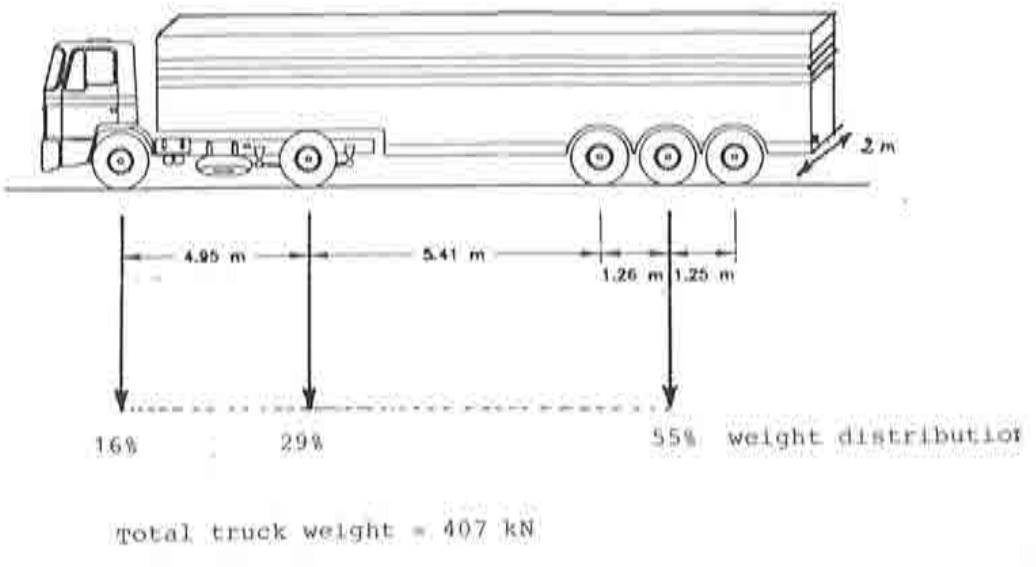

Figure 3.5. Definition of the truck used in the analysis

box girder.

Although the grid model is known to provide a good representation of the global behavior of the bridge including the distribution of the load to the main longitudinal members, it is questionable whether modeling the slab as beam elements is sufficiently accurate to study the failure of the slab. This is because the grid model ignores several factors that contribute to the capacity of bridge deck slabs. Examples of such factors include the two-dimensional moment interaction of the slab and the effect of membrane action. Due to the contributions of these factors several research studies have shown that bridge slabs in reality possess much higher strengths than indicated by typical simple analysis procedures. For these reasons, another analysis is performed for the box girder bridge assuming that the slab will continue to carry loads beyond the level at which the strain in the transverse slab elements reaches its limiting value of 0.0035. In this case, system failure is assumed to occur at the point at which concrete crushes in a main longitudinal member. This level was reached at a load factor equal to 10.92 for the three-cell bridge.

System serviceability limit is defined as the load at which the maximum deflection in a main longitudinal member is equal to the span length/200 (0.125 m). This limit is reached at a load factor equal to 9.03 for the 11 girder bridge and at a load factor of 9.17 for the box girder bridge.

Figure 3.6 shows a comparison between the load factor versus maximum displacement curve for the two bridge configurations analyzed. One should note the similarities between the two curves except for the final failure points.

A sensitivity analysis is performed to study the effect of the boundary conditions of the box-girder bridge. In this example, two pin supports are placed at the end of each box beam to restrain its torsional rotation. First member failure assuming linear elastic response occurs in the external member at a load factor equal to 9.08. Accounting for

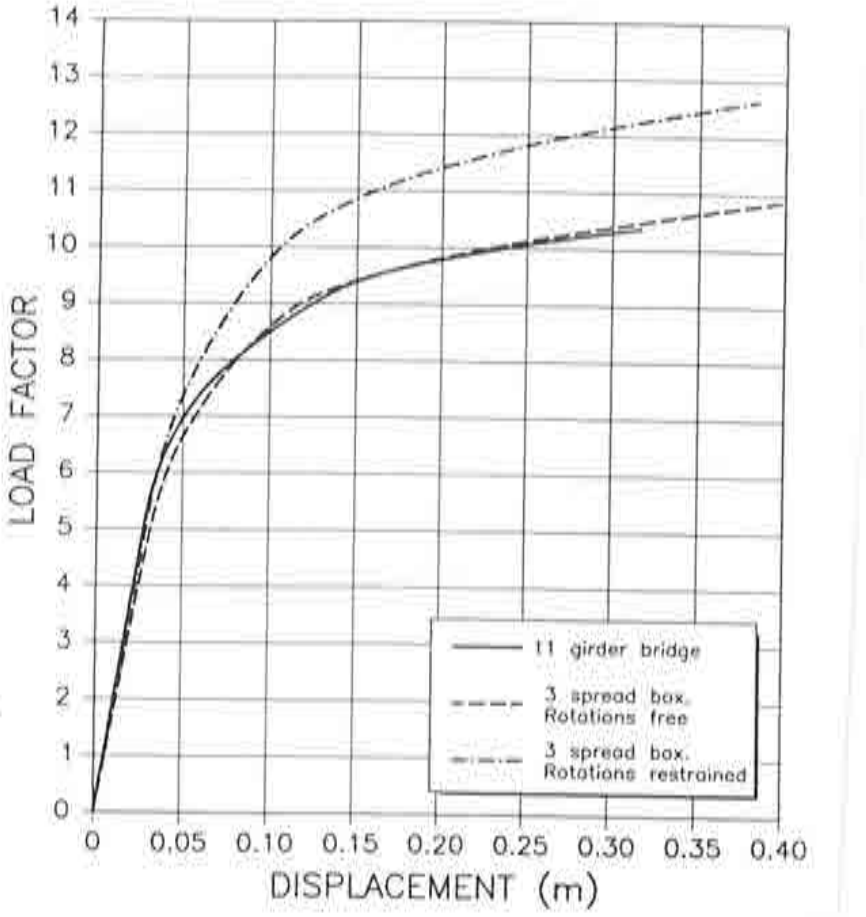

Figure 3.6. Comparison of load deflection curves of the two configurations analyzed

the nonlinear behavior, slab crushing in the transverse direction occurs at a load factor equal to 10.41. If the nonlinear analysis is continued beyond this load level then system failure would occur at a load factor equal to 12.67 when the exterior longitudinal member crushes. The serviceability displacement limit of 0.125 m under a main longitudinal member is obtained at a load factor equal to 10.43.

If we assume that the external member of the 11-girder bridge is completely damaged, the nonlinear analysis shows that failure of the slab occurs at a load factor of 1.91. If the slab is assumed to be able to sustain this load, crushing in a main longitudinal member would then occur at a load factor of 6.92. Damage to the three-box girder bridge is simulated by assuming complete damage of the external web of the external girder. For the box girder with only one pin support at each section end, the slab would fail under the effect of the dead load alone. If loading is continued assuming that slab failure is only a local failure, then system failure would occur at a load factor of 5.67. For the box girder bridge with supports under each web, the load factor at which transverse slab failure occurs is 1.3 and the load factor at which longitudinal member failure occurs is 6.21. The load factors calculated for the damaged box girder bridge are lower than those observed for the 11-girder bridge because damage to one web will not only reduce the

external box's moment capacity by one half but will also reduce the torsional rigidity of the member to a practically negligible level. The results of all the analyses performed herein are summarized in Table 3.4.

CONFIGURATION	LIMIT STATE	LF	$\beta^{(*)}$	$\Delta\beta$	target	$\beta^{(**)}$	$\Delta\beta$	target
11-GIRDER BRIDGE	1st member–Linear elastic	8.98	5.56	x	x	5.84	x	x
	Transverse slab failure	x	x	x	x	x	x	x
	Long. member failure	10.40	6.09	0.53	1.00	6.41	0.57	1.00
	System serviceability	9.03	5.84	0.28	- 1.00	6.14	0.30	- 1.00
	Damage condition	6.92	4.90	- 0.66	- 0.50	5.13	- 0.71	- 0.50
3-SPREAD BOX BEAM BRIDGE one pin support at center of end section	1st member–Linear elastic	8.53	5.38	x	x	5.64	x	x
	Transverse slab failure	9.18	5.64	0.26	x	5.92	0.28	x
	Long. member failure	10.92	6.27	0.89	1.00	6.60	0.96	1.00
	System serviceability	9.17	5.90	0.52	- 1.00	6.20	0.56	- 1.00
	Damage condition	5.67	4.22	- 1.16	- 0.50	4.41	- 1.23	- 0.50
3-SPREAD BOX BEAM BRIDGE two pin support under webs of end section	1st member–Linear elastic	9.08	5.60	x	x	5.88	x	x
	Transverse slab failure	10.41	6.09	0.49	x	6.41	0.53	x
	Long. member failure	12.67	6.82	1.22	1.00	7.20	1.32	1.00
	System serviceability	10.43	6.36	0.76	- 1.00	6.70	0.82	- 1.00
	Damage condition	6.21	4.53	- 1.07	- 0.50	4.74	- 1.14	- 0.50

(*) LF COV = 13 %
(**) LF COV = 10 %

Table 3.4. Summary of results

3.3.4 Reliability Analysis

To account for bridge strength and load uncertainties, a reliability analysis is performed. The safety margin Z for a bridge system is defined as:

$$Z = (R - D) - (L + I) \tag{3.17}$$

$$Z = LF - LL \tag{3.18}$$

where the incremental load factor, LF, is equal to the resistance R minus the dead load D ($LF = R - D$). LF determines the capacity of a bridge system to support the applied live load. LL is the maximum applied live load effect expected in a given return period. LL depends on the static truck load effects L and the dynamic effect I. Since in this study the calculation of the bridge system capacity is presented as a function of the typical average truck configuration shown in Figure 3.5, both LF and LL are herein normalized with respect to the effect of the typical average truck.
Bridge failure occurs when Z in equations (3.17) and (3.18) is less than zero or when LF is less than LL. Both LF and LL are random variables. LF is random due to the uncertainties in determining the system resistance R and the dead load D. A deterministic estimate of LF for each of the four limit states previously identified is obtained using the nonlinear analysis program as seen in the previous section.
LL is random due to the uncertainties associated with predicting the maximum expected load in a given return period. It is a function of the number of trucks that cross the

bridge during the return period, the number of trucks that are simultaneously on the bridge when the maximum load effect is measured, the positions of the trucks on the bridge deck, the weights of the trucks, the distribution of the weights to the individual axles and the axle configuration. In addition, the load effect is a function of the dynamic impact. All these factors are random and produce a high level of uncertainty in estimating the maximum expected truck load effect in a given return period. Reference [14] provides a simple truck live load model which has been proven to be valid for the Spanish truck traffic. The model gives the maximum expected lifetime load effect as a function of a typical truck configuration with a characteristic weight. The total truck load effect $L + I$ is given as:

$$L + I = a\, m\, W_{95}\, H\, i \tag{3.19}$$

where "a" is the effect of a representative truck configuration with a one unit total load. "m" is factor representing the variation of the random trucks from the configuration of the representative truck. W_{95} is the characteristic 95 percentile value of the truck weight histogram for a given jurisdiction. H is the headway factor representing the number of representative trucks of weight W_{95} that will produce the same effect as the maximum expected lifetime load effect. "i" is the impact factor. When normalized with respect to the effect of the average truck shown in Figure 3.5, equation 3.19 becomes:

$$LL = \frac{m\, W_{95}\, H\, i}{407^{(kN)}} \tag{3.20}$$

Since the analysis performed in the previous section uses an average truck configuration "m" is herein assumed to be equal to 1.0 and its coefficient of variation (COV) is assumed to be equal to 8 percent [7]. W_{95} for typical Spanish truck gross weights is given as 559 kN with a COV of 10 percent [84]. The dynamic impact factor for two trucks is shown to be about 1.10 with a COV of 8 percent [82].
H is a function of the return period, thus two different loading conditions are identified: Extreme loading condition and regular truck traffic condition. Extreme loading condition is defined as the maximum expected lifetime load. The expected bridge lifespan is usually around 50 to 75 years. The extreme loading condition is normally used in the evaluation of member safety and for the safety for the ultimate limit state. Reference [14] shows that for 25 m span and for a 50-year return period H is on the order of 2.78 times the effect of one representative truck (or 1.39 times the effect of two side-by-side trucks). Regular traffic condition is defined as the recurrent load expected to be regularly applied on the bridge. A two-year exposure period is used herein to define the maximum load expected under regular traffic conditions. This condition is used for the analysis of the serviceability limit state and for the analysis of damaged bridges. Reference [82] shows that expected 2 year load is about 93 percent of the maximum lifetime load. Thus H becomes equal to 1.30 times the effect of two side-by-side trucks. Reference [14] recommends a COV equal to 7 percent for H.
In addition, a COV of 10 percent is added to LL to account for possible future changes in truck traffic patterns and growth in truck traffic rates. The final COV obtained for the normalized live load effect LL is then equal to 20 percent.

According to reference [82] prestressed concrete member capacities are on the average higher than the nominal or code specified resistances by a factor of 1.05 with a COV of 7.5 percent. Additionally, actual dead load values are on the average 1.04 times higher than the estimated values obtained from bridge plans with a COV of 9 percent. For the bridges studied in this paper, this would produce a bias of 1.05 on LF ($LF = R - D$) and a COV of 10 percent. In addition, a COV of 8 percent is added herein to account for the variability in the lateral and longitudinal positions of the trucks. The final bias on LF is then equal to 1.05 and the final COV is equal to 13 percent. Cornell [80] explains that such a COV on member capacity would result in a lower COV (on the order of about 10 percent) for the complete system. However, in this study it is proposed to use the same COV for member capacity as well as system capacity to account for the uncertainties associated with modeling the nonlinear behavior and predicting the system capacity. Thus, it is herein assumed that a bias of 1.05 and a COV of 13 percent are valid for all four limit states studied.

Knowing the mean values and the COV of LF and LL and assuming that LF follows a lognormal distribution while LL follows an extreme type I distribution, the probability of failure P_f can be calculated as:

$$P_f = \Phi(-\beta) = Pr(LF < LL) \tag{3.21}$$

where Φ is the Gaussian cumulative distribution function and β is defined as the safety or reliability index. The safety index β can be calculated to satisfy equation (3.21) using a first order reliability program [88].

Redundancy is defined as the capability of a bridge system to continue to carry load after the failure of its most critical member. Hence, to study the redundancy of a system, it is useful to examine the difference between the safety indices of the system and the safety index of the most critical member. If the safety index of the system for the ultimate limit state is defined as $\beta_{ult.}$, the safety index of the system for the serviceability limit state is $\beta_{serv.}$, the safety index for the damaged condition is $\beta_{damaged}$ and the safety index for member failure assuming linear elastic response is β_{member} then the redundancy indices as defined in section 3.1 are given for the ultimate limit state as, $\Delta\beta_u$, the serviceability limit state $\Delta\beta_s$, and the damaged condition $\Delta\beta_d$, are defined as:

$$\begin{aligned} \Delta\beta_u &= \beta_{ult.} - \beta_{member} \\ \Delta\beta_s &= \beta_{serv.} - \beta_{member} \\ \Delta\beta_d &= \beta_{damaged} - \beta_{member} \end{aligned} \tag{3.22}$$

Reference [11] proposed a set of reliability conditions that adequately redundant bridge systems should satisfy. For example, to be classified as adequately redundant, a bridge system must produce $\Delta\beta_u$, $\Delta\beta_s$, and $\Delta\beta_d$, values respectively equal to or higher than +1.0, -1.0 and -0.5.

A first order reliability program [88] is used to perform the calculations of β, for the four

limits and for all the cases analyzed above. The results are summarized in Table 3.4. The results show that in all the cases analyzed, the safety index for member is above 5.38. Knowing that a target member safety index of 3.5 was used in North America for the development of bridge design and evaluation codes, the member safety index values obtained herein indicate that these bridges provide highly conservative levels of safety. This however does not necessarily mean that these bridges are adequately redundant. In fact it is observed that only the bridge with end torsional rotations restrained provide an adequate level of redundancy for the ultimate limit state. None of the bridge configurations studied provide adequate redundancy for the damaged condition. However, it is observed that the 11-girder bridge shows the best performance for this case. On the other hand, all the bridges provide adequate levels of system serviceability performance.

To study the sensitivity of the results to the assumed values of COV for LF, the same calculations are repeated assuming that the COV is equal to 10 percent. It is interesting to note that the effect of the change in this COV is relatively small because this produces a change in the system safety indices as well as a change in the member safety indices such that the net effect on the redundancy indices is small. Similar observations are also made in reference [3] indicating that the measures of redundancy proposed in equation (3.22) are not very sensitive to variability in the data base.

3.3.5 Conclusions

The system performance of two alternate bridge configurations is analyzed. The results indicate that the three-cell bridge configuration provides the best system performance for the ultimate limit state. However, it is the 11-girder bridge that provides the best system performance in case of damage to one critical member. Although, the redundancy indices obtained are relatively low, the values of the system safety indices obtained are high (greater than 4.2 even for the damaged condition), indicating that these bridges are conservatively designed and provide overall high levels of system safety.

4. OPTIMIZED REHABILITATION OF DAMAGED BRIDGE SYSTEMS

4.0 Introduction

The evaluation of an existing bridge must accurately reveal the present load carrying capacity of the structure and predict future loads and any future changes in bridge capacity due to deterioration. Many studies on different aspects of bridge diagnostics, evaluation, rehabilitation techniques and management strategies have been initiated throughout the world. For example, models for deterioration rates of bridge members are under investigation [23,24] and innovative methods for bridge strengthening and rehabilitation are being implemented in current practice [25,26,27,28]. In addition, reliability–based techniques for bridge member as well as bridge system evaluation have been developed [29,30]. The results of these investigations however, were never assembled into a comprehensive and coherent framework that can be directly used by a bridge engineer during the routine evaluation of existing bridges.

The objective of this chapter is to develop an outline for a comprehensive framework for the evaluation of damaged highway bridge systems based on reliability techniques. The proposed framework takes into account both the life cycle costs and the structural safety of the bridge. The optimum repair strategy is the strategy that would minimize the lifetime cost while ensuring a minimum acceptable level of safety. This can be formulated as lifetime cost optimization problem subject to the constraint that the probability of failure be always lower than a target level that is determined based on current practice.

4.1 Bridge Life Cycle Costs

Bridges are normally designed and constructed for an estimated 75 to a 100 year lifespan. During their lifespan, bridges may be subjected to aging, increased loading conditions and environmental contamination as well as unforeseen accidents that might cause structural damage. To ensure the safety of the public and ascertain their structural reliability, bridges require regular maintenance and frequent inspections. In addition, a bridge's life cycle costs should also reflect the consequences of the bridge's failure. Thus, a bridge's life cycle costs are function of the bridge maintenance costs, bridge inspection costs, the cost of failure and the probability of failure. In addition, if a damage is detected, the life cycle costs should reflect the cost of damage inspection and the cost of damage repair.

If during bridge inspection a damage is detected, the evaluating engineer has the option of making his safety evaluation of the bridge based on the initial observations or performing more in depth inspections to assess the level of damage. The cost of inspection is a function of the methods used to perform the bridge diagnostics. It may be reasonable to assume that the cost of inspection is proportional to the level of reliability of the inspection technique.

The costs of repairs and the subsequent maintenance as well as the probability of failure of the repaired structure are functions of the repair strategy. For example, if no repairs are performed, then the cost of repair is zero and the probability of failure is the probability of failure of the damaged structure. On the other hand, if the whole structure is replaced after damage, then the cost of repair is equal to the cost of a new structure including the cost of demolition. In addition, the more information is obtained about bridge damage and deterioration through inspection, the more knowledge the engineer has about the repair techniques that would be most appropriate.

The probability of bridge failure is a function of the applied lifetime loads, the resistance of the damaged structure at inspection time, the uncertainty in estimating this resistance capacity, the resistance capacity after repair, the strength degradation function and the time at which the repair takes place. In addition, the probability of failure of the bridge system will be a function of the importance of the damaged or deteriorated members to the overall structural integrity of the complete system. Therefore, to solve the cost optimization problem, data on bridge member deterioration rates, repair techniques and bridge load statistics are required. The effect of member damage and deterioration on the overall reliability of the bridge structural system will also have to be considered.

In summary, the object of an optimum bridge evaluation system would be to minimize

the life cycle costs of a repaired bridge. This cost can be mathematically represented by a function of the form:

$$C_{life} = C_{insp.} + C_{repair} + P_f C_{failure} + C_{maint.} + C_{damage}$$

where C_{life} is the expected lifetime cost, $C_{insp.}$ is the cost of inspection, C_{repair} is the cost of repair, P_f is the probability of failure, $C_{failure}$ is the cost of failure, $C_{maint.}$ is the cost of maintenance of the repaired structure and C_{damage} is the cost of maintenance of the damaged structure between the time of damage detection until damage repair.
It is reasonable to assume that the cost of inspection is proportional to the reliability of the inspection technique utilized. Thus, one can assume that the cost of inspection is a function of the coefficient of variation of the estimate of the strength of the damaged member(s). Similarly, the cost of repair is a function of the reliability of the repair technique utilized. It is thus reasonable to assume that the cost of repair is both a function of the strength of the member(s) after repair and the coefficient of variation of the repaired member strength.
The cost of failure $C_{failure}$ is a function of the cost of the structure and the societal costs. The latter include the costs for loss of life as well as economic costs due to traffic congestion, increased travel distances, etc.
The probability of failure P_f is a function of the system strength and the applied load. P_f can be either calculated at a given point in time or can be the expected (average) lifetime probability of failure. If for example, one is interested in evaluating the probability of failure at the end of the useful lifespan (normally the time with the highest risk), then P_f is calculated at that point in time. On the other hand, in a second optimization model the expected costs can be expressed in terms of the average probability of failure over the entire lifespan of the structure. The first model is used to ensure that the probability of bridge failure remains below an acceptable (target) level for the whole lifespan. The target value is normally determined based on the experience of the engineering community with the performance of similar structures. Thus, in this model, the optimization problem is subject to reliability constraints. This constraint can be either expressed in terms of the probability of failure or in terms of the safety index β as defined in chapter 3.
The second model with an expected lifetime probability of failure is used when the optimum level of bridge reliability is based on cost considerations. This means that there are no artificially imposed reliability constraints and that the optimum safety level would be determined solely based on costs. This latter situation assumes that all the tangible and intangible costs, including the costs of loss of life and the societal costs due to bridge failure can be exactly determined. In addition, this model allows each bridge to have a different optimum reliability level than other similar bridges. For these reasons, it is herein suggested that this model should not be used when the required cost estimates are difficult to obtain. The rest of this chapter uses the constraint optimization model where the target reliability level is predetermined.
Maintenance costs $C_{maint.}$ are the costs of maintaining the repaired structure. These can be expressed in terms of the time period between damage repair and demolition of the structure at the end of its useful life. C_{damage} are the costs of maintaining the damaged

structure. These can be expressed in function of the period between damage detection and damage repair. They may include tangible costs such as the costs of providing traffic control, and intangible costs such as the economic costs due to increased congestion or temporary bridge closures, etc.

4.2 Optimization Problem

Upon detecting a damage, the goal of the evaluating engineer is to find the most cost efficient strategy to rehabilitate the bridge structure. The evaluating engineer has to chose between a number of alternate options. Examples of the decisions that have to be made include:

1. Whether to perform a more careful inspection to better estimate the true strength capacity of the bridge member and the bridge system. The costs will depend on the chosen method of inspection.
2. What method of repair to use and to which level of strength should the damaged members be strengthened. The costs will depend on the method of repair and the new level of strength.
3. Whether to repair the damaged members immediately or delay the repair until a later date. The costs will depend on the method of repair, the time of repair and the economic returns of delaying the repair.
4. Ensure that the bridge will provide a minimum level of safety at all times. This will depend on the loading applied and the rate of bridge strength deterioration.

The bridge rehabilitation problem can then be formulated as an optimization problem, where the best rehabilitation strategy is chosen to minimize the expected life cycle costs subject to the constraint that the bridge safety levels are always above a certain minimum safety level. A common measure of bridge safety that account for the uncertainties in evaluating member and system strengths as well as the uncertainties in evaluating load intensities is the safety index, β, that was defined in chapter 3 of this report. The safety index has been used by code writing groups to calibrate bridge design specifications to achieve minimum levels of safety. For example, the LRFD AASHTO code in the US and the OHBDC Ontario code have been calibrated to achieve a target safety index values on the order of 3.5 for new design. On the other hand, for existing bridges Moses *et al.* recommend the use of a safety index of 2.5.
The object of the optimization is to determine the level of inspection, the level of repair (the strength of the member after repair) and the time at which the repair should take place. A simple example illustrating how these decisions can be made is presented in the next section.

4.3 Illustration

As a simple illustration of how a bridge rehabilitation program can be developed using the model proposed in this chapter, let us consider a reinforced concrete bridge with members that deteriorated after 25 years in service. We assume that the inspector determined that the members of this bridge have deteriorated to an unacceptably low

level. The inspector's report estimated the member moment capacity at this point of time to be 3.87 kN.m. It is also estimated that if left in its current damaged state, the bridge members will further deteriorate at an exponential rate. This deterioration can be modeled as:

$$R = K\ (d - \alpha\tau)^2 \tag{4.1}$$

where K is a constant reflecting the member material and cross sectional properties. d is the diameter of the reinforcing bars. α is the rate of deterioration in bar diameter. τ is the time increment.

At the time when the damage was measured, K was estimated as 11.51 units, while the diameter of the bars was estimated to be 0.58 units. If left untreated, the bars are assumed to lose their diameter at a rate of 8.5 10^{-3} units per year.

It is herein assumed that the bridge is assumed to survive at least 25 additional years beyond the time at which a damage is observed. It is also assumed that member capacities are estimated with a coefficient of variation on the order of 3 % while the maximum lifetime load is estimated at 3.25 units with a coefficient of variation of 10 %. It is further assumed that the cost of inspection is 500,000 units. The cost of failure is 186,000,000 units, the cost of maintenance is 300,000 units per year for the damaged structure, while it is 100,000 units per year after damage repair. It is further assumed that the structure should always maintain a minimum reliability level corresponding to a safety index β equal to 1.0. Three different repair options are presented below. Each repair option is associated with a different cost of repair. The object of this exercise is to find the best repair strategy and the time at which repair should take place in order to minimize the life cycle costs.

Option 1

The first repaired option consists of simply treating the bars to arrest any further reduction in member capacity. It is estimated that this repair option will cost about 24,000,000 units. If left untreated, the bars are assumed to lose their diameter at a rate of 8.5 10^{-3} units per year. On the other hand, it is assumed that the treatment would reduce this rate to 1.0 10^{-3} units per year. Performing the optimization indicated that this repair option will not satisfy the reliability constraint set for this problem. If repair is performed as soon as the damage is detected, the lifecycle costs are estimated to be 58,500,000 units but the safety index β after 25 years of service is 0.83 which is below the set target level.

Option 2

The second repair option consists of strengthening the member by adding additional reinforcement. In this option, the value of K in equation 4.1 is increased at repair time to 12.2 and in addition, new reinforcement of diameter equal to 2.5 units is added such that its effect is associated with a K constant equal to 4.3 units. It is herein assumed that after repair, the rate of deterioration α is 1.5 10^{-3}. This repair option is estimated to cost 37,000,000 units. For this option, the optimization recommends that repair should be performed immediately upon detection of the damage. The estimated

lifecycle costs are 45,000,000 units and the target safety index is satisfied. In fact this repair option will produce a safety index value of 14.4 at the end of 25 years after repair.

Option 3

Repair option 3 consists of placing lateral plates at the bottom of the member to enhance its capacity. This option alters the behavior of the member and the new resistance model will be of the form:

$$R = k' \left(A - \alpha' \tau\right) \tag{4.2}$$

It is herein assumed that k' is equal to 184 units while A is 0.3. The costs of repair are estimated to be 34,000,000 units. The optimization indicated that minimum lifetime costs of 42,000,000 units are obtained when the repair is performed immediately when the damage is detected. The safety index target level is achieved at all times. At the end of the useful life (25 years after detection of damage), the safety index value β is equal to 5.25.

Summary

The results of this exercise indicate that the best repair strategy consists of using the third option and performing the repairs as soon as the damage is detected.

4.4 Conclusions

This chapter presents a framework for using an optimized reliability–based model for decision making on bridge rehabilitation and repair. The model is illustrated through the use of a realistic example. Future research should be directed toward further refinement and collection of actual cost data in order to verify the applicability of this model in engineering practice.

5. CONCLUSIONS

This report is the outcome of a one year study on the reliability of existing highway bridge systems conducted at the Department of Construction Engineering at the Technical University of Catalunya. The objective of this study was to develop preliminary ideas toward proposing a framework for the evaluation of existing bridges. The long term goals of this study and future research is to develop a methodology to help the bridge engineer devise optimum strategies for the evaluation and repair of damaged bridges. The proposed methodology considers the randomness in assessing the extent of damage, the randomness in assessing the capacity of the repaired member, as well as consider the cost implications of the final decision. The proposed approach accounts for the time dependent reliability of the member and the importance of the member to the overall structural integrity of the bridge system.

To achieve these goals, this report presents a simple practical method to perform the nonlinear analysis of bridge systems. The report also outlines a method to use the results of such analyses to obtain estimates of the reliability of the complete system as

an expansion to current methods that only consider the reliability of individual members. The results of such member or system reliability models can be used to devise optimum bridge repair strategies as illustrated in this study.
Future research should concentrate on expanding the models proposed herein by collecting additional data on bridge repair and lifecycle costs; develop methods to include recent findings on bridge deterioration rates, bridge materials, diagnostic procedures and rehabilitation techniques in the proposed framework; and further verify the applicability of the proposed live load and reliability models.

Acknowledgement

This report was written during the sabbatical leave of the first author from the City College of The City University of New York. The author is grateful to his co–author Prof. Juan Ramon Casas for inviting him to spend his 1994 sabbatical year with the Department of Construction Engineering at the Technical University of Catalunya (UPC).
The first author appreciates the informative technical discussions with Prof. Casas and the others members of the bridge group including Prof. Angel Aparicio and Gonzalo Ramos as well as the other faculty of the department.
The author is also thankful for the friendship extended during this year by his hosts and all the members and staff of the department.
The financial support provided by the Generalitat of Catalunya (Direccio General d'Universitats) by means of a fellow ship for visiting professors is greatly appreciated.

REFERENCES

[1] "The 1991 Status of the Nation's Highways and Bridges: Conditions, Performance, and Capital Investment Requirements", US Department of Transportation, Federal Highway Administration, July, 2, 1991.
[2] OECD: "Bridge Management", *Road Transportation Research.* Paris, 1992.
[3] Dunker, K.F. and Rabbat, B.G., "Why America's Bridges Are Crumbling", *Scientific American*, March 1993.
[4] Shanafelt, G.O. and Horn, W.B., "Guidelines for Evaluation and Repair of Prestressed Concrete Bridge Members", NCHRP report 280, TRB, Washington D.C., December 1985.
[5] Nowak, A.S. and Tharmabala, T.: "Bridge reliability evaluation using load tests". ASCE, *Journal of Structural Engineering*, Vol. **114**, No. 10 (1988), pp. 2268–2279.
[6] Standard Specifications for Highway Bridges, 1989, AASHTO, Washington D.C.
[7] CEB–FIP Model Code 1990. *Comite Euro–International du Beton. Lausanne.*
[8] Ontario Highway Bridge Design Code, 1983, Ontario Ministry of Transportation and Communications. Toronto, Ontario, CANADA.
[9] Kulicki, J.M., "Development of Comprehensive Bridge Specification and Commentary", NCHRP 12–33, Draft Report, March 1993.

[10] EP–93: Instrucción para el proyecto y la ejecución de obras de hormigón pretensado, Comisión permanente del hormigón. Ministerio de Obras Públicas y Medio Ambiante. Madrid.

[11] Ghosn, M. and Moses, F., "Redundancy in Highway Bridge Superstructures", NCHRP project 12–36, *Transportation Research Board*, Washington D.C., 1994.

[12] Daniels, J.H., Kim, W. and Wilson, J.L., "Guidelines for Redundancy Design and Rating of Two–Girder Steel Bridges", NCHRP 12–28 (10), November, 1988.

[13] *"Proceedings of the III International Workshop on Bridge Rehabilitation"*. Editors Gert Konig and Andrzej S. Nowak. Ernst and Sohn, Berlin, 1992.

[14] Ghosn, M. and Moses, F., *"A Comprehensive Study of Bridge Loads and Reliability"*, Department of Civil Engineering, Case Western Reserve University, Cleveland, Ohio, 1984.

[15] Miesseler, H.J., Lessing R.: "Monitoring of load bearing structures by means of optical fiber sensors". Proceedings of the IABSE Congress on Durability of structures, pp. 853–858, Lisbon, 1989.

[16] Chatelain, B. Godart and Duchene J.L., *"Detection, Diagnosis and Monitoring of Cracked Prestressed Concrete Bridges"*. Bridge Evaluation, Repair and Rehabilitation, Edt. A. Nowak, Kluwer Academic Publishers, pp. 145–160, 1990.

[17] Flesch, R.,Kernbichler,K.: "A dynamic method for the safety inspection of large prestressed bridges". Proc. of Int. Workshop on nondestructive evaluation for performance in civil structures. Univ. of Southern California, Los Angeles, 1988.

[18] Bakht B. and Jaeger L.G. *"Utilization of Service Loads in Bridge Evaluation"*. Bridge Evaluation, Repair and Rehabilitation, Edt. A. Nowak, Kluwer Academic Publishers, pp. 379–390, 1990.

[19] Casas, J.R., and Aparicio A.C. "Dynamic Testing of Bridges Using Traffic Induced Vibration", Proceedings of the International RILEM–IMEKO Conference on Diagnosis of Concrete Structures, pp. 374–378, Bratislava, 1991.

[20] Moses, F., Ghosn, M. , Gobieski, J.: "Evaluation of steel bridges using in–service testing", Transportation Research Record 1072, Washington D.C., 1986.

[21] Casas, J.R., Sobrino, J.A.,: "Determinacion del coeficiente de amplificacion dinamica en puentes a partir de registros de aceleracion". (in spanish). *Hormigon y Acero*, n. 179, pp. 21–36.

[22] Moses, F., Lebet J.P., and Bez, R., *"Use of Testing for Bridge Evaluation"* Bridge Rehabilitation, Edited by Gert Konig and Andrzej S. Nowak. Ernst and Sohn, Berlin, pp. 571–580, 1992.

[23] Schiessl, P. and Raupach M., *"Monitoring the Corrosion Risk of Reinforcements of Bridges"*. Bridge Rehabilitation, Edited by Gert Konig and Andrzej S. Nowak. Ernst and Sohn, pp. 741–752, Berlin, 1992.

[24] Hergenroder, M., Rackwitz, R.: "Investigations on the statistics of carbonation depths in concrete", Proc. of the Second International RILEM/CEB Symposium. "Quality Control of Concrete Structures", Gent 1991, EFN Spon, London, pp. 451–460.

[25] Fisher J.W. and Menzemer C.R. *"Bridge Repair Methods: US–Canadian Practice"*, Bridge Evaluation, Repair and Rehabilitation, Edt. A. Nowak, Kluwer

Academic Publishers, pp. 495–512, 1990.

[26] Klaiber, F.W., Dunker, K.F. and Sanders, W.W.: "Strengthening of existing bridges (simple and continuous span) by post–tensioning". *External Prestressing in Bridges, ACI SP–120*, pp. 207–228.

[27] Saadatmanesh, H, Ehsani, M.R.: "Fiber composite plates can strengthen concrete beams", *ACI*, Concrete International, 12(3), pp. 65–71, 1990.

[28] Swamy,R.N., Jones, R. Bloxham, J.W.: "Structural behavior of reinforced concrete beams strengthened by epoxy–bonded steel plates". *The Structural Engineer* (London), 65A(2), pp. 59–68, 1987.

[29] Ghosn M., Moses, F. and Khedekar, N. "Response Functions and System Reliability of Bridges", IUTAM conference on Advances in Reliability of Structural Systems, San Antonio, TX, April, 1993.

[30] Tabsh S.W. and Nowak A.S., "Reliability of Highway Girder Bridges", *ASCE Journal of Structural Engineering*, Vol. **117**, No. 8, August 1991.

[31] Tilly, G.P., *"Evaluation of Bridges: European Perspective"*, Bridge Evaluation, Repair and Rehabilitation, Edt. A. Nowak, Kluwer Academic Publishers, pp. 367–378, 1990.

[32] Gordon S., O'Connor D., "Bridge Management, Evaluation and Rehabilitation – A Survey of Current Practice". Bridge Rehabilitation, Edited by Gert Konig and Andrzej S. Nowak. Ernst and Sohn, Berlin, pp. 79–88, 1992.

[33] Ahlskog, J.J., *"Bridge Management – The answer to the Challenge"*, Bridge Evaluation, Repair and Rehabilitation, Edt. A. Nowak, Kluwer Academic Publishers, pp. 3–10.

[34] Hambly E.C., "Bridge Deck Behavior", Chapman and Hall, Second Edition, London, 1991.

[35] Livesley, R.K., "Matrix methods of structural analysis". Pergamon Press Ltd., Oxford, 1970.

[36] Park, R. and Pauley, T, "Reinforced Concrete Structures", *Wiley and Sons*, New York, 1975.

[37] Naaman, A.E., Harajali, M.H., and Wight, J.K., "Analysis of Ductility in Partially Prestressed Concrete Flexural Members", *PCI Journal*, Vol. **31**, No.3, May–June 1986.

[38] Mattock, A.H., "Rotational Capacity of Hinging Region in Reinforced Concrete Beams", Int. Symp. on Flexural Mechanics of Reinforced Concrete, PCA, Miami, Fl, 1964.

[39] Joint ACI, ASCE Task Committee 426, "The Shear Strength of Reinforced Concrete Members", *ASCE Journal of the Structural Division*, Vol. **99**, No. ST6., June, 1973.

[40] Leonhardt, F. and Walther R. "The Stuttgart Shear Tests, 1961", *Cement and Concrete Association*, No. 111, London, 1962.

[41] Seible, F., *"Nonlinear Analysis and Ultimate Strength of Multi–Cell Reinforced Concrete Box Girder Bridges"*, UCB/SESM–82/02, Department of Civil Engineering, University of California at Berkeley, Berkely, CA, 1982.

[42] Zsutty, T.C., "Shear Strength Prediction for Separate Categories of Simple Beam

Tests", *ACI Journal*, Vol. **68**, No. 2, Feb. 1971.

[43] Bazant, Z, P. and Ozbolt, J., and Eligehausen, R., "Fracture Size Effect: 1. Review of Evidence for Concrete Structures", *ASCE Journal of Structural Engineering*, Vol. **120**, N. 8, pp. 2377–2398, 1994.

[44] Maheu, J., "Redistribution of Moments in Slab on Girder Bridges", Ontario Ministry of Transportation.

[45] Schilling, C.G., "A Unified Autostress Method", Report 51, *American Iron and Steel Institute*, November 1989.

[46] Grubb, M.A., "The AASHTO Guide Specifications for Alternate Load–Factor Design Procedures for Steel Beam Bridges", *ASCI Engineering Journal*, Vol. **2**, No. 1, 1987.

[47] Rabbat, B.G., Kaar,P.H., Russell H.G. and Bruce Jr., R.N., "Fatigue Tests of Full–Size Prestressed Girders", State of Louisiana Technical Report No. 113, June 1978.

[48] Hawkins, N.H., Sozen, M.A., and Siess C.P., "Behavior of Continuous Prestressed Concrete Beams".

[49] López, A., *"Estudio de la Evolución hasta la Rotura de Tableros Continuos de Puentes de Hormigón Pretensado de Planta Curva o Esviada"*, Tesis Doctoral, Universidad Politécnica de Cataluña, Escuela Técnica Superior de Ingenieros de Caminos, Canales y Puertos de Barcelona, España, 1987.

[50] Serrano, T.B., "Ensayo a rotura por esfuerzo cortante de vigas en T parcialmente pretensadas", *Hormigon y Acero*, Asociación Técnica Espanola del Pretensado, No. 143, España, 1981.

[51] Serra, I.M. and Marí, A.B. and López, F.A., "Estudio experimental del comportamiento de vigas de hormigón armado descimbradas a tempranas edades", *Hormigon y Acero*, Asociación Técnica Española del Pretensado, España, 1993.

[52] Leonhardt, F., and Walther, R., "Torsion and Shear Tests on Prestressed Box Girders", *Cement and Concrete Association*, No. 130, London, 1968.

[53] Calgaro, J.A., and Virlogeux, M. "Projet et Construction des Ponts: Analyse Structurale des Tabliers de Ponts", Presses de L'Ecole Nationale des Ponts et Chaussees, Paris, 1988.

[54] Buckle, I.G. and Dickson A.R. and Phillips M.H., "Ultimate Strength of Three Reinforced Concrete Highway Bridges", *Canadian Journal of Civil Engineering*, Vol. **12**, pp. 63–72, 1985.

[55] Burdette, E.G. and Goodpasture, D.W., "Full Scale Bridge Testing: An Evaluation of Bridge Design Criteria", University of Tennessee, December 1971.

[56] Choudhury, D. *"Analysis of Curved Nonprismatic Reinforced and Prestressed Concrete Box Girder Bridges"*, Report No. UCB/SEMM–86/13, Department of Civil Engineering, University of California, Berkeley, CA, December 1986.

[57] Scordelis, A.C., Bouwkamp, J.G., and Wasti, S.T., "Structural Behavior of a Two Span Reinforced Concrete Box Girder Bridge Model", Vols. **1,2** and **3**, Report Nos. UC SESM, 71–5, 71–6, 71–7, University of California, Berkeley, CA, 1971.

[58] Soliman, M.I., and Ghali, M.K., "Effect of Diaphragms on the Behavior of R.C. Box Girder Bridges", Fourth International Conference on Short and Medium Span

Bridges, CSCE, Halifax, Nova Scotia, CA, Aug. 1994.
[59] Zokaie, T., Osterkamp, T.A., Imbsen, R.A., "Distribution of Wheel Loads on Highway Bridges", NCHRP project 12–26, TRB, Washington D.C., March 1991.
[60] Powell, G.H., and Buckle I.G., "Computer Programs for Bridge Deck Analysis", Report No. UC SESM 70–6, University of California, Berkeley, April, 1970.
[61] Mondkar, D.P., and Powell, G.H., "CURVBRG–A Computer Program for Analysis of Curved Open Girder Bridges", Report No. UC SESM 74–17, University of California, Berkeley, December, 1974.
[62] Lin, C.S., and Scordelis, A.C., "Computer Program for Bridges on Flexible Bents", Report, No. UC SESM 71–24, University of California, Berkeley, December, 1971.
[63] Peterson, W.S., and Kostem, C.N., *"User's Manual for Program BOVA"*, Fritz Engineering Laboratory Report No. 378B.6A, Lehigh Univ., Bethlehem, PA, 1975.
[64] Hall, J.C., and Kostem, C.N., *"User's Manual for Program BOVAS"*, Fritz Engineering Laboratory Report No. 435.3A, Lehigh Univ., Bethlehem, PA, 1981.
[65] Idriss, R.L. and White, K.R., "Secondary Load Paths in Bridge Systems", Transportation Research Record No. 1290., TRB Bridge Engineering Conference March 1991.
[66] ANSYS Users' Manual of Operations, Swanson Analysis Systems, Houston, TX.
[67] Scordelis, A.C., *"Berkeley Computer Programs for the Analysis of Concrete Box Girder Bridges"*, Department of Civil Engineering, Division of Structural Engineering, University of California, Berkeley, CA.
[68] Hand, T. and Kostem, C.N., "Inelastic Analysis of Prestressed Concrete Spread Box–Beam Bridges", Fritz Engineering Laboratory Report No. 432.8, Lehigh University, Bethlehem, PA, Oct. 1984.
[69] López, L.A., Rehak, D.R., Dodds, R.H., and Schmidt, R.J., "POLO–FINITE, A Structural Mechanics System for Linear and Nonlinear, Static and Dynamic Analysis, Civil Engineering Systems Laboratory, University of Illinois at Urbana–Champaign.
[70] Hibbitt, H.D., Karlsson, B.I., and Sorenson, J., "ABAQUS general purpose finite element code", Hibbitt, Karlsson and Sorensen Inc. Providence, R.I.
[71] Helba, A. and Kennedy, J.B., "Collapse Loads of Continuous Skew Composite Bridges", *ASCE Journal of Structural Engineering*, Vol. **120**, No. 5, May, 1994.
[72] *"NONSAP User Manual"*, Structural Mechanics Computer Laboratory, University of Southern California, Jan., 1981.
[73] Hallquist, J.O., *"DYNA3D User's Manual (Nonlinear Dynamic Analysis of Structures in Three Dimensions)"*, Lawrence Livermore National Laboratory, April, 1988.
[74] Cornell, C.A., Some Thoughts on System and Structural Reliability , Nuclear Engineering and Design, Vol. **71**, 1982.
[75] Bennett, R.M., and Ang, H.S., "Formulation of Structural System Reliability", *ASCE Journal of the Engineering Mechanics Division*, Nov. 1986.
[76] Gorman, M.R., and Moses, F., *"Reliability of Structural Systems"*, Report 79.2, Civil Engineering Department, Case Western Reserve University, Cleveland, OHIO, May, 1979.

[77] Moses, F., "System Reliability Developments", *Journal of Structural Safety*, Vol. **1**, No. 1, 1982.

[78] Ghosn, M., Moses F., and Khedekar, N., Response Functions and System Reliability of Bridges, IUTAM Symposium on Advances in Structural Reliability, San Antonio, TX, April, 1993.

[79] Verma, D., and Moses, F., Efficient Structural System Reliability Assessment by Monte Carlo Methods, Proceedings of ICOSSAR 89, San Francisco, CA, August, 1989.

[80] Cornell, C.A., *"Risk–Based Structural Design"*, Proceedings of a Symposium on Risk Analysis, Department of Civil Engineering, University of Michigan, Ann Arbor, MI, August, 1994.

[81] Thoft–Christensen, P., and Baker, M.J., Structural Reliability Theory and its Applications, Springer–Verlag, New York, 1982.

[82] Nowak, A.S., Calibration of LRFD Bridge Design Code, NCHRP 12–33, May 1992.

[83] R. Bez, Cantieni, R. and Jacquemoud., *"Modelisation du Traffic Routier Suisse*, Ingenieurs et Architectes Suisses, No. 23, Nov. 1985.

[84] Sobrino, J.A., *"Evaluación del comportamiento funcional y de la seguridad estructural de puentes existentes de hormigón armado y pretensado"*, Tesis Doctoral, Departament d'Enginyeria de la Construcció, Universitat Politècnica de Catalunya, Barcelona, Diciembre, 1993.

[85] Vrouwenvelder, A. and Waarts, P.H., "Traffic loads on bridges". *Structural Engineering International*, Vol. **3**, No. 3, pp. 169–177, 1993.

[86] Ad Hoc Committee on Serviceability Research, "Structural Serviceability: A Critical Appraisal and Research Needs", *ASCE Journal of Structural Engineering*, Vol. **112**, No. 2, December, 1986.

[87] Burdette, E.G., and Goodpasture, D.W., "Tests of Four Highway Bridges to Failure", *ASCE Journal of the Structural Division*, Vol. **99**, No. ST3, March 1973.

[88] Rackwitz, R., and Fiessler, B., "Structural Reliability under Combined Random Load Sequences", Computers and Structures, No. 9, 1978.